MICROSYSTEMS FOR *IN VITRO* CNS NEURON STUDY

A Dissertation

by

JAEWON PARK

Submitted to the Office of Graduate Studies of
Texas A&M University
in partial fulfillment of the requirements for the degree of

DOCTOR OF PHILOSOPHY

December 2011

Major Subject: Electrical Engineering

MICROSYSTEMS FOR *IN VITRO* CNS NEURON STUDY

A Dissertation

by

JAEWON PARK

Submitted to the Office of Graduate Studies of
Texas A&M University
in partial fulfillment of the requirements for the degree of

DOCTOR OF PHILOSOPHY

Approved by:

Co-Chairs of Committee,	Arum Han
	Jianrong Li
Committee Members,	Xing Cheng
	Jun Kameoka
	Gladys Ko
Head of Department,	Costas Georghiades

December 2011

Major Subject: Electrical Engineering

ABSTRACT

Microsystems for *in vitro* CNS Neuron Study. (December 2011)

Jaewon Park, B.E., Korea University

Co-Chairs of Advisory Committee: Dr. Arum Han
Dr. Jianrong Li

In vertebrate nervous system, formation of myelin sheaths around axons is essential for rapid nerve impulse conduction. However, the signals that regulate myelination in CNS remain largely unknown partially due to the lack of suitable *in vitro* models for studying localized cellular and molecular basis of axon-glia signals.

We utilize microfabrication technologies to develop series of CNS neuron culture microsystems capable of providing localized physical and biochemical manipulation for studying neuron-glia interaction and neural progenitor development.

First, a circular neuron-glia co-culture platform with one soma-compartment and one axon/glia compartment has been developed. The device allows physical and fluidic isolation of axons from neuronal somata for studying localized axon-glia interactions under tightly controlled biochemical environment. Oligodendrocyte (OL) progenitor cells co-cultured on isolated axons developed into mature-OLs, demonstrating the capability of the platform. The device has been further developed into higher-throughput devices that contain six or 24 axon/glia compartments while maintaining axon isolation. Increased number of compartments allowed multiple experimental

conditions to be performed simultaneously on a single device. The six-compartment device was further developed to guide axonal growth. The guiding feature greatly facilitated the measurement of axon growth/lengths and enabled quantitative analyses of the effects of localized biomolecular treatment on axonal growth and/or regeneration. We found that laminin, collagen and Matri-gel^{TM} promoted greater axonal growth when applied to somata than to the isolated axons. In contrast, chondroitin sulfate proteoglycan was found to negatively regulate axon growth only when it was applied to isolated axons.

Second, a microsystem for culturing neural progenitor cell aggregates under spatially controlled three-dimensional environment was developed for studies into CNS neural development/myelination. Dense axonal layer was formed and differentiated OLs formed myelin sheaths around axons. To the best to our knowledge, this was the first time to have CNS myelin expressed inside a microfluidic device. In addition, promotion of myelin formation by retinoic acid treatment was confirmed using the device.

In conclusion, we have developed series of neuron culture platforms capable of providing physical and biochemical manipulation. We expect they will serve as powerful tools for future mechanistic understanding of CNS axon-glia signaling as well as myelination.

To my family, for their love and support

ACKNOWLEDGEMENTS

First and foremost, I would like to express my heartfelt gratitude to my advisor Dr. Arum Han for all his contributions of time, ideas, guidance, and funding to make my Ph.D. experience productive and stimulating. He provided me with an excellent atmosphere to be an independent thinker, an engineer as well as a researcher. I not only learned a lot but also had lots of fun while working on the project with him and this dissertation could not have been written without him.

I also thank Dr. Jianrong Li and her lab members. Dr. Li taught me everything I know about neuroscience and was always there to answer any questions I had for the biology. Lengthy discussions we had inspired me to develop my project in the right direction and her attitude of enjoying the research motivated me to become an active researcher like her. I thank Andrew and Jeffery for their valuable advice and time they spared for helping me with the cell culture. I would like to give special thanks to Hisami and Sunja. Hisami had patience to help me with most of my neuroscience work from the very beginning and taught me everything I need to know to work at a neuroscience lab. Without her help, my project couldn't have developed this far. I thank Sunja not only for helping me with the dissection and cell culture but also for encouraging me to further develop my neuroscience project. I probably couldn't have finished all of my projects without her help and advices.

I would like to extend my thanks to all of my committee members Drs. Xing Cheng, Jun Kameoka, Gladys Ko for their support. Advice they have given me during the

collaboration projects has inspired me in many ways and helped me to think outside the box.

I thank all my group members in NanoBio Systems laboratory for their support, help, and opinions from different angles. I want to express special thanks to Huijie and Chiwan for their valuable and acute advice over years, Dr. Younghak Cho for sharing his past research experiences.

My time at Texas A&M was made enjoyable due to many friends that became a part of my life. Time I spent with Sungwook, Jaewon and Hyun Soo is the most valuable memories I have from College Station. I would also like to thank Jungho, Sangick and their families for always taking care of me.

Most importantly, none of this would have been possible without the love and patience of my family. My family has been a constant source of love, concern, support and strength all these years. To them I dedicate this dissertation.

TABLE OF CONTENTS

Page

Page

Page

Page

LIST OF TABLES

Page

LIST OF FIGURES

Page

Page

Page

Page

Page

Page

I. INTRODUCTON

1.1. Microdevices for bio/medical applications

Conventional *in vitro* cell culture methods, where cells are cultured in plastic culture plates, have been an essential tool in biological science and have made significant contribution in understanding various properties of cells. However, it had limitations in physically or biochemically manipulating cells or culture environments during the culture. Recent advances in microfluidics and micro/nano fabrication lead to the development of miniaturized chemical and biological analysis systems, including cellular analysis and treatment.[1-6] Some microfluidic devices even provide manipulation and control at single cell level which was difficult to perform using culture plate based conventional methods.[7-9] These applications utilize the unique characteristics of microfluidics, such as small volume and large surface to volume ratio, laminar flow, and compact system size for fast and accurate analysis of biological samples at low cost.[10-12] In addition, the "Lab-on-a-chip" concept allows integration of multiple functional microfluidic components such as electrochemical sensors, microfluidic PCR devices, or electroporators into a single system, thereby all the necessary steps for a particular process could be done on a single chip with minimized processing time and labor.[13-15] Another recent development in microsystems is devices that can apply localized chemical stimuli to cells or precisely control the fluidic microenvironment for on-chip cell culture.[16-23] These devices typically have integrated

---

This dissertation follows the style of *Nature Biotechnology*.

microfluidic functionalities such as microvalves or sensors for real-time and continuous monitoring of the cellular microenvironment.[24-27]

The microfluidic devices can be built in various polymers, glass, or silicon using microfabrication techniques.[28-31] The development of soft-lithography technology[32], a method where hundreds of polymer replicas can be simply stamped out from a single master mold, proliferated the use of microfluidic chips and related technologies from a limited number of researchers having access to sophisticated sets of equipment to numerous researchers outside of the engineering discipline, enabling easy access to such microchips, master molds or even custom microfluidic chips.[33, 34] Typically, a biocompatible polymer such as poly(dimethylsiloxane) (PDMS) is mixed and poured on top of the master, cured, peeled off, and placed against a culture surface to form an assembled microfluidic device.

1.2. CNS neuron and glia

The proper function of vertebrate nervous system depends on rapid nerve impulse conduction achieved by insulating axons with multi-layered myelin sheaths. Myelin sheaths are formed by oligodendrocytes (OLs) in the central nervous system (CNS) and Schwann cells in the peripheral nervous system (PNS).[35, 36] In the CNS, OLs extend their processes, align and spirally wrap around certain axons to form multi-segments of compact myelin layers that maximize the axonal conduction velocity.[37] Dysfunction of myelin-forming cells and/or loss of myelinating sheath underline many neurological disorders including multiple sclerosis, Alzheimer's disease and psychological disorders

such as schizophrenia. To develop effective treatments for diseases originated from neural damages, intensive research have been carried out to reveal how neuronal cells grow, differentiate, network, and respond to various external stimuli.[38, 39] Despite recent progress in understanding the molecular signals in PNS myelination[40], very little is known about how CNS axons regulate the unique feature of OLs – i.e. forming myelin sheath around axons. OLs are post-mitotic cells that arise from their progenitors, oligodendrocyte progenitor cells (OPCs), which proliferate and migrate throughout the CNS during late embryonic development and subsequently mature into pre-myelinating oligodendrocytes before finally differentiating into myelinating cells (i.e. mature OLs) in the white matter.[41, 42] Regulation of OL development has been studied extensively and the development of an efficient method to grow pure OPCs in culture[43] greatly facilitated the identification of many signaling molecules that control OPC proliferation, survival and differentiation.[44-46] However, the CNS myelination process of recognition, myelin synthesis, enwrapping, extension, and formation of nodes of Ranvier are highly regulated by reciprocal signaling between myelinating OLs and the axons to be ensheathed[47-49], and the mechanisms underlying how myelination is initiated and regulated in the mammalian CNS remain largely unknown. This is partly due to the lack of appropriate *in vitro* culture models that are easily accessible for experimental manipulations to unravel the cellular and molecular basis of axon-glia interactions. An *in vitro* culture model system that can mimic physiological axon-glia interactions with ease manipulating capability will allow detailed understanding into axon-glia communications.

1.3. Neuron culture microsystems

There have been numbers of microfluidic devices developed for culturing neurons *in vitro* for overcome limitations from conventional culture methods. Millet *et al.* developed a microfluidic platform for low density neuron culture and optimized PDMS fabrication process and microfluidic environment that enhances the neuron growth the most inside the PDMS device.[50] Microfluidic devices capable of guiding axon growth using micro/nanostructures and controlling cell culture chemical environments with incorporated microfluidic channels have also been reported by multiple research groups.[51-54] One of the most actively studied fields is microfluidic culture platforms with integrated microelectrode arrays (MEAs). Neuron studies relating to electrical stimulation or recording is commonly done by immersing electrode wires in the cell culture wells.[55, 56] However, the stimulation affects all cells in the culture well and the recording from high number of cells within a cell culture well hindered it from obtaining cell level response. Microfluidic culture plates integrated with MEAs allow localized electrical stimulation or recording by culturing neurons directly on top of micro-size electrodes that are electrically insulated with each other. James *et al*. successful recorded the signals from patterned neuronal network using MEAs and Wagnaar *et al*. showed that externally applied electrical stimulation can substitute for natural inputs to cortical neurons.[57]

1.4. Compartmentalized neuron culture

1.4.1. Campenot chamber

An *in vitro* culture device allowing compartmentalized culture of neurons was first developed by Campenot in 1977.[58] Since then, Campenot chambers have been widely used to study axon-glia interaction and axonal biology of dorsal root ganglion (DRG) neurons.[59-61] This chamber utilizes a Teflon® divider attached to a substrate via a thin layer of silicone grease. The Teflon® divider separates the chamber into three compartments, confining cells in the center compartment while the axons can grow through the silicone grease into the neighboring compartments. Nerve growth factor (NGF) is typically used to promote axonal growth through the grease layer and many researches using Campenot chamber have been focused on the influence and the transport of NGF on DRG neurons. However, there are several limitations and challenges to this method. The main drawbacks of Campenot chambers are their tendency to leak due to imperfect grease seal, difficulty in assembly, and limitation in adapting to sophisticated microscopy.

1.4.2. Microfluidically compartmentalized neuron culture microsystem

A microfluidically compartmentalized neuron culture device that can potentially replace the Campenot chamber was first introduced by Taylor *et al.* in 2003.[62] They have fabricated a poly(dimethylsiloxane) (PDMS) microfluidic device composed of one soma compartment and one axon compartment that are connected via arrays of shallow microfluidic channels. The shallow height of the microchannels confines neuronal cell

bodies inside the soma compartment during the culture. At the same time, axons grown from the neuronal somata pass through microchannels into the axon compartment. The height and the length of microchannels successfully isolated axons inside the axon compartment from neuronal cell bodies and dendrites. Since the introduction of this device in 2003, several microdevices with similar scheme have been used for isolating axonal mRNA from CNS neurons and for studying regeneration/degeneration of CNS and PNS axons. [63-67] Recently, Zhang *et al.* locally treated isolated DRG axons with nerve growth factor (NGF) for imaging the axonal transport of NGF and Hur *et al.* utilized compartmentalized neuron culture device to demonstrate that inhibition of NMII ATPase activity promotes axon regeneration over inhibitory molecules. [68, 69]

Conventional CNS neuron-glia interaction studies *in vitro* have been conducted by co-culturing high density of neurons and glia cells on a polystyrene cell culture plate in a mixed form. It is the most widely used co-culture method and made significant contribution in discovering many neurological mechanisms.[70-72] However, the conventional co-culture method provides no means to spatially control cells during the culture and makes it extremely hard to study localized axon-glia interactions. Microfluidic compartmentalized co-culture platform that utilizes the axon isolation feature can enable glia cells to interact only with isolated axons, thereby providing more chemically and physically controlled surroundings. A high-throughput microfluidic platform capable of co-culturing isolated axons with glial cells can be a unique and a powerful tool for studying localized axon-glia interaction *in vitro*.

1.5. Three-dimensional neuron culture

1.5.1. Three-dimensional aggregate culture models

Three-dimensional (3D) cell culture systems have received significant interests in recent years in tissue engineering, stem cell biology, and cancer biology. The *in vivo* like culture environment of 3D culture systems, where cells grow in a 3D space with ample interacting signaling among cells, are thought to result in more physiologically relevant growth, leading to *in vivo* like functionality of cells and tissue *in vitro*. In tumor cell research, 3D multi-cellular aggregates have been used for simulating the tumor microenvironment and providing authentic cell-to-cell interactions, as well as for the establishment of uniform mass transfer to study anticancer drugs.[73-76] A few neuron aggregate culture models have been also recently developed for studying neurons in more *in vivo* like environments.[77-79] Ziegler *et al*. showed differentiation of human embryonic stem cells into Schwann cells using aggregate culture model. Studies including the contribution of astrocytes to the rate of myelin wrapping as well as the effects of OL maturation stage in myelin formation are also being investigated using different type of aggregate culture model.[80]

1.5.2. Microfluidics cell aggregate culture systems

Due to the advantages of microfluidic cell culture systems described above, their application to aggregated cell culture models is actively being pursued.[81-85] Such effort can be categorized into two approaches, generating cell aggregates with microfabricated devices and culturing aggregated cells inside the microfluidic devices to provide a more

physically/chemically controlled environment. So far, only very few research groups have developed microfluidic aggregated cell culture devices, such as tumor aggregate culture devices for finding and screening anticancer drugs[86, 87] or embryonic stem cell culture devices for studying cell differentiation.[77, 83, 85]

Among methods to generate cancer or stem cell aggregates, the most commonly used method is culturing dissociated cells on top of microwell arrays of desired sizes. Dissociated cells on the microwell form uniformly sized clusters of cells after 1-3 days of culture and are collected for use.[82, 83] This simple method can easily generate aggregates of different sizes depending on the microwell sizes. A microfluidic device that allows active control over the sizes of cell aggregates by using hydrodynamic micro-rotational flow has also been introduced but the aggregate formation throughput was significantly lower compared to microwell type cell aggregation devices that can simultaneously generate hundreds and thousands of cell aggregates in a single batch. Several other methods such as micro-droplet or cell sieve based aggregate formation devices that integrate cell aggregate generating modules with cell culture chambers have been recently introduced.[85, 86]

II. CIRCULAR CNS NEURON/GLIA CO-CULTURE MICRODEVICE*

2.1. Motivation

The square design neuron cell culture platform previously introduced by Taylor *et al.* capable of isolating axons from cell bodies is composed of two 100 μm high compartments that are connected by 3μm high microfluidic channels. The shallow height of the microchannels confine neurons inside the soma compartment into which neurons are initially loaded, while allowing axons to grow through the channels into the axon compartment and be isolated from their cell bodies and dendrites. This square design device has two reservoirs for each compartment for loading cells and changing culture medium. The square device was initially used to co-culture neurons with OLs for studying axon/glia interaction, but the fluidic flow from one reservoir to the other within the same compartment caused neurons to be washed away from the soma compartment during the cell loading and culture medium exchange process. Due to this flow, number of neurons inside the soma compartment could not be accurately controlled or reproduced. Also, this flow caused neurons to move away from the microchannel inlets, reducing the probability of axons to grow into the axon compartment. In order to overcome these issues and for the microdevice to be routinely

used as a robust *in vitro* neuron/glia co-culture platform, a circular design neuron co-culture microdevice have been developed.

The circular design co-culture microdevice provides the same function as the square device, but has only one reservoir for the soma compartment which itself is the soma compartment with an open reservoir structure. The configuration keeps fixed number of neurons within the soma compartment throughout the culture and allows neurons to be directly loaded around the microchannel inlets using a pipette to enhance the probability of axons crossing into the axon/glia compartment. Minute radial culture medium flow from the soma compartment to the axon/glia compartment during the cell loading process further promotes neurons to position close to the axon-guiding microchannel arrays. In addition, the open-compartment configuration facilitates better CO_2 exchange and reduces any possible negative effects of a closed-compartment for better cell growth.

2.2. Design

The circular microfluidic co-culture platform is composed of two cell culture compartments, one for neurons and the other for OLs. Two compartments are connected by arrays of 15-30 μm wide, 2.5-3 μm high microchannels (n = 140 to 180). Typical sizes of embryonic cortical neurons isolated from E16-18 rats and OL progenitor cells (OPCs) from P1-2 rat range from 5-15 μm. These shallow microchannel arrays that connect the two compartments work as a barrier to keep neuron cell bodies in the soma compartment, while allowing axons to pass through and grow into the axon/glia compartment. The length of microchannels (200-800 μm) restricts the growth of

dendrites into the axon/glia compartment, leaving only axonal network layer formation in the axon/glia compartment. This enables OPCs loaded into the axon/glia compartment to interact only with axons, but not with neuronal somata or dendrites (Figure 2.1A). This microfluidic co-culture platform also fluidically isolates the axonal microenvironment. Fluidic isolation of the microfluidic co-culture platform was established by creating a minute fluidic level difference of culture medium between the two compartments. When the levels of culture medium inside the two compartments are at equilibrium, molecules resolved in one compartment can diffuse into the other compartment through the microchannel arrays. On the other hand, slight difference in fluidic levels between the two compartments produce small but sustained flow from the higher fluidic level side to the lower side that counters diffusion, thus enabling fluidic isolation (Figure 2.1B). This fluidic isolation between the two compartments is essential for localized treatments of axons or OLs with various growth factors, inhibition factors, and also potentially with drugs.

The platform is composed of one circular open compartment (soma compartment) located in the middle for neurons and one closed co-centric ring compartment (axon/glia compartment) for glia. The open circular soma compartment is 7 mm in diameter and the closed outer ring compartment is 100 μm high and 2 mm wide, and distanced away from the soma compartment by the length of the axon-guiding microchannels (200-800 μm long). Culture medium for the neuron cells can be held in the soma compartment whereas culture medium for the OLs is held in the two reservoirs connected to the

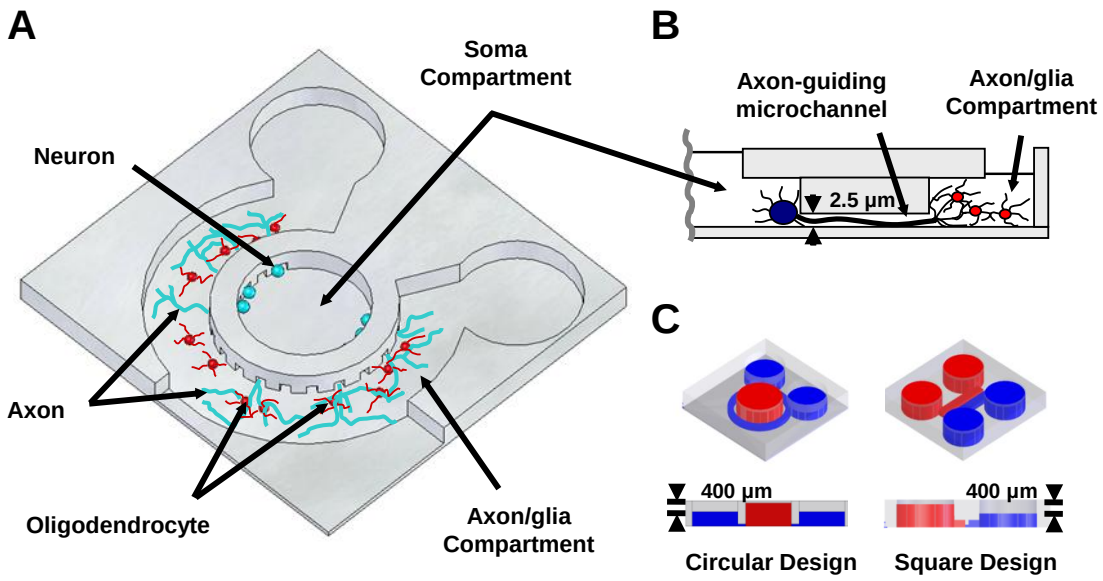

Figure 2.1. Schematic illustration of the microfluidic compartmentalized CNS neuron co-culture platform. (A) A 3D-view of the circular device. (B) A cross-sectional view showing the physical isolation of axons and OLs from neuronal soma and dendrites. (C) Cross section views of the circular and square design culture platforms showing a minute difference in fluidic levels for fluidic isolation. The circular compartment in the center of the circular device is an open access compartment for neurons and is connected to the outer ring-shaped axon/glia compartment for OLs through arrays of axon-guiding microfluidic channels.

axon/glia compartment. The soma compartment is an open compartment to provide better cell living conditions by facilitating CO_2 exchange. Although PDMS is known to be gas permeable, primary cultured neurons are often very sensitive to small environmental changes and an open access compartment design reduces possible negative effects of a closed compartment. The open compartment design also reduces mechanical stress to cells during culture medium exchange compared to a closed compartment design by reducing the shear stress during such processes.

To characterize our design and also to compare the design to other previously reported neuron culture design such as that from Taylor *et al.*[63], we have also fabricated and tested a square design co-culture device (Figure 2.1C). This square design is composed of two rectangular compartments connected through arrays of axon-guiding microchannels. The compartment width and height varied from 1.2 to 5 mm and 60 to 100 μm, and the channel length and width varied from 200 to 800 μm and 15 to 30 μm, respectively, to optimize the geometry of the design.

2.3. Fabrication

Microfluidic co-culture platforms with different designs were fabricated in PDMS using the soft-lithography technique. First, the master mold was fabricated on a 3 inch diameter silicon substrate using a two-layer photolithography process. Two layers of photosensitive epoxy (SU-8, Microchem, Inc., Newton, MA) with different thicknesses were sequentially patterned on the substrate. The first layer forming 2.5-3 μm thick axon-guiding microchannels was obtained by spin-coating SU-8™ 2002 at 1000 rpm

and soft-baking at 95°C for 4 min. It was then exposed to ultraviolet (UV) light followed by post-exposure bake at 95°C for another 4 min. The second layer forming the cell culture compartment was 60-100 μm thick and patterned by spin-coating SU-8™ 2075 at 2000 rpm, soft baking in two steps at 65°C for 20 min and at 95°C for 40 min, followed by UV exposure and post-exposure baking in two steps at 65°C for 5 min and at 95°C for 15 min. The SU-8 ™ master was coated with (tridecafluoro-1,1,2,2-tetrahydrooctyl) trichlorosilane (United Chemical Technologies, Inc., Bristol, PA) to facilitate PDMS release from the master after replication. Devices were replicated from the master by pouring PDMS pre-polymer (10:1 mixture, Sylgard® 184, Dow Corning, Inc., Midland, MI), followed by curing at 85°C for 45-60 min. The reservoirs to hold culture medium were punched out using a 7 mm diameter punch bit (Technical Innovations, Angleton, TX) mounted on a drill press. To improve the bonding of PDMS devices onto substrates and to make the device hydrophilic for easy cell and culture medium loading, the PDMS culture devices were exposed to oxygen plasma (Harrick Plasma, Ithaca, NY) for 90 sec. For sterilization, the device was immersed in 70% ethanol for 30 min prior to bonding on poly-d-lysine (PDL) or Matrigel™ coated glass coverslips or polystyrene culture plates. However, substrates coated with Matrigel™ resulted in all axon-guiding microchannels being blocked due to rehydration of the Matrigel™. Therefore, all following experiments were conducted on PDL coated substrates. PDL coating was done by applying PDL solution to the substrate and either incubating inside a 37°C incubator for 3-5 hours or leaving at room temperature

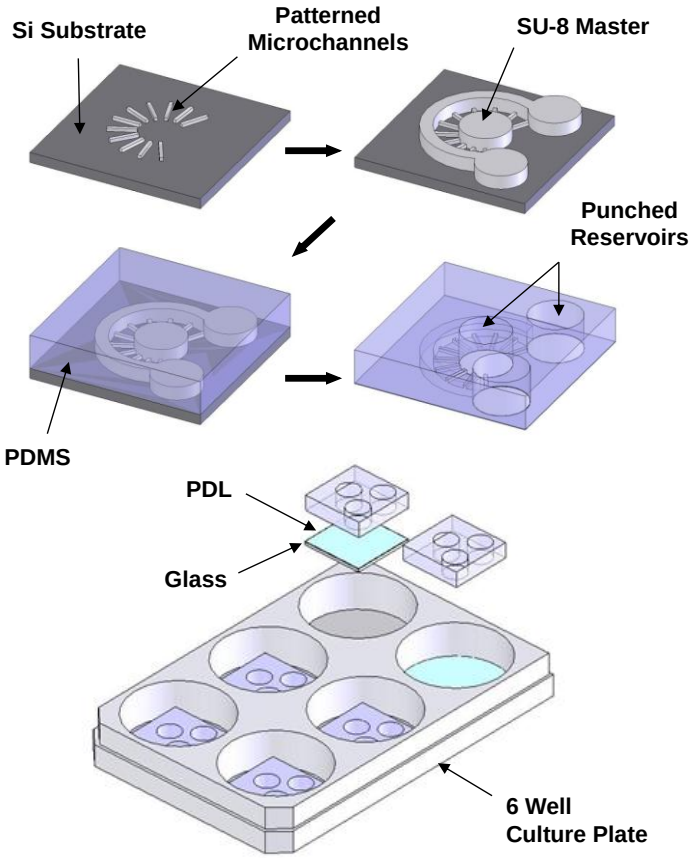

Figure 2.2. Fabrication and assembly steps for the microfluidic co-culture device. Two SU-8 layers with different thicknesses were patterned on top of a silicon substrate to form the axon-guiding microchannel array and the two cell culture compartments (soma, axon/glia). PDMS devices were replicated from the SU-8 master using soft-lithography process and 7 mm diameter reservoirs were punched out followed by sterilization in 70% ethanol for 30 min and bonding onto PDL or Matrigel^{TM} coated substrates. Each device fits into one well of a conventional 6-well polystyrene culture plate.

overnight. Each device was placed inside each well of a conventional 6-well polystyrene cell culture plate. Figure 2.2 shows the overall fabrication steps and assembly processes.

Figure 2.3 shows images of the microfabricated PDMS co-culture device. The scanning electron micrographs show arrays of 15 μm wide axon-guiding microchannels separated from one another by approximately 60 μm distance. The inset in Figure 2.3A shows the overall device (22 x 22 mm^2) placed inside a conventional 6-well polystyrene culture plate. Axon-guiding channel having width of 30 μm with 30 μm distance between channels and 15μm with 60-500 μm distances have been tested to find the optimal dimension that maximizes the channel area between the compartments (i.e. maximum channel width and minimum distance between channels) for high density axon growth into the axon/glia compartment while maintaining a stable fluidic seal. Too wide of a channel caused the PDMS channel to sag and block the channel. Too short of a distance between channels resulted in insufficient contact area between the PDMS structure and the substrate, preventing a tight fluidic seal. Experimental results showed that axon-guiding channels with 15 μm width and 60 μm distance provided maximum opening between the two compartments while maintaining a robust fluidic seal between the PDMS device and the substrate throughout the culture period of four weeks without leakage. Without the oxygen plasma treatment, the fluidic seal between the device and the PDL or Matrigel™ coated substrate broke after several hours, and the hydrophobic property of the PDMS caused bubbles to be trapped inside the compartment while

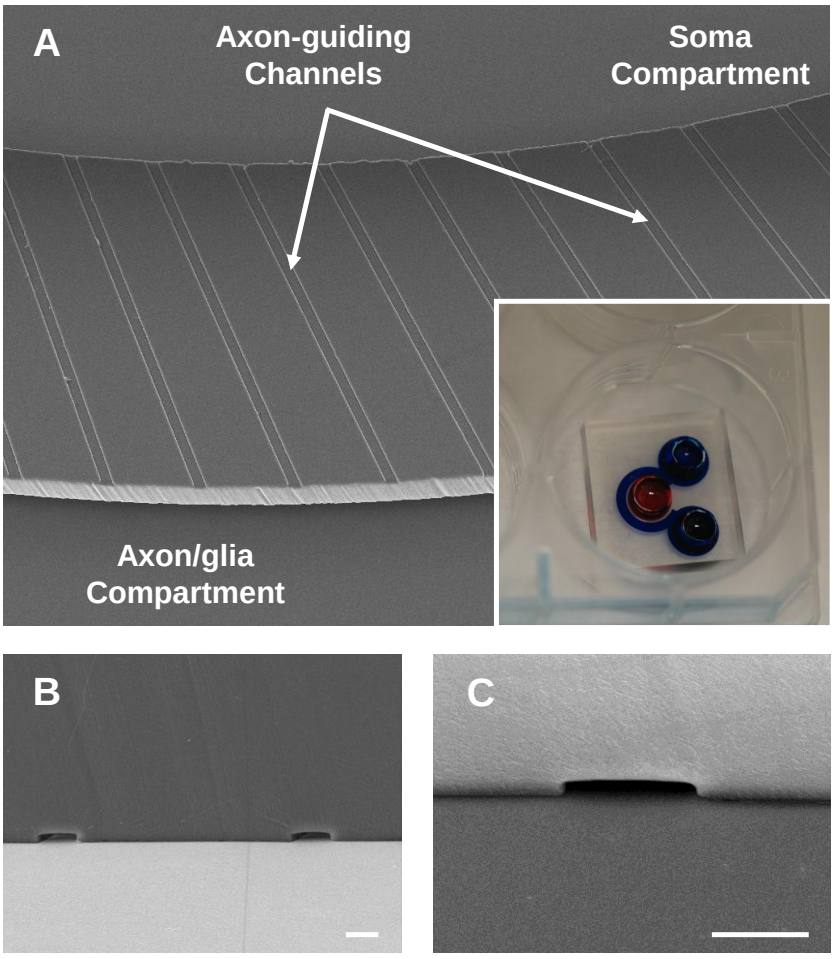

Figure 2.3. Scanning electron micrographs (SEMs) and an optical photograph of the PDMS co-culture device showing (A) bottom side of the axon-guiding channel arrays before bonding (Inset: Device placed inside a conventional 6-well polystyrene culture plate and filled with color dye for visualization), (B) PDMS device bonded onto a glass coverslip showing two 15μm wide axon-guiding micro channels with approximately 60 μm separation, and (C) close up view of one axon-guiding microchannel. Scale bars: 10 μm.

loading cells or changing out the culture medium. The 30 μm wide channels with 30 μm distances provided more than two folds of area connecting two compartments, but the short distance between the channels deteriorated the adhesion of the PDMS device to the substrate, resulting in a fluidic seal failure after several hours.

2.4. Tissue dissociation

Primary CNS neurons were prepared from forebrains of embryonic day 16 Sprague-Dawley rats. Briefly, forebrains free of meninges were dissected in ice-cold dissection buffer (Ca^{2+}/Mg^{2+}-free Hank's Balanced Salt Solution containing 10 mM HEPES), dissociated with L-cysteine activated papain (10 units/ml) in dissection buffer for 5 minutes at 37°C, and resuspended in dissection medium containing trypsin inhibitor (10 mg/ml) for 2-3 minutes. Following two more washes with the trypsin inhibitor solution, the tissue was resuspended in a plating medium (NBB27 + glutamate: neurobasal medium containing 2% B27, 1 mM Glutamine, 25 M glutamic acid, 100 units/ml penicillin, and 100 g/ml streptomycin) and triturated with a fire-polished glass Pasteur pipette until all clumps disappeared. The cells were then passed through a 70 μm cell sieves and live cells were counted using a hemocytometer and trypan blue exclusion assay. The viability of isolated cells was constantly greater than 90-95%.

Primary OLs cultures were prepared from the cerebral hemispheres of Sprague-Dawley rats at postnatal day 1-2 as previously described.[36, 88] Forebrains free of meninges were chopped into 1 mm^3 blocks and placed into HBSS containing 0.01% trypsin and 10 μg/ml DNase. After digestion, the tissue was collected by centrifugation

and triturated with the plating medium DMEM20S (DMEM, 20% fetal bovine serum and 1% penicillin-streptomycin). Cells were plated onto PDL-coated 75 cm^2 flasks and were fed with fresh DMEM20S medium every other day for 10-11 days at 37℃ in a humidified 5% CO_2 incubator. The flasks were pre-shaken for 1 hour at 200 rpm to remove lightly attached microglia followed by overnight shaking to separate OLs from the astrocyte layer. The suspension was plated onto uncoated petri-dishes and incubated for 1 hour to further remove contaminating microglia and astrocytes. Purified OLs were then collected by passing through a 15 μm sieve and centrifuged. OLs isolated in this study were primarily OL progenitors (OPCs) and precursors.

2.5. Fluidic isolation

The efficiency of fluidic isolation was tested on both the circular design and the square design by creating a minute fluidic level difference between the reservoirs that resulted in difference in hydrostatic pressure. Initially, color dye (red and blue) was mixed with PBS and loaded into each reservoir. Fluidic level differences of 130, 400, 650, and 1000 μm were achieved by creating volume differences of 5, 15, 25, 40 μl between reservoirs, respectively. Successful fluidic isolation between the compartments was achieved with as small as 400 μm fluidic level difference that was maintained for over 70 hours in both the circular and the square design culture platform (Figure 2.4). Fluidic pressure from the soma compartment (red color, higher fluidic level) to the axon/glia compartment (blue color, lower fluidic level) through the 2.5-3 μm high microchannel array

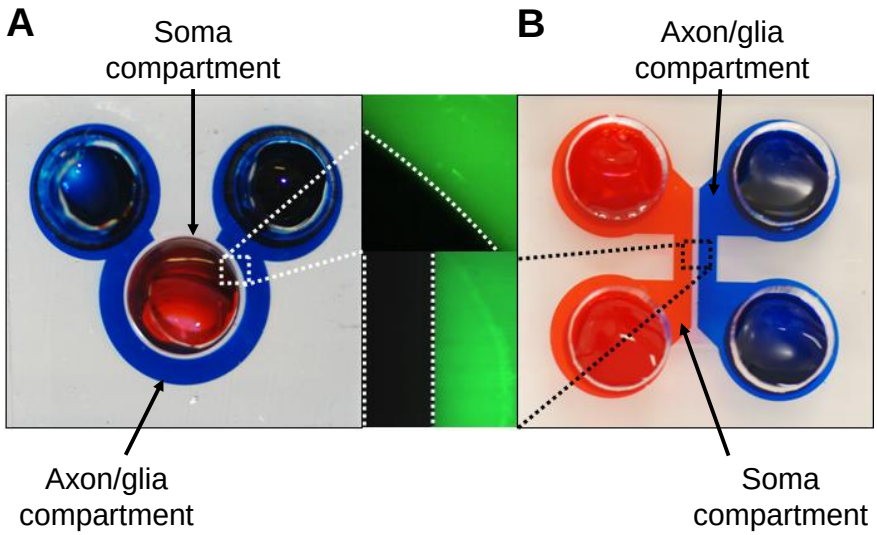

Figure 2.4. Fluidic isolation in the (A) circular design and (B) square design neuron culture platforms. Dotted white lines in fluorescence images delineate compartment boundaries. Green fluorescent part indicates the axon/glia compartment while the black part indicates the array of axon-guiding microchannels.

counteracted diffusion. For more accurate test, the axon/glia compartment and the soma compartment were filled with fluorescent dye (FITC) and PBS respectively, with the soma compartment having a slightly higher fluidic level. With a fluidic level difference of 400 μm between the two compartments, FITC was successfully confined to the axon/glia compartment, where a sharp boundary can be seen between the compartment and the axon-guiding microchannel arrays (Figure 2.4).

2.6. Isolation of axons

The microdevice was designed so that neuron cell bodies are isolated from axons by the height of the axon-guiding microchannels (2.5-3 μm) that block the cell bodies from moving into the axon/glia compartment. On the other hand, isolation of dendrites from axons is achieved by controlling the length of the axon-guiding channels because both axons and dendrites can grow through the axon-guiding microchannels but dendrites can grow only for a short distance. Microchannels with length ranging from 200 to 800 μm were tested to find the minimum length required for axon/dendrite isolation. Axons and dendrites successfully developed from neurons loaded inside the co-culture platform, and no toxicity or contamination issues were observed throughout four weeks of culture. Axons crossed and filled most of the axon-guiding microchannels by DIV 6 and started to spread out rapidly inside the axon/glia compartment. The microchannel arrays were not only efficient in guiding axons but also successful in physically isolating cell bodies and dendrites from axons. The height of the microchannels prevented cell bodies from

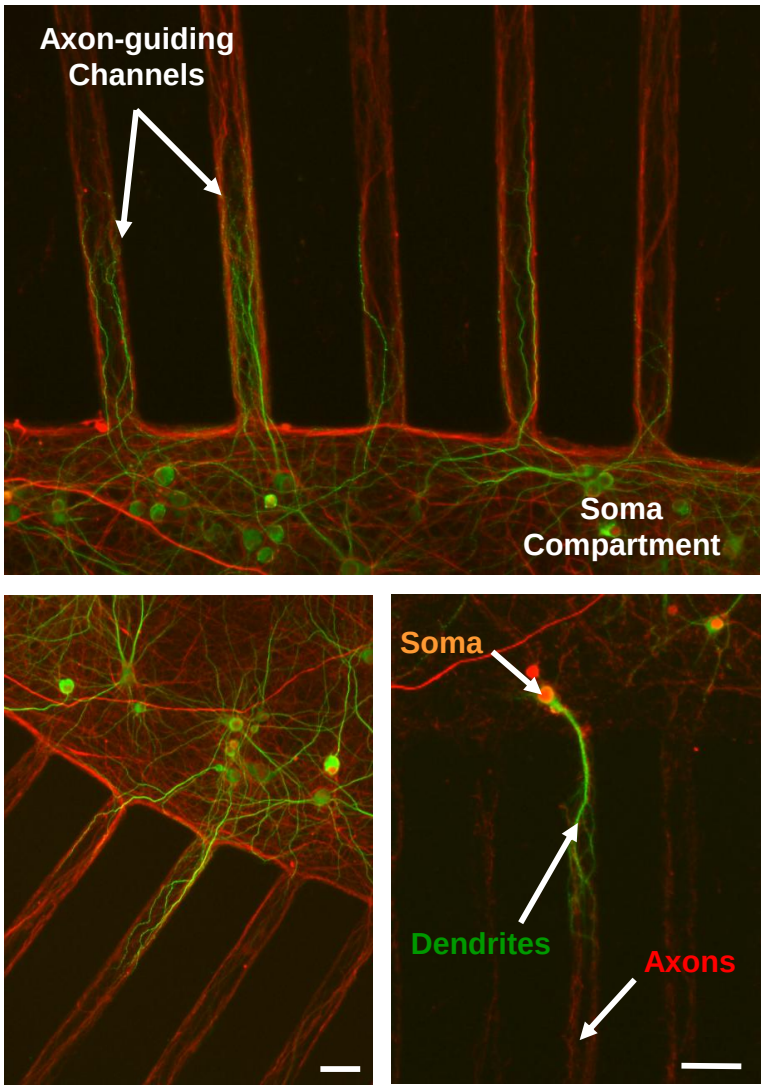

Figure 2.5. Immunocytochemistry images of neurons at two weeks in culture demonstrate that axons grew from the soma compartment into the axon/glia compartment through the arrays of axon-guiding microchannels but dendrites and neuronal soma could not reach into the axon/glia compartment due to the length and the height of the microchannels. Axons were immunostained for NF (red) and dendrite for MAP2 (green). Scale bars: 20 μm.

moving into the axon/glia compartment, and the length of the microchannels kept dendrites from reaching the axon/glia compartment. Figure 2.5 clearly demonstrates the physical isolation of axons from neuronal somata and dendrites via the axon-guiding microchannels. A shorter axon-guiding channel has the advantage to form an extensive axonal network inside the axon/glia compartment at earlier stage, and axon-guiding channel as short as 200 μm was sufficient to isolate dendrites from growing into the axon/glia compartment.

2.7. Neuron cell loading efficiency

To facilitate highly efficient axon crossing into the axon/glia compartment through the axon-guiding microchannels to achieve high-density axonal network, neurons loaded into the soma compartment of the microfluidic co-culture platform have to be positioned close to the entrance of the microchannels during the initial cell loading process. Neuron cells were loaded into the soma compartment to characterize and compare the distances between the loaded cells and the entrance of the axon-guiding microchannels in the two different microdevice designs (circular design vs. square design). The areal cell density was kept identical in both designs (500 cells/mm^2). We first tested the square design neuron culture platform. In our initial experiments, 120 μl per reservoir of additional culture medium was added to each reservoir immediately after loading the neurons to the soma compartment. This cell loading protocol, however, resulted in many of the cells inside the soma compartment washing out to the outlet reservoir due to the rather strong culture medium flow from one reservoir to the other reservoir. To prevent such washing

out of cells, a short incubation step was added before loading culture medium since neurons loaded inside the compartment attach to the substrate after a while and their locations remain relatively stable. Incubation times of 10-60 min were tested to optimize the incubation step. Sufficient adhesion of the cells to the substrate was achieved after 30 min of incubation that prevented cell wash-out while maintaining good cell viability. Longer incubation times (more than 30 min) provided stronger adhesion of the cells but with a drop in cell viability. Neurons incubated for 60 min before adding culture medium showed slight aggregation of neurons inside the soma compartment after 24 hours, and most of them were observed dead at DIV 4. Short incubation times (less than 30 min) resulted in many cells still being washed out to the other side of the reservoir while adding the culture medium. Although cell adhesion to the substrate is an important factor and the loading method has been optimized for the square design, the chances of axons entering the axon-guiding microchannels and growing into the axon/glia compartment are low unless neurons are positioned close to the inlet of the axon-guiding microchannels during the initial loading process. The location of the cells during the initial cell loading step is heavily influenced by the microfluidic design of the culture compartments and cell loading inlets/outlets.

The circular design co-culture platform developed here has one open access compartment in the center for neurons. This design allows neuron cells loaded into the center compartment to flow radially toward the axon-guiding channel inlets. This small but sustained flow keeps cells close to the entrance of the axon-guiding channels. The

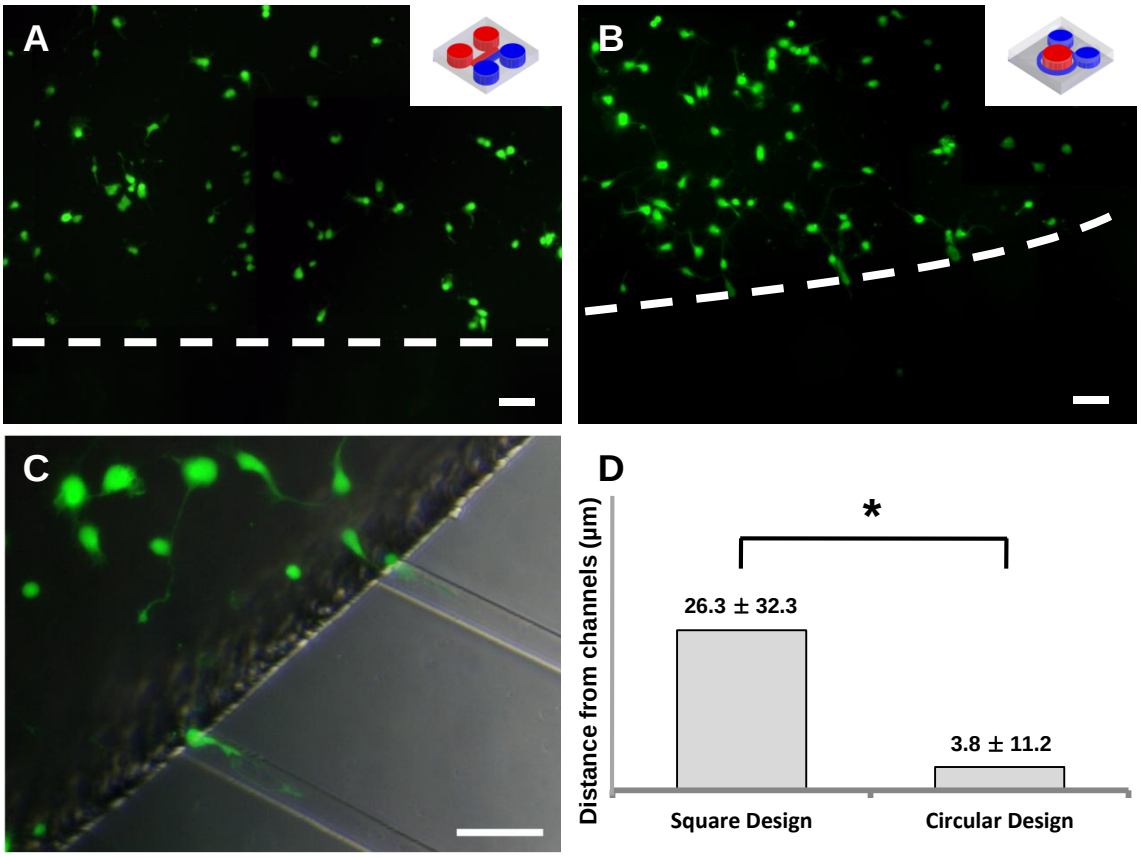

Figure 2.6. Fluorescent images of neuron cells inside the soma compartment at DIV 1. (A) Cells inside the square design device. (B-C) Cells inside the circular design device. (D) Average distance of the closest cells from the axon-guiding channel inlets (square design, $n = 263$; circular design, $n = 225$). White dotted lines indicate where the axon-guiding microchannels start. Cells were stained with Calcein-AM at DIV 1 before fixing. Scale bars: 50 μm. *$p < 0.001$.

"cell loading efficiency" in the two different microfluidic co-culture platform designs was analyzed by measuring the average distance of the closest cells from the inlets of the axon-guiding microchannels. Cells loaded into the square design co-culture platform moved smoothly into the soma compartment; however, the average distance of the cells from channel inlets, measured from 263 cells in multiple devices, was 26.0 ± 32.3 μm (means ± SD). In contrast, the circular design co-culture platform showed an average distance of 3.8 ± 11.2 μm, measured from 225 cells in multiple devices, which indicates that the loaded cells are located almost exactly at the inlet of the axon-guiding microchannels (Figure 2.6). This shows that the cells are located closer to the inlets of the axon-guiding microchannels when using the circular design compared to the square design, increasing the probability of axons growing into the microchannels. Cells loaded into the open soma compartment were naturally positioned close to the channel inlets due to the radial flow pressure resulting from the circular fluidic design, and the fluidic pressure from the added culture medium of 120 μl moved the cells even closer to the channel inlets. Although neurons were located at the channel inlets, channel openings were not blocked by the neurons, and axons could successfully pass through the channels into the axon/glia compartment.

The cell loading efficiency was not analyzed for the OPCs since they have to attach uniformly on top of the axonal network layer inside the axon/glia compartment rather than being concentrated to the axon-guiding channel outlet area. OPCs were loaded into the axon/glia compartment at DIV 14 for the co-culture experiments with a final areal cell density of 400 cells/mm^2. A total culture medium volume of 10 μl was added

through the axon/glia compartment reservoir after aspirating out the excessive culture medium inside the reservoir. It is important not to remove the culture medium inside the axon/glia compartment during aspiration, since axons inside the axon/glia compartment can be damaged. OPCs were uniformly distributed over the axonal network inside the axon/glia compartment in both the circular and the square designs.

2.8. Axon growth

Two different types of substrates, glass coverslips and 6-well polystyrene culture plates, were coated with PDL prior to assembly with the PDMS microfluidic co-culture devices. To compare how the two microfluidic culture platform designs and the different substrates influence axon growth inside the co-culture platform, neurons were cultured in both the circular and the square design assembled on PDL coated polystyrene culture plates and PDL coated glass coverslips. The axon growth efficiency by different conditions was analyzed by the axon coverage ratio (ACR), defined as the percentage of area covered with axons inside the axon/glia compartment. To analyze the ACR by the different device designs, neuron cells were cultured at an areal density of 500 cells/mm^2 on top of PDL coated polystyrene culture plates and fixed at DIV 14.

After two weeks of neuron cell culture, the average ACR of the circular design co-culture platform attached on polystyrene culture plate was 51.0 ± 11.8% (means ± SD), which is significantly higher than that of the square design on the same substrate showing 14.1 ± 4.6% (Figure 2.7A, $p < 0.0001$). Therefore, we concluded that the novel

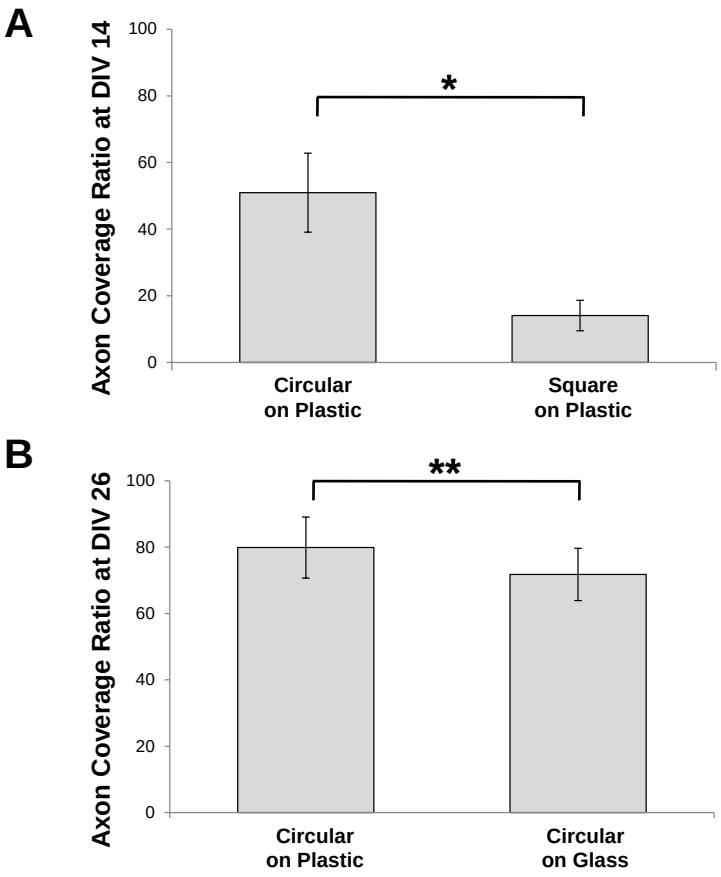

Figure 2.7. Axon coverage ratio (ACR) of the axon/glia compartment by (a) different culture platform designs at DIV 14 and by (B) different substrates (polystyrene, glass) at DIV 26. Neurons cultured on the polystyrene culture plate using the circular design shows enhanced axon growth when compared to the square design on plastic or the circular design on glass coverslip (* $p < 0.0001$, ** $p < 0.05$).

circular co-culture design developed here enables the formation of a denser axonal network layer when compared with the square design. The ACR was also affected by the substrate type. Neurons with an areal cell density of 3100 cells/mm^2 were cultured inside the circular design culture platforms assembled on PDL coated glass coverslips and PDL coated polystyrene culture plates, respectively. After four weeks of culture, including two weeks of co-culture period, neurons cultured on glass coverslips showed an average ACR of 71.8 ± 7.9% (means ± SD), while the neurons cultured on polystyrene culture plates showed an ACR of 79.9 ± 9.2% (means ± SD) (Figure 2.7B). In addition, the adhesion of cells to substrates was also different depending on the substrate types. Axons grown on top of polystyrene culture plates were firmly attached to the substrate while many axons cultured on glass coverslips peeled off when detaching the PDMS devices for fixing and staining at the end of the culture periods.

2.9. Co-culture of neuron and oligodendrocyte

The co-culture capability of the developed platform was tested by plating OPCs on top of the axonal network inside the axon/glia compartment that was already formed during the initial 2 week culture period. OPCs with an areal cell density of 400 cells/mm^2 were loaded uniformly on top of the axonal layer inside the axon/glia compartment without any disturbance to the existing axonal network layer. The 2.5-3 μm high axon-guiding microchannels physically prevented OPCs from crossing through the channels, and no OPCs were observed inside the soma compartment upon loading. After loading, neurons

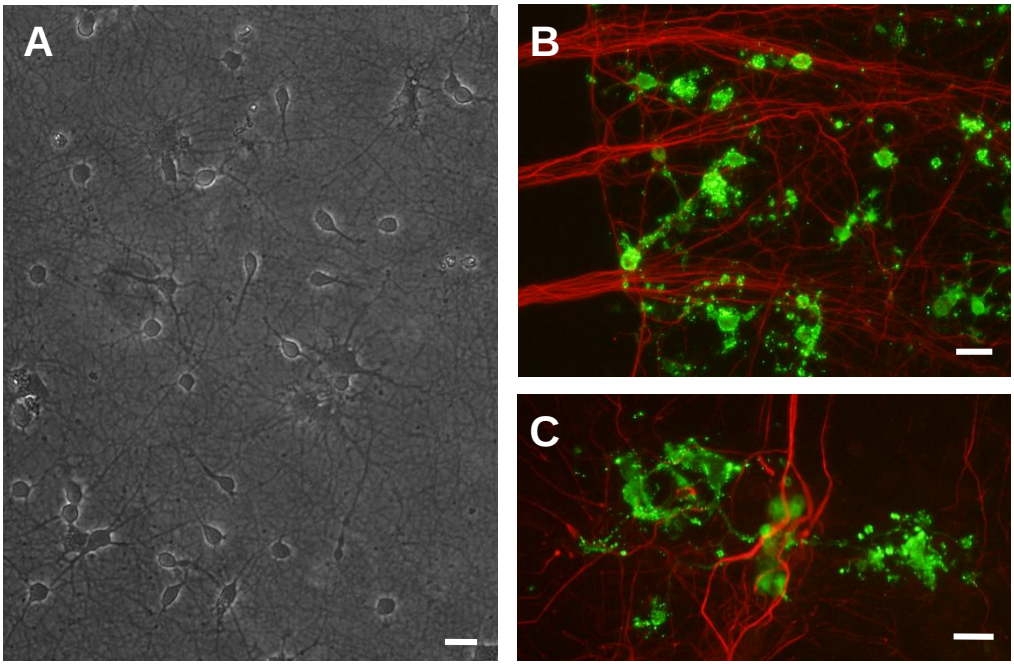

Figure 2.8. A phase contrast image and Immunocytochemistry images of axons and OLs co-cultured inside the axon/glia compartment for two weeks. (A) Phase contrast image of the axon/glia compartment. (B-C) Immunostained images showing mature OLs grown on top of axonal network layer inside the axon/glia compartment. Axons were stained for NF (red) and mature OLs were stained for MBP (green). Scale bars: 20 μm.

and OPCs were co-cultured for up to two more weeks and fixed at DIV 26. Figure 2.8 shows axons and mature OLs (stained for MBP, green) inside the axon/glia compartment. Myelin basic protein (MBP), stained with green fluorescence, expresses only in mature OLs, thus, the expression of MBP is a clear indication that OPCs co-cultured on top of the axonal network successfully developed into mature OLs inside the PDMS microfluidic co-culture platform.

2.10. Conclusion

A circular design PDMS microfluidic compartmentalized co-culture platform composed of two compartments connected via arrays of shallow axon-guiding microfluidic channels has been developed. These microfluidic channels allowed both physical and fluidic isolation between the soma compartment and the axon/glia compartment. Fluidic isolation between the compartments was achieved with a 400 μm fluidic level difference between the compartments. Neuron cell bodies and dendrites inside the soma compartment were successfully isolated from the axons growing into the axon/glia compartment. This novel circular design allowed cells to be positioned right next to the inlets of the axon-guiding channel as well as showed enhanced axonal growth characterized by the significantly increased axon coverage ratio inside the axon/glia compartment. The co-culture capability of the device was confirmed by successfully co-culturing OPCs with axons inside the axon/glia compartment that resulted in maturation of OLs. This work has been published in *Biomedical Microdevices*.[89]

III. SIX-COMPARTMENT CNS NEURON/GLIA CO-CULTURE MICRODEVICE*

3.1. Motivation and design

The circular design microfluidic neuron/glia co-culture device in Section II was successfully demonstrated as an efficient tool for studying localized axon/glia interactions. However, the device allowed only one experimental condition to be tested in one device. Considering that 40-60 devices are used for each experimental run lasting about five weeks, with 2-3 replicates for each condition, only 20-30 conditions can be tested at a time. To overcome such low throughput, a novel six-compartment neuron co-culture platform, capable of conducting up to six independent experimental conditions in parallel within a single device occupying the same footprint as the circular design co-culture device (20 x 20 mm^2), has been developed.

The new six-compartment neuron/glia co-culture microsystem is composed of one 7 mm diameter circular soma compartment and six square-shaped satellite axon/glia compartments that are 400 μm apart from the soma compartment (Figure 3.1). The soma compartment and six surrounding axon/glia compartments are connected by arrays of 3 μm high and 20 μm wide axon-guiding microfluidic channels. The device shares the same configuration with the previously introduced circular device for isolation of

*Reprinted with permission from "Micro-macro hybrid soft-lithography master (MMHSM) fabrication for lab-on-a-chip applications" by Jaewon Park, Jianrong Li, Arum Han, 2010. *Biomedical Microdevices*, 12, 345-351, Copyright 2009 by Springer Science.

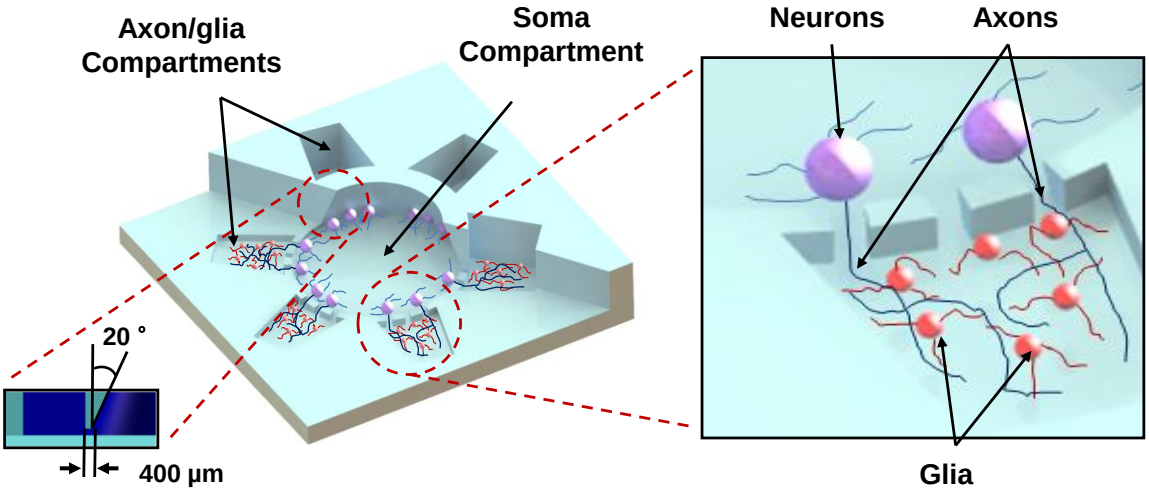

Figure 3.1. 3D Illustrations of the six-compartment CNS neuron co-culture platform (Inset 1: Isolation of axons inside the axon/glia compartment from neuronal soma and dendrites by the axon-guiding channels, Inset 2: Cross-sectional view showing truncated cone shaped soma compartment).

axons. The six axon/glia compartments are fluidically isolated from each other by minute hydrostatic pressure driven flow from the axon/glia compartments to the soma compartment. This allows six independent experimental conditions to be conducted in parallel on a single device.

3.2. Micro-macro hybrid soft-lithography master fabrication technique

3.2.1. Motivation

To fabricate the six-compartment neuron/glia co-culture device using the same fabrication process applied for the circular device, one soma compartment and six axon/glia compartments in the proposed design have to be manually punched out in a single device. However, the soma compartment and the surrounding axon/glia compartments are only 400 μm apart and it is practically impossible to punch compartments via a manual process. Even if the process results in occasional success, the length of the channels connecting the soma compartment and the axon/glia compartments will vary from on device to another since the axon-guiding channel length is determined by the distance between two punched compartments. Using the manual punching process is also very labor intensive. Therefore, a simple fabrication method that is capable of fabricating PDMS microfluidic devices having both macroscale and microscale structures by a single PDMS soft-lithography process without any manual punching step have been developed. The fabrication technique, named micro-macro hybrid soft-lithography master (MMHSM), allowed fabricating neuron co-culture

platforms composed of six axon/glia compartments that are exactly 400 μm apart from the soma compartment at much reduced time.

This novel technique has broader utility in PDMS based microfluidic device fabrication requiring features in both micro-scale and micro-scale. For example, integrated fluidic reservoirs in cell culture microdevices need to hold a certain volume of reagents, samples, or buffers. Therefore, they typically require millimeter scale dimensions not only in the planar direction, but also in the vertical direction, which is a challenging size-scale for most microfabrication techniques. The most commonly used methods for making fluidic reservoirs is manually punching the PDMS device using either blunt needles or punch bits.[89-91] The soft material property of PDMS makes it easier to punch holes on these devices compared to other materials such as silicon, glass or hard polymers. Although this manual process is simple and does not require any sophisticated tools, poor alignment and time consumption make this step a bottleneck when accurate alignment or many reservoirs/devices are needed. Methods such as attaching tubes or pins on the microstructure patterned master molds to define reservoirs or fluidic interfaces in the replicated PDMS devices have been introduced previously, but the processes were still manual and time consuming.[92, 93] The processing step of the proposed MMHSM fabrication technique is simple and significantly reduces the fabrication time. Also, it eliminated misalignment issue associated with the manual punching process, hence enabling high-throughput microdevice fabrication with good batch-to-batch quality control. The MMHSM fabrication technique can be widely used to mass fabricate various high-throughput bio/medical PDMS microdevices at low cost.

3.2.2. Fabrication

Macroscale reservoirs were first machined into a 76.2 x 76.2 mm^2 PMMA block (McMaster-Carr, Atlanta, GA) using a bench-top CNC milling machine (MDX 40, Roland, Irvine, CA). The PMMA block was then sonicated in isopropyl alcohol (IPA) (Sigma Aldrich, St. Louis, MO) for 10 min and dried with N_2 gas to remove residual debris from the milling process. The hot-embossing master that defines arrays of microchannels was fabricated by wet etching a glass slide. Micro-ridge patterns were created on a cleaned Cr/Au deposited glass substrate with a positive photoresist (S1818™, Microchem Corp., Newton, MA) followed by wet etching of the glass substrate in buffered oxide etch (BOE) (J. T. Baker, Phillipsburg, NJ) at room temperature for 5-7 min to obtain 20 μm wide and 3 μm high glass ridge structures. This imprint master was then aligned and hot-embossed against a PMMA block having CNC machined reservoirs to transfer the microridge patterns into the PMMA block as microchannel patterns. The hot-embossing process was conducted at 115°C with 1,082 kPa of pressure for 5 min using a temperature controlled hydraulic press (Specac Ltd., London, UK). A PDMS master was then replicated from this PMMA master by pouring PDMS pre-polymer on the master (10:1 mixture, Sylgard® 184, Dow Corning, Inc., Midland, MI), followed by curing at 85°C for 60 min. The final PDMS device with reservoirs and microchannels was replicated from the PDMS master by a single soft-lithography process, same as described above, and assembled on a PDL coated 6-well culture plate after oxygen plasma treatment (Plasma cleaner, Harrick Plasma, Ithaca, NY)

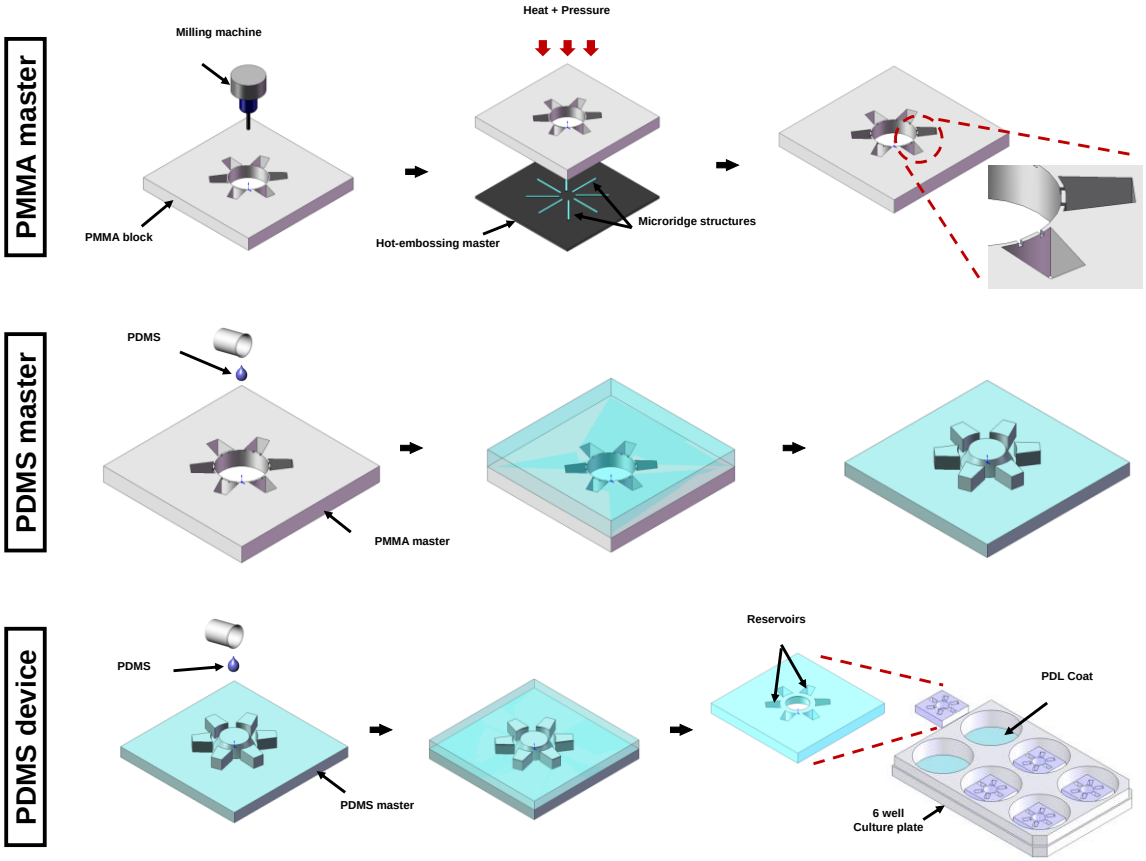

Figure 3.2. Fabrication and assembly steps of the six-compartment neuron/glia co-culture platform.

and ethanol sterilization process. Figure 3.2 shows the overall MMHSM fabrication process.

Figure 3.3 shows the PDMS six -compartment neuron co-culture device showing millimeter-scale compartments connected via arrays of 3 μm high microchannels. It can be seen that microscale channels and macroscale compartment reservoirs were successfully replicated to the final PDMS device. The average width and depth of the axon-guiding microchannels changed from 20.7 ± 1.02 μm and 2.96 ± 0.02 μm (PMMA master), 20.7 ± 1.17 μm and 3.0 ± 0.03 μm (PDMS master) to 20.2 ± 0.25 μm and 3.34 ± 0.06 μm (PDMS device), showing that no significant changes in dimension occurred throughout the process. In addition, the surface roughness changed from 14.20 ± 2.44 nm (PMMA master), 17.95 ± 4.36 nm (PDMS master) to 38.63 ± 7.70 nm (PDMS device) and the device bonding on the PDL coated substrate was not affected by the change from the MMHSM process. The PDMS master was easily released from the PMMA master after the soft-lithography process without any surface treatment of the PMMA master. However, the final PDMS devices firmly adhered to the PDMS master after the curing process and could not be peeled off without damaging the microstructures when no coating was used. In order to facilitate the release process, the PDMS master was vapor coated with (tridecafluoro-1,1,2,2-tetrahydrooctyl) trichlorosilane (United Chemical Technologies, Inc., Bristol, PA) for 10 min and rinsed with IPA to remove excessive coating residues. Chemical treatment of the PDMS master solved the adhesion issue, but the high aspect ratio of the PDMS walls separating

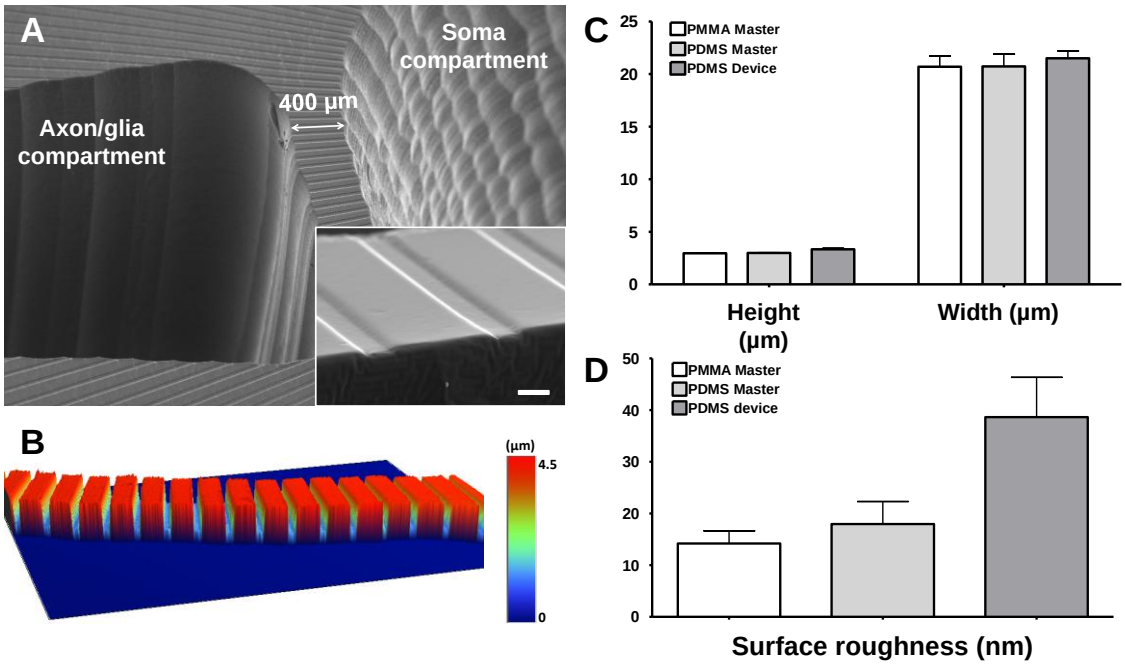

Figure 3.3. (A) SEM images of the PDMS neuron culture device fabricated by the 'MMHSM' technique. Scale bar: 20 µm. (B) 3D reconstructed optical profilometry image of the axon-guiding microchannels connecting the soma and the axon/glia compartment. (C) Average height and width of the axon-guiding microchannels on the PMMA master, PDMS master and the PDMS device (mean ± SD). (D) Changes in surface roughness throughout the fabrication process (mean ± SD).

reservoirs still posed a challenge, and careful attention had to be paid when designing the reservoirs on the PMMA master. When reservoirs were too close from each other compared to the final thickness of the PDMS device, for example when the aspect ratio of the PDMS wall was 9:1, the wall part of the PDMS was torn during the PDMS device replication process.

For the six-compartment neuron co-culture platform, the soma compartment and the axon/glia compartments were only 400 μm apart and it was challenging to replicate a 3.5 mm thick PDMS device from its master without damaging the device. Therefore, the design of the soma compartment was modified from a cylinder shape into a truncated cone shape with sidewalls tilted 20° toward the center (Figure 3.1 lower left inset). This modified structure not only strengthened the PDMS walls separating the compartments, but also facilitated the release of the device. Reservoirs on the PMMA master were engraved using a 0.8 mm square end mill (Roland, Irvine, CA). Only the area where macroscale structures exist was engraved with the CNC milling machine. The rest of the PMMA surface was left intact to preserve the smooth and polished surface to obtain PDMS devices with smooth surfaces. Average surface roughness, measured using an optical surface profilometer (Veeco NT9100, Veeco, Plainview, NY) of the PMMA master and the imprint master before the hot-embossing process was 9.89 ± 0.88 nm and 14.14 ± 1.06 nm respectively. After the hot-embossing process, surface roughness of the PMMA master changed to 14.19 ± 2.44 nm, showing that no significant changes had been made to the surface roughness during the hot-embossing process other than due to the imprint master surface roughness. The results matches well with recent results

reported by Desai *et al.* that multiple self-replications, making a new master from a master fabricated by a soft-lithography process, have little effect on the surface roughness and dimensions of the final replica.[94]

3.3. Tissue dissociation

Neurons were prepared as described in Section 2.4. Primary OLs and astrocytes cultures were prepared from the cerebral hemispheres of Sprague-Dawley rats at postnatal day 1-2 as previously described.[36, 88] Forebrains free of meninges were chopped into 1 mm^3 blocks and placed into HBSS containing 0.01% trypsin and 10 μg/ml DNase. After digestion, the tissue was collected by centrifugation and triturated with the plating medium DMEM20S (DMEM, 20% fetal bovine serum and 1% penicillin-streptomycin). Cells were plated onto PDL-coated 75 cm^2 flasks and were fed with fresh DMEM20S medium every other day for 10-11 days at 37℃ in a humidified 5% CO_2 incubator. The flasks were pre-shaken for 1 hour at 200 rpm to remove lightly attached microglia followed by overnight shaking to separate OLs from the astrocyte layer. The suspension was plated onto uncoated petri-dishes and incubated for 1 hour to further remove contaminating microglia and astrocytes. Purified OLs were then collected by passing through a 15 μm sieve and centrifuged. OLs isolated in this study were primarily OL progenitors (OPCs) and precursors. Astrocytes were purified (> 95%) from the astrocyte layer in the flask after being exposed to a specific microglia toxin L-leucine methyl ester (1 mM) for 1 hour and were sub-cultured one to two times. Astrocytes were purified

(> 95%) from the astrocyte layer in the flask after being exposed to a specific microglia toxin L-leucine methyl ester (1 mM) for 1 hour and were sub-cultured one to two times.

3.4. Axon growth

Primary neurons, loaded into the soma compartment of the co-culture platform at an areal density of 500-1000 cell/mm^2, were cultured healthily for up to four weeks with no toxicity issues. Neuronal somata were successfully confined only inside the soma compartment throughout the culture period due to the shallow height of the axon-guiding microchannels. In contrast, axons from the confined neuronal somata passed through the axon-guiding microchannels and grown into the surrounding six axon/glia compartments, being successfully isolated from neuronal somata. The circular well-type soma compartment enhanced neurons plated inside the soma compartment to position close to the axon-guiding microchannel inlets due to surface tension and radial culture medium flow toward the satellite axon/glia compartments during the cell loading process (Figure 3.4A-B). The average distance of the closest cell from channel inlets was 23.8 ± 12.15 μm (Figure 3.4C). This resulted in increased axon isolation efficiency, and more than 90% of axon-guiding microchannels were filled with axons after two weeks of culture (Figure 3.4D).

The growth of the axons as well as the isolation capability of the multi-compartment neuron-glia co-culture platform was investigated by analyzing the axon coverage ratio (ACR) within the axon/glia compartment (1.6 x 0.8 mm^2, white dotted area in Figure

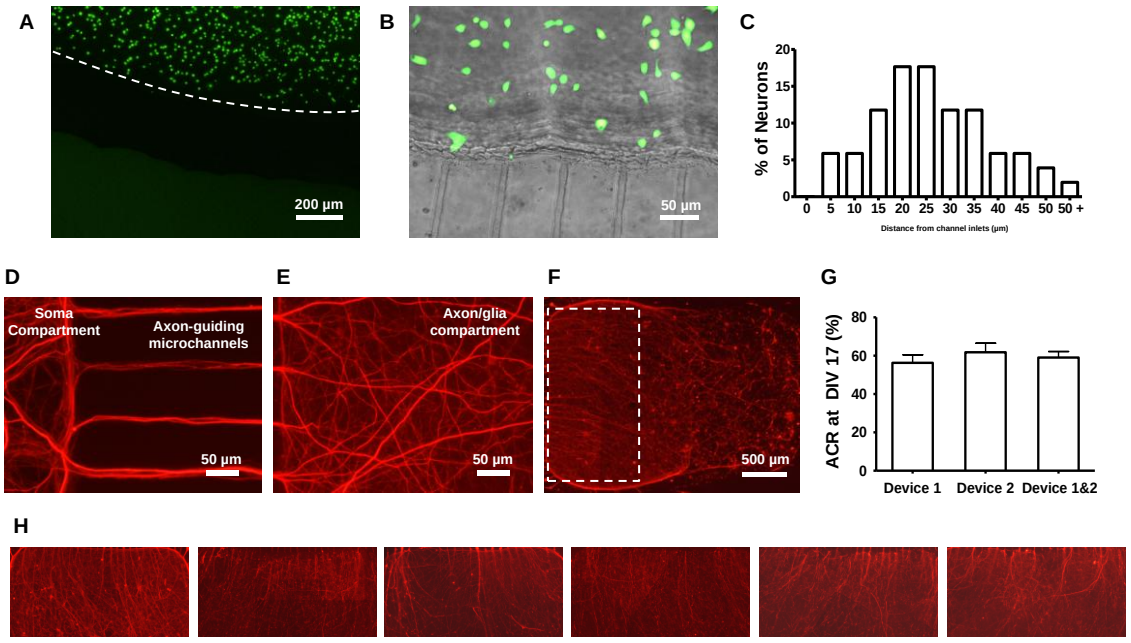

Figure 3.4. (A-B) Calcein-AM (green) stained images of neurons plated inside the soma compartment at DIV 1. (C) Histogram showing the distances of the closest neuron cells from the axon-guiding microchannel inlets. (D-E) Axons passing through the axon-guiding microchannels for isolation. More than 90% of channels were filled with axons and dense axonal layer formed inside the axon/glia compartment after two weeks of culture. (F) Reconstructed image of isolated axons labeled against NF-red inside an axon/glia compartment at DIV 17. White dotted box delineates ACR analyzed area (0.8 x 1.6 mm^2). (G) ACR of the multi-compartment neuron co-culture platform showing device-to-device repeatability and axon/glia compartment-to-compartment variations (mean ± SEM). (H) Isolated axons inside the six axon/glia compartments of a single device (Stained for NF = red).

3.4F). Here, ACR was defined as the percentage of the area covered with isolated axons. Isolated axons started to form dense axonal network layer inside the axon/glia compartments after two weeks of culture (Figure 3.4E) and were fixed and immunostained against neurofilament (NF) at DIV 17 for ACR analysis. Average ACR of the isolated axons inside the axon/glia compartments of the multi-compartment device was 59 ± 10% (mean ± SD, n = 12, Figure 3.4G-H), which is comparable to the previously reported results obtained from a circular neuron co-culture platform.[89] The small ACR variation (around 10%) among multiple axon/glia compartments indicates that the establishment of isolated axonal layer in each axon/glia compartment was uniform and the results from each axon/glia compartment can be directly compared with others.

3.5. Fluidic isolation

In order to carry out multiple localized experimental conditions in parallel to isolated axons for increased throughput, each of the six axon/glia compartment has to be fluidically isolated from each other. During the multiple treatments to isolated axons inside the axon/glia compartments, 80 µl of culture medium was loaded to the soma compartment, while only 15 µl was applied to each of the six axon/glia compartments. The fluidic level difference between the soma compartment and the axon/glia compartments generates small flow from the soma compartment toward the axon/glia compartment and prevents any diffusion or flow of locally treated chemicals or drugs to

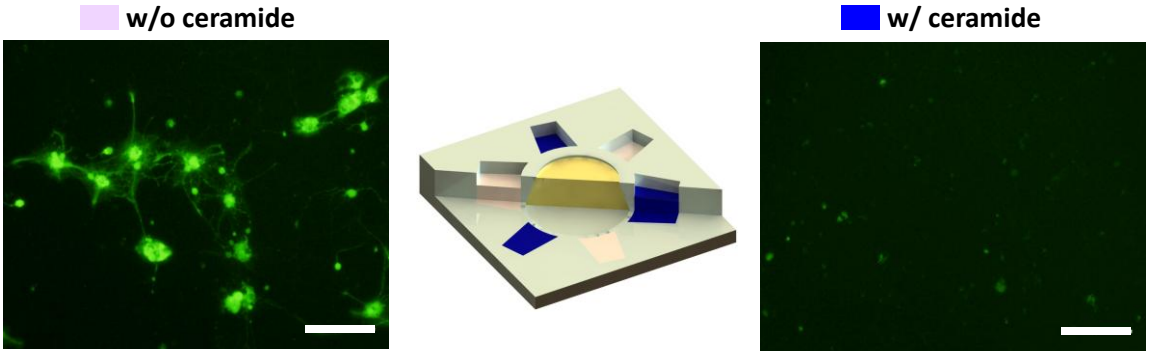

Figure 3.5. Calcein-AM stained fluorescent images of OLs inside the six axon/glia compartments with and without the 150 μM of ceramide treatment. Cell viability checked 6 hours after the treatment. Scale bars: 50 μm.

isolated axons from entering into the soma compartment or the neighboring axon/glia compartments. To demonstrate its parallel performance, OLs inside the six axon/glia compartments were treated with high concentration of ceramide (150 μM: concentration that would cause neuronal cell death). Ceramide is a signaling molecule that regulates cell proliferation, growth, differentiation, and programmed cell death.[95-99] First, OLs from P1-2 rats were cultured inside the six axon/glia compartments at an areal density of 500 cells/mm^2. Ceramide was then added to every other axon/glia compartments as shown in Figure 3.5. OL viability was checked after 6 hours of ceramide treatment by staining cells with Calcein-AM. All OLs in the ceramide treated axon/glia compartments were observed dead, while OLs inside the axon/glia compartments without the ceramide treatment remained unaffected. This indicates that independent culture conditions can be maintained in each compartment and the six axon/glia compartments are fluidically isolated from each other for carrying out multiple experimental conditions in parallel.

3.6. Co-culture of CNS neuron and glia

To study the interaction between the CNS axons and glia cells, OPCs and astrocytes dissected from P1-2 rats were co-cultured on top of isolated axons that have been cultured for two weeks at an areal cell density of 500 cells/mm^2 respectively. Due to non-flow characteristic of the well-type compartment, OPCs and astrocytes were uniformly loaded on top of the isolated axons and the cell density could be accurately controlled. After two weeks of co-culture period, cells were fixed and stained against

neurofilament (NF-red) and myelin basic protein (MBP-green). MBP is expressed only in mature OLs, therefore the expression of MBP is a clear indication that the OPCs successfully differentiated into mature OLs. Regarding the astrocytes, phase contrast images showed nice growth of glia cells and confluent sheath formation of astrocytes; however, fluorescent images revealed that most of isolated axons inside the axon/glia compartments were lost and only thick bundle of axons around the axon-guiding microchannel outlet area could be observed.

Our hypothesis is that this phenomenon may have been caused by the co-cultured astrocytes. Astrocytes tend to stretch out and form sheath layer on the substrate under 2D *in vitro* culture and this property seemed to physically push away previously established axonal layers. In order to verify this hypothesis, three of the axon/glia compartments were loaded with astrocytes and OPCs while other compartments were loaded only with OPCs. As it can be seen in Figure 3.6A-D, isolated axonal layer co-cultured only with OPCs formed dense axonal network layer inside the axon/glia compartment and OPCs cultured on top of axonal layer successfully differentiated into mature OLs, expressing MBP. On the other hand, isolated axons co-cultured with both the astrocytes and the OPCs were again damaged and the remaining axons showed the morphology as if they were pushed toward the axon-guiding microchannel inlet area (Figure 3.6E-G, from lower right toward upper left). In contrast, OPC growth, unlike axons, was promoted by co-cultured astrocytes and more MPB expressed OLs were observed compared to OPCs co-cultured only with axons (Figure 3.6H).

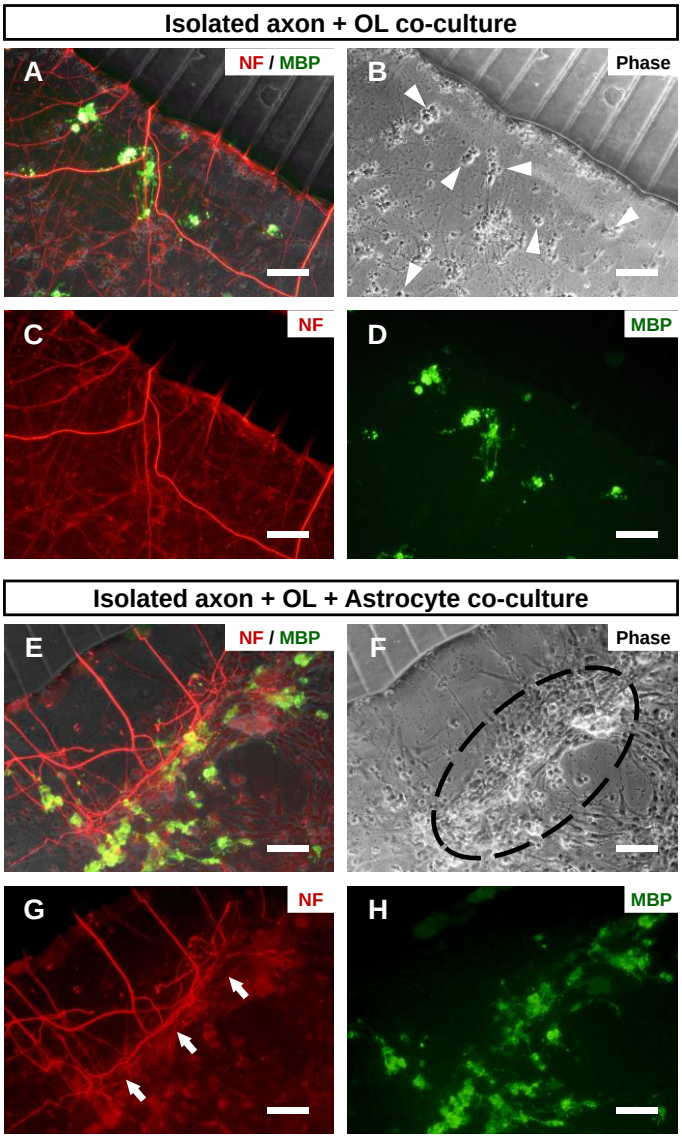

Figure 3.6. Images showing co-cultured axons and glial cells at DIV 27. Isolated axons co-cultured with (A-D) OLs and (E-H) OLs and astrocytes. Co-cultured astrocytes physically damaged established axonal layer while forming sheath on the substrate (White arrow head indicate axons pushed away by astrocyte sheath layer). Axons were stained against NF (red) and mature OLs were stained against MBP (green). Scale bars: 100 μm.

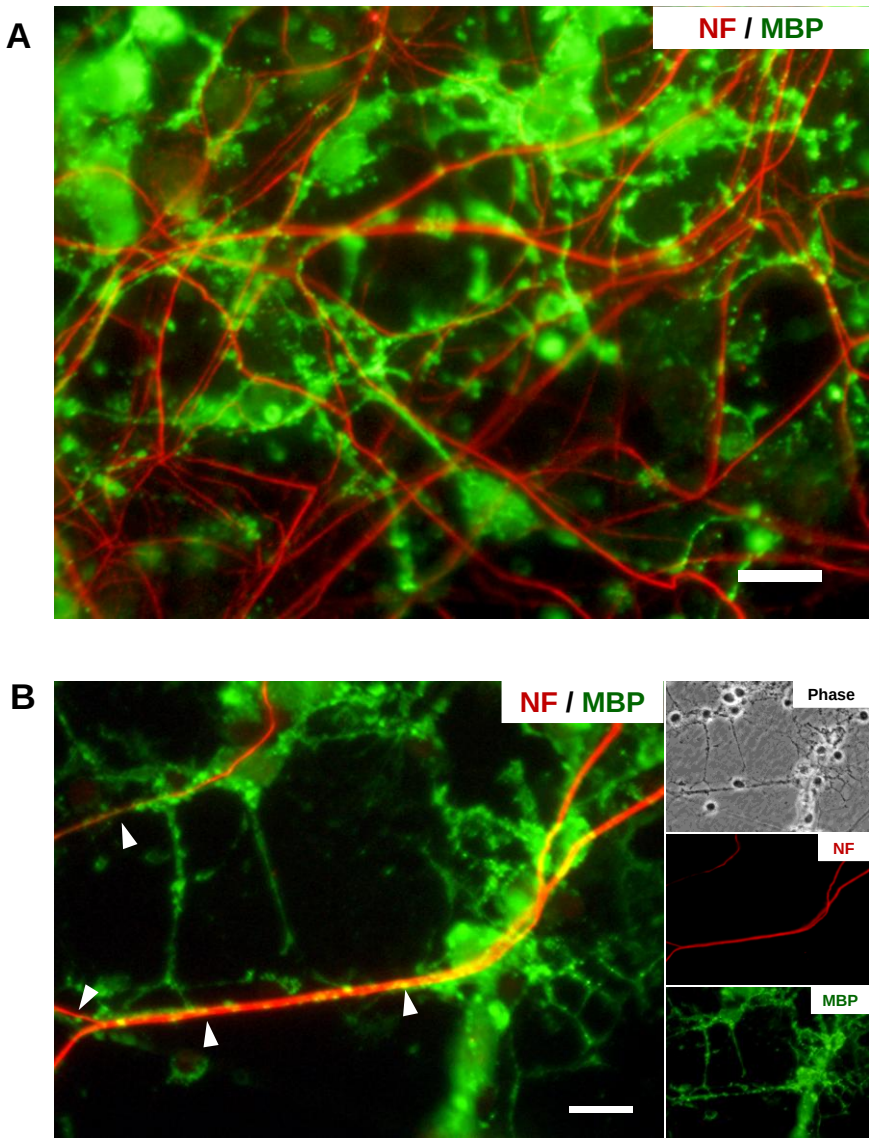

Figure 3.7. Immunostained images of axons and OLs inside the axon/glia compartment at DIV 29. (A) OPCs co-cultured on top of isolated axonal layer successfully differentiated into mature OLs and expressed MBP. (B) Myelinating OLs aligned with co-cultured neighboring axons inside the axon/glia compartment to form myelin sheaths. (White arrow heads indicate OLs aligned with axons to form myelin sheaths). Axon: NF-red, mature OL: MBP-green). Scale bars: 20 μm.

Due to the damage of isolated axon layer inside the axon/glia compartments by astrocytes, only OPCs (2000 cells/mm^2) were co-cultured on top of isolated axons for studying axon-glia interaction and CNS myelination. After two weeks of co-culture, OPCs successfully differentiated into mature OLs, without causing any noticeable damage to isolated axon layers (Figure 3.7A). Among mature OLs, some showed perfect alignment with neighboring axons to form myelin sheath (Figure 3.7B, white arrowhead). Although we did not see robust myelin formation inside the neuron co-culture platform with axon and OPC co-culture, myelinating OLs indicate pre-stage of myelin sheath formation. This also demonstrates that the developed device can be applied for studying CNS axon myelination process to provide more controlled environment.

3.7. Conclusion

We have developed a novel multi-compartment neuron-glia co-culture platform where multiple localized treatments only to axons can be performed on a single device in parallel. The device is fabricated by utilizing the newly developed MMHSM process that allows exact same replicates of PDMS devices having both macroscale and microscale structures to be made in significantly reduced time. Also, the ceramide treatment result to six axon/glia compartments showed that they are fluidically isolated from each other during the parallel localized drug treatments. Glial cells were co-cultured on top of isolated axonal layer inside the axon/glia compartments under several different conditions and revealed that astrocytes physically damage axons when co-

cultured on top of established axonal layer. OPCs did not physically affect the isolated axonal layer and successfully differentiated into mature OLs with some perfectly aligning to neighboring axons as a prelude for myelin sheath formation. Part of this work has been published in *Biomedical Microdevices*.[100]

IV. SIX-COMPARTMENT NEURON CULTURE PLATFORM FOR QUANITATIVE CNS AXON GROWTH AND REGENERATION ANALYSIS

4.1. Motivation

Adult mammalian central nervous system (CNS) cannot be functionally recovered after injury, unlike peripheral nervous system (PNS), and often results in permanent deficits. This is mainly due to the failure of spontaneous regeneration of damaged CNS axons. It has been thought that extrinsic environmental factors such as glia scars or myelin-associated inhibitors dominantly attribute to the suppression of CNS axon regeneration.[101, 102] However, it has been reported recently that neutralization of known axon regeneration inhibitors allows only limited amount of axons to regenerate *in vivo* and that the manipulation of intrinsic axon growth control pathways promotes axon regeneration in CNS.[103-105] This indicates that not only the extrinsic environmental factors but also the intrinsic growth capability of CNS neurons plays a critical role in CNS axon regeneration.

In order to investigate the effects of different molecular factors and drugs in promoting CNS axon growth, precise control over the biochemical environment of cell growth as well as easiness of tracking and quantifying axon growth is necessary. Conventional culture-plate based *in vitro* neuron culture methods however hold several limitations in analyzing the effects of various biomolecular factors or drugs on axon growth. First, in conventional cell culture methods, it is not easy to perform localized

biochemical treatments. In most cases, both the neuronal cell bodies and the axons are treated simultaneously, hence, making it difficult to investigate the influence of biomolecular treatments on either the soma or the axon independently. In brain tissue, axons are often far apart from cell bodies and experience different biochemical environment from the neuronal somata. Therefore, localized biomolecular treatment capability is necessary in understanding detailed mechanisms of axon growth and regeneration. Campenot chamber, first introduced in 1977[58], enables localized treatment of neuron cells. However, as described in the Section II, unstable fluidic seal and complicated assembly process hinders it from being routinely used for CNS axon growth studies. Second, because of the random directional growth of axons, tracking and analyzing the growth of large number of axons over long culture period is challenging. *In vitro* neuron culture typically requires certain areal cell density in order for them to grow properly because of various secretion factors that neurons release.[106] However, conventional axon growth studies are often performed at very low cell density (< 5 cells/mm^2) and that only during very short period.[107] This is mainly due to the technical difficulties in tracking and measuring randomly grown axons that result in intensively tangled network when they are cultured at high cell density. Other analysis methods such as quantitative comparison of proteins involved in axonal growth such as growth associated protein-43 (GAP-43) by western blot is also available but the process requires time consuming and labor intensive preparation steps.[108, 109] Therefore, a neuron cell culture platform that provides physical and biochemical microenvironment isolation of axons from neuronal somata with a means to easily analyze and quantify axon growth

would be an important tool in finding biochemical factors or drugs that promote the intrinsic growth capability of CNS axons.

4.2. Design and fabrication

The microfluidic platform is built on the conceptual framework of our previously developed device that isolates axons in radial directions[110], however has many distinct and novel features. The platform is composed of two poly(dimethylsiloxane) (PDMS) layers; a top culture compartment layer and a bottom axon-guiding microgroove layer (Figure 4.1A). The culture compartment layer has one soma compartment in the center and six surrounding axon compartments that are only 800 μm apart from the soma compartment. The layer is replicated from a PDMS master that has been cast molded from a PMMA master mold, fabricated by a bench-top CNC milling machine (MDX 40, Roland, Irvine, CA). The PDMS master was vapor coated with (tridecafluoro-1,1,2,2-tetrahydrooctyl) trichlorosilane (United Chemical Technologies, Inc., Bristol, PA) and rinsed with IPA prior to the replication for facilitating the PDMS release from the master. The bottom layer was replicated from a SU-8™ (Microchem, Inc., Newton, MA) patterned Si master mold and has arrays of 3 μm deep and 20 μm wide axon-guiding microgrooves. Theses microgrooves connect the soma compartment and the satellite axon compartments. Approximately 70 axon-guiding microgrooves are connected to each of the six axon compartment.

The shallow depth of the microgrooves confines neuronal somata only to the soma compartment during the neuron culture while allowing axons to cross into the

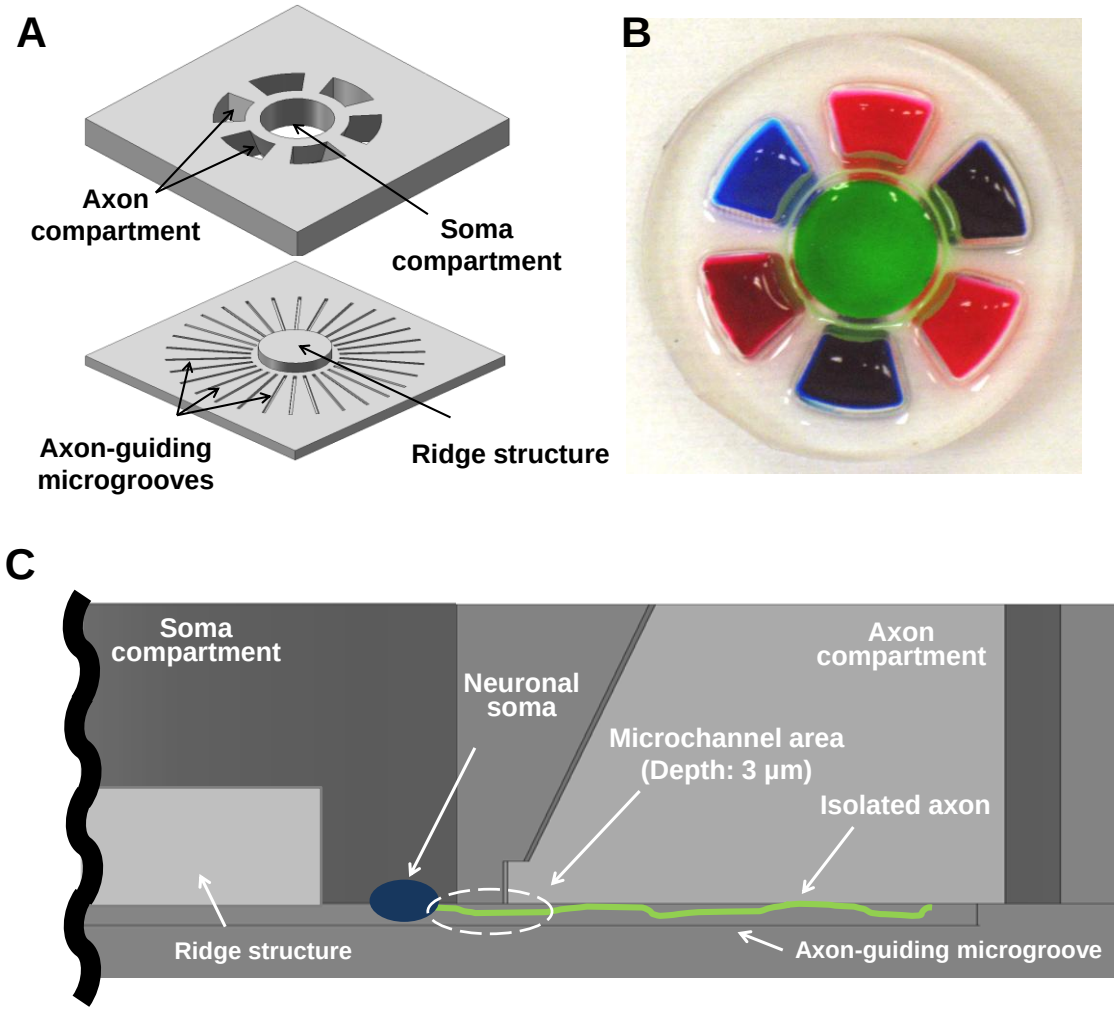

Figure 4.1. (A) Top and bottom PDMS layers composing the multi-compartment neuron culture platform. (B) Photographic image of the PDMS culture platform (45 x 45 mm^2) filled with different color dyes for visualization. (C) Cross-sectional illustration showing axon isolation from neuronal soma by a microgroove (depth: 3 μm, width: 20 μm).

neighboring axon compartments, isolating them from the neuronal somata (Figure 4.1C). These microgrooves, unlike previously reported microchannel-based axon guiding schemes, continue to physically guide axons within the axon compartment. This axon guiding feature facilitates quantitative analyses of axon growth even at high density cultures since axons continue to grow straight inside the microgrooves without tangling with each other. Effects of various localized biomolecular treatments on axonal growth can be directly compared by measuring the length of the straightly grown isolated axons inside the axon/glia compartments. More than 2,000 isolated axons from high density cell culture (2000 cells/mm^2) could be analyzed within two hours using the proposed neuron culture platform.

In order to reduce the number of neurons required per device and to increase the axon isolation efficiency, a cylindrical ridge structure was added at the center of the soma compartment. The ridge structure helped to decrease the number of cells required per device by reducing the surface area of the soma compartment. In addition, it enforced neurons to position close to the microchannels and reflected the axon-growing directions toward the neighboring axon compartments for increased axon crossing efficiency (Figure 4.2A).

4.3. Tissue dissociation and cell culture

Neurons were prepared as described in Section 2.4. Dissected primary neuron cells were loaded into the soma compartment of the device at an areal density of 1000 cells/mm^2 and cultured at 37℃ in a humidified 5% CO_2 incubator. Cells were initially fed with the

plating medium (NBB27 + glutamate) and changed to NBB27 medium at DIV 4. ECMs were diluted in NBB27 medium and locally treated at DIV 7. Half of culture medium was changed out every 3-4 days.

4.4. Axon growth and isolation

The ridge structure decreased the surface area of the soma compartment from 177 mm^2 to 82 mm^2, thereby reducing the number of neurons required to approximately 46% while maintaining the same areal density. It was also effective in enhancing axon crossing efficiency. Efficiency of axons crossing with and without the center ridge structure was compared by counting the number of microgrooves inside the axon compartment filled with axons after 11 days of culture. Axons were successfully guided by the microgrooves and were isolated inside the six axon compartments from neuronal somata for localized biochemical treatments (Figure 4.2B). The isolated axons were stained with Calcein-AM (green) for visualization. The result revealed that more than 91 ± 9% (n = 463) of microgrooves were filled with axons in the presence of the ridge structure, while only 60 ± 16% (n = 434) were filled without the center ridge structure, which is a 50% improvement.

4.5. Fluidic isolation

Axons inside an axon compartment are not only physically isolated from the neuronal somata but also can be fluidically isolated from the soma compartment and other

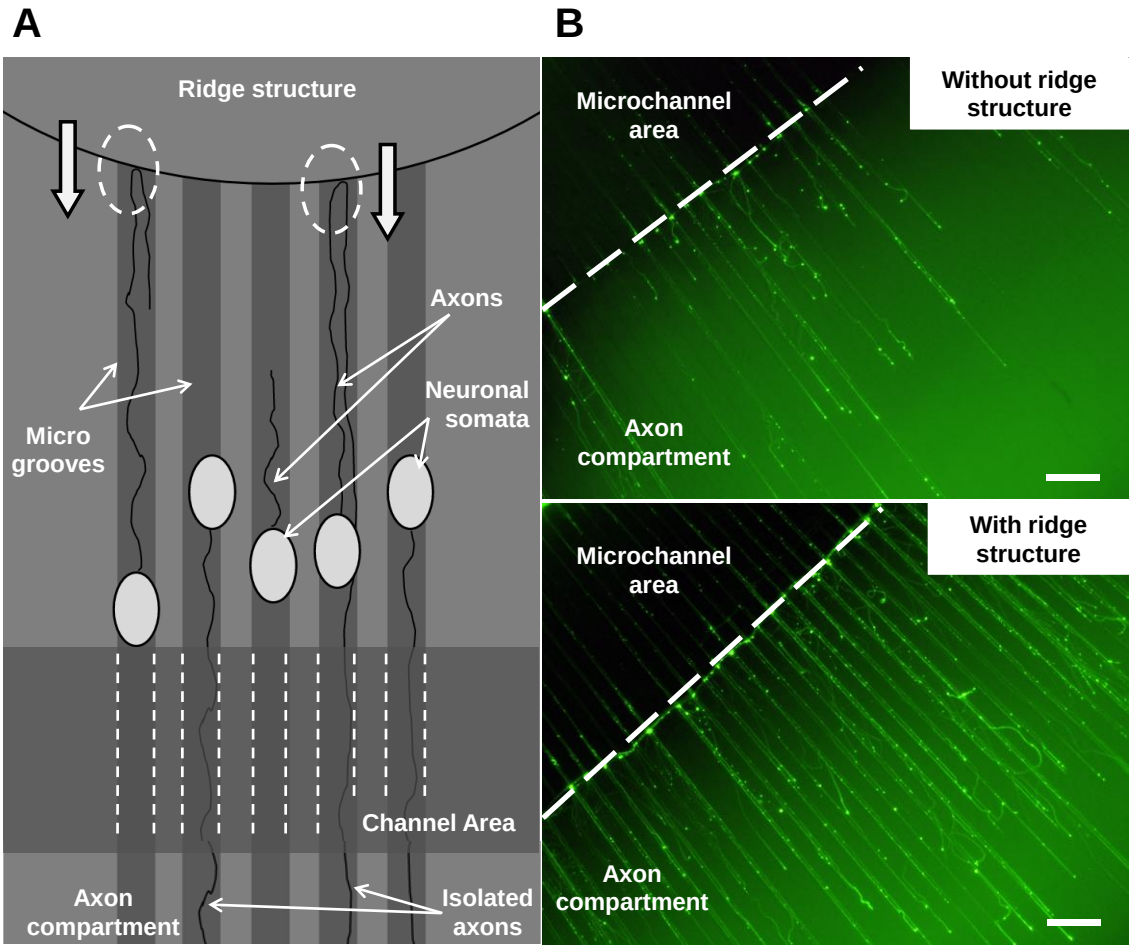

Figure 4.2. (A) Illustration showing axon guidance by the microgroove arrays inside the soma compartment. The ridge structure bounces back axons towards the axon compartment direction, increasing the number of axons crossing into the axon compartment. (B) Isolated and guided axons inside the axon compartment without (top) and with (bottom) the ridge structure. White dotted lines indicate the microchannel and compartment boundary. Scale bars: 200 μm.

neighboring axon compartments for carrying out multiple localized biochemical treatments in parallel. During the localized soma compartment treatment, small but sustained flow from the axon compartment toward the soma compartments, generated by the culture medium fluidic level difference, prevents biochemicals applied to the soma compartments from flowing or diffusing into the axon compartments. In the case of localized axon treatment, the small flow from the soma compartment toward the axon compartments maintains fluidic isolation among the six axon compartments. This allows six different localized biomolecular treatments to isolated axons to be performed in a single device simultaneously for screening drugs or factors that promote axon growth at higher throughput. This fluidic isolation of compartmentalized neuron culture platforms have been demonstrated with the device presented in Section III, as well as by others.[63, 111] The soma compartment was filled with 600 µl of culture media while the axon compartments were filled with 300 µl of culture medium during the localized neuronal somata treatment. For the parallel biomolecular treatments to isolated axons inside the axon compartments, 800 µl and 200 µl of culture medium was applied to the soma compartment and the axon compartments respectively.

4.6. Chondroitin sulfate proteoglycan screening

Fluidic isolation capability of the multi-compartment neuron culture platform having similar design scheme has been demonstrated in Section III by localized ceramide treatment. In order to demonstrate the fluidic isolation as well as the parallel localized

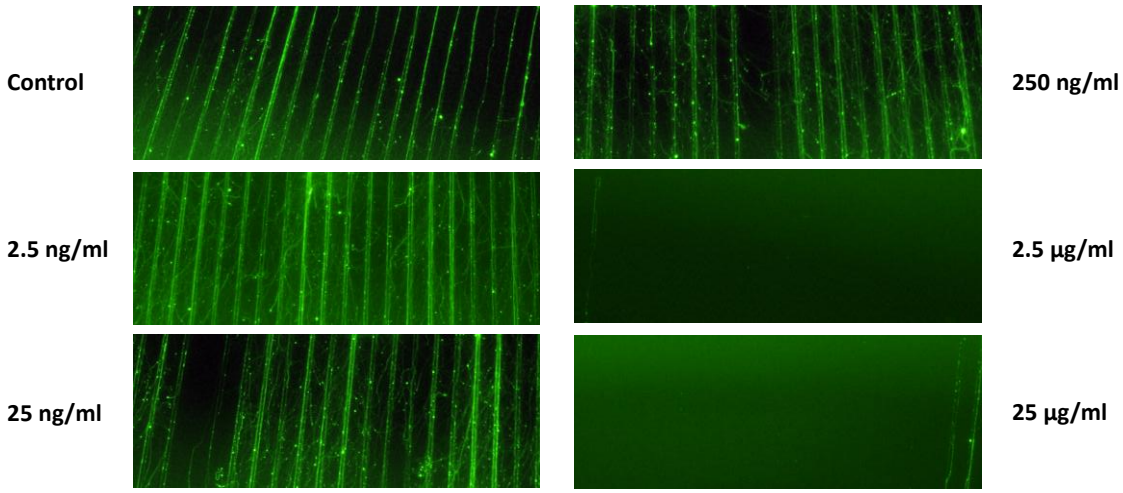

Figure 4.3. Isolated axons inside the axon compartment treated with six different concentrations of CSPG for cytotoxicity concentration screening.

biomolecular screening capability of the culture platform, isolated axons were locally treated with six different concentrations of chondroitin sulfate proteoglycan (CSPG), a protein that is known to negatively regulate axon growth and causes retraction of the established axons.[112] First, neurons were cultured for two weeks for establishing dense isolated axonal layer inside the axon/glia compartments. Six different concentrations of CSPG (0, 2.5, 25, 250, 2500, 25000 ng/ml) diluted in culture medium were then loaded into each axon compartment of a single device. CSPG treated axons were observed under microscope by staining them with Calcein-AM after 72 hours. It has been found that most of isolated axons treated with CSPG concentration higher than 2.5 μg/ml were retracted as it can be seen in Figure 4.3. On the other hand, no noticeable changes were observed to axons treated with CSPG concentration lower than 250 ng/ml. This screening result conveys well with previously reported screening result from conventional cell culture method where CSPG concentration as low as 3 μg/ml was found to be effective in inhibiting neurites outgrowth.[113] Axons inside the axon-guiding microchannels were not significantly affected by the localized CSPG screening in either concentration. This indicates that the CSPG treatment to isolated axons was confined within the axon compartment and the fluidic isolation between the soma compartment and the axon compartments was successfully maintained during the localized screening. The result reflects that the six compartment culture platform is capable of screening biomolecules that promote axon growth at higher throughput.

4.7. Localized extracellular matrix treatment

In order to investigate localized conditions that promote CNS axon growth, CNS neurons cultured inside the six-compartment platform were treated with five different ECMs (CSPG, Matrigel^{TM}, laminin, fibronectin, and collagen). First, effects of localized somata treatment with ECMs were investigated by adding ECMs to the soma compartment at DIV 7. ECMs were diluted in the culture medium to have protein concentrations of 50 μg/ml, with the exception of CSPG (5 μg/ml). Average lengths of the isolated axons inside the axon compartments were measured after four days of treatment to compare the effect of ECM treatments on CNS axonal growth. Average length of the isolated axons was analyzed by measuring the longest grown axons inside the axon-guiding microgrooves using a commercial software (NIS-Element, Nikon Instruments, Inc., Tokyo, Japan) after fluorescently staining axons with Calcein-AM for visualization. Due to the axon-guiding feature of the culture platform, lengths of axons could be easily measured for quantitative analysis. As it can be seen in Figure 4.4, the average length of the isolated axons inside the axon compartments varied by ECMs. Results from three independent experiments showed that laminin, collagen, and Matrigel^{TM} treatments to the neuronal somata promoted axons to grow approximately two fold longer than the control (T-test $p < 0.001$).

To further investigate the effect of locally treated ECM on axonal growth, six different concentrations of collagen (0-100 μg/ml) were treated to neuronal somata. The average length of the isolated axons increased with increasing concentration of collagen,

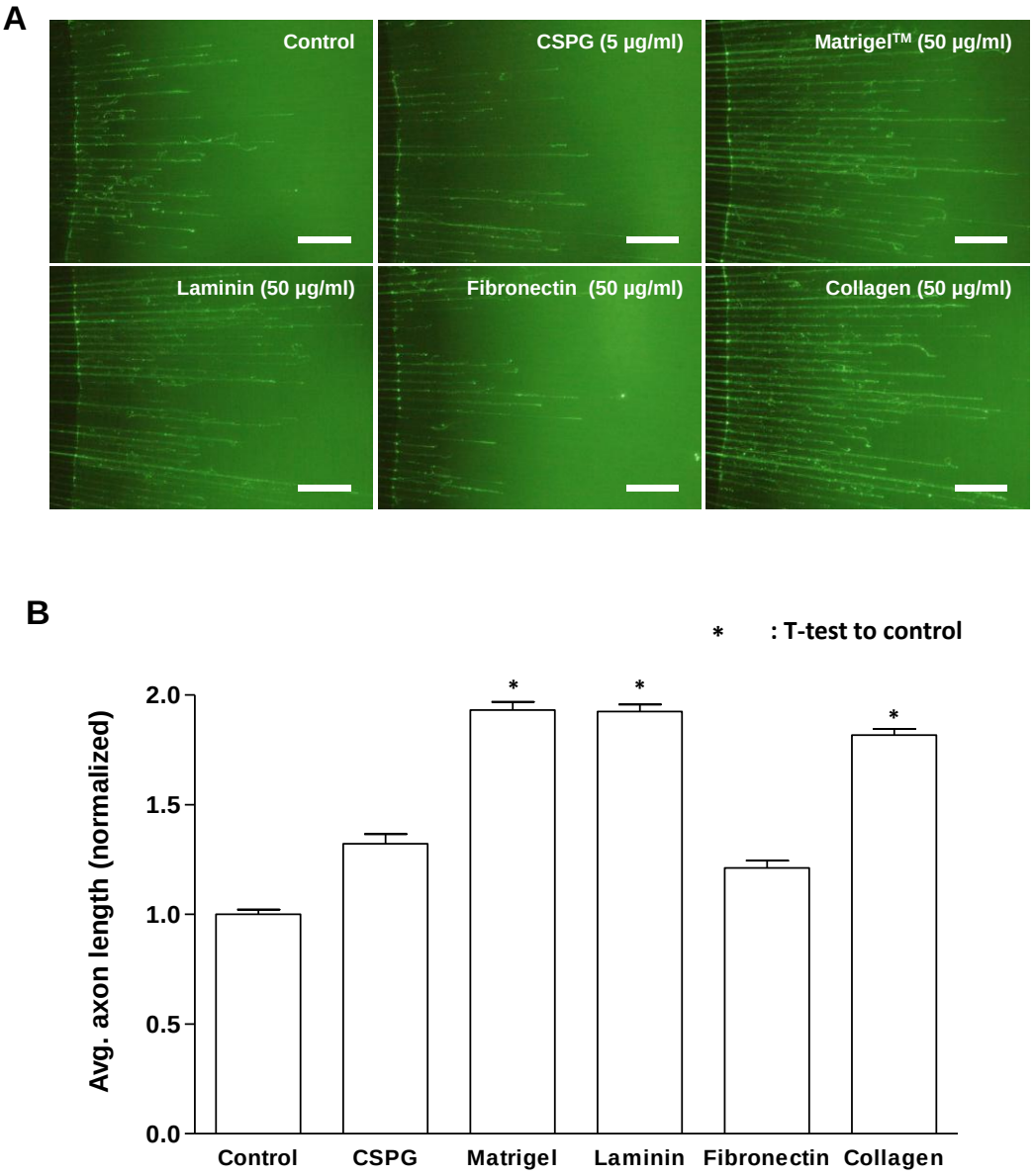

Figure 4.4. Growths of isolated axons after 4 days of localized ECM treatments to the neuronal somata. (A) Fluorescence images of isolated/guided axons inside the axon compartment. Scale bars: 500 µm. (B) Average length of the isolated axons by different ECM treatment (mean + SEM, *$p < 0.001$).

however then started to saturate at around 20 μg/ml. It then sharply dropped with 100 μg/ml of collagen treatment (Figure 4.5). Results that enable direct quantitative axon growth comparison could be obtained by utilizing the multi-compartment culture platform. In conventional culture, quantitatively analyzing the axon growth at DIV 11 with the tested cell density (1000 cells/mm^2) is almost impossible. More importantly, conducting axon growth comparison and analyses between conditions that result in only small but meaningful differences, such as that of 20 μg/ml and 50 μg/ml of collagen treatments as shown in Figure 4.5, is difficult.

Next, to investigate how localized ECM treatments to isolated axons instead of to somata influence the axonal growth, ECMs at 50 μg/ml (CSPG: 5 μg/ml) concentrations were applied to each axon compartment of a single device (Figure 4.6A). With the exception of CSPG, all ECMs were found to promote isolated axons to grow approximately 50% longer than the control. In the case of the neuronal somata treatment, fibronectin was not as effective as other ECMs such as laminin, collagen, or Matrigel™ (Figure 4.4B), but no significant difference was observed when ECMs were locally treated to isolated axons (Figure 4.6B).

Unlike other ECMs, CSPG had significantly different influence whether they were treated to neuronal somata or isolated axons. Although CSPG is known to negatively regulate axon growth, it was not inhibited when only the neuronal somata were exposed to the CSPG, where it actually promoted the growth by about 30% over 4 days of culture. However, direct CSPG treatment to isolated axons completely abrogated axonal growth

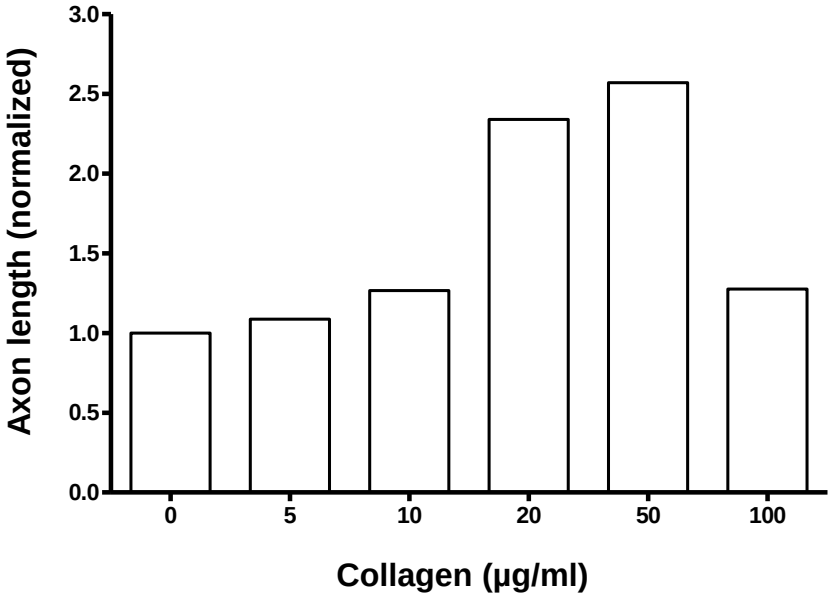

Figure 4.5. Neuronal somata locally treated with different protein concentrations of collagen for screening.

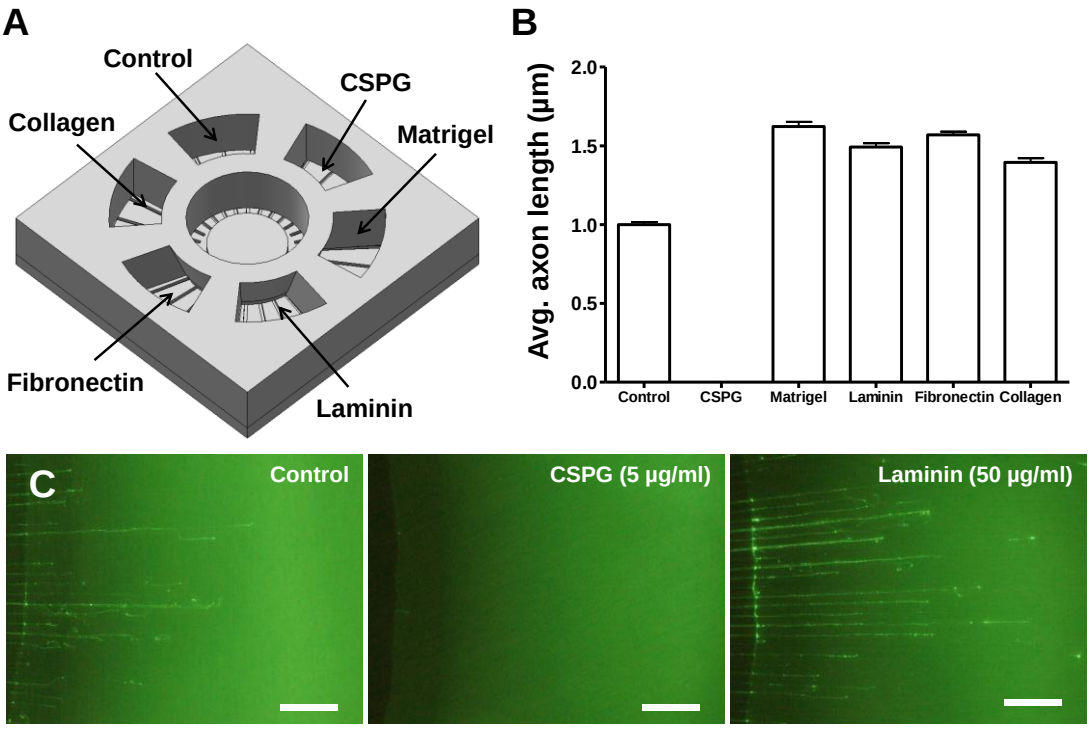

Figure 4.6. (A) Schematic illustration showing localized ECM treatment to the isolated axons using a single device. (B) Average length of the isolated axons by ECM treatment at DIV 11 (mean + SEM). (C) Calcein-AM stained images of isolated/guided axons inside the axon compartments after the ECM treatment. Scale bars: 500 µm.

and caused retraction of the established axons (Figure 4.6C). This is an indication that known biomolecular inhibition or promotion factors need to be further characterized and investigated by devices that enable localized treatment such as the developed multi-compartment culture platform presented here.

4.8. Conclusion

A PDMS CNS neuron culture platform capable of isolating and guiding axons from neuronal somata for quantitative axon growth analysis has been developed. The neuron culture platform successfully demonstrated its capability to physically and fluidically isolate axons from neuronal somata for localized biochemical manipulation to either the neuronal somata or the axons. Parallel localized biomolecular treatment capability of the developed device was demonstrated by locally applying CSPG of six different concentrations to the isolated axons in a single device, and 2.5 μg/ml was screened to be the minimum effective concentration in inhibiting axonal outgrowth. Effects of localized ECM treatments to axonal growth were quantitatively analyzed using the device and revealed that laminin, collagen and Matrigel™ promote the axonal growth the most when applied to neuronal somata. Localized treatment of laminin, collagen and Matrigel™ to isolated axons also promoted axonal growth, but was not as effective as localized neuronal somata treatment. In addition, CSPG treatment to the isolated axons caused complete retraction of the established axon layer while it had limited effect on neuronal somata. The axon guiding feature of the culture platform significantly facilitated the quantitative analysis of axon growths even at high density neuron culture

(1000 cells/mm^2), and more than 2,000 isolated axons could be analyzed within two hours.

V. 24-COMPARTMENT NEURON CULTURE MICROSYSTEM

5.1. Motivation

The six-compartment neuron/glia co-culture device presented in Section III successfully showed six-fold increase in throughput compared to the square or the circular design co-culture platform initially developed (Section II). In order to even further increase the throughput, a microfluidic platform with 24 axon/glia compartments was designed. With increased number of axon/glia compartments, the device can be used for high-throughput drug screening for axon regeneration and degeneration studies. However, designing a 24-compartment co-culture device required more than simply extending the previous six-compartment device into a 24-compartment device by fabricating a co-culture device with 24 satellite compartments. Merely increasing the number of axon/glia compartments with the same configuration as the previously introduced six-compartment device requires tens of pipetting steps per device for changing culture medium or treating drugs, yet the small compartment size (8 x 2.5 mm^2) this step very challenging. Typically, medium is replenished once every 3-4 days in these microdevices. This is a critical bottleneck that needs to be solved before such devices can be truly used as a high-throughput screening tool. Since most experiments require 3-4 replicates for each condition being tested, a culture platform design that enables to manipulate 3-4 compartments with same treatment simultaneously would minimize the manual time consuming pipetting steps. Therefore, a 24-compartment neuron/glia co-

culture microdevice capable of conducting four sets of six different experimental conditions, where culture medium can be exchanged altogether has been developed.

5.2. Design

The schematic illustration of the 24-compartment neuron/glia co-culture microsystem is shown in Figure 5.1. One rectangular open access soma compartment is surrounded by 24 axon/glia compartments. The soma compartment and the neighboring axon compartments are connected via arrays of 3 μm high and 400 μm long microfluidic channels for axon isolation from neuronal cell bodies and dendrites, same as the circular or the six-compartment co-culture devices introduced in previous sections. The 24-compartment co-culture device is composed of three layers. The bottom layer is a cell culture substrate layer with a ridge structure in the center. The ridge structure is slightly smaller than the size of the soma compartment and enforces neurons loaded into the soma compartments to be positioned closer to the microfluidic channel inlets (Figure 5.1B). The middle layer is the compartment layer incorporating axon-guiding microfluidic channels. Two through-holes, one for the culture medium inflow and the other for the culture medium outflow, are made on top of each axon/glia compartment for culture medium exchange (Figure 5.1C). Culture medium outflow holes from each compartment are connected to a medium exchange port through the medium outflow channel patterned on the bottom side of the top layer. The top layer is the culture medium reservoir layer composed of one reservoir for the soma compartment, six

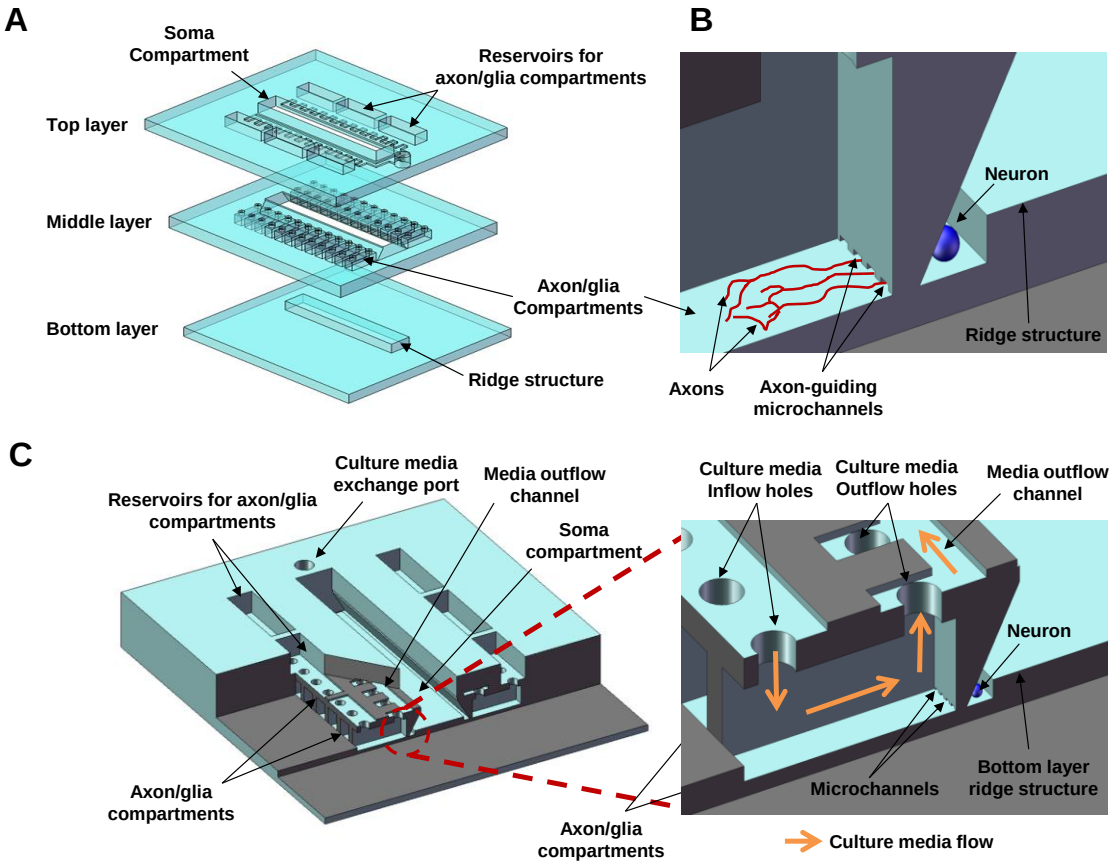

Figure 5.1. (A) Three layers composing the 24-compartment neuron/glia co-culture microdevice. (B) Illustration showing axon isolation from neuronal soma by microfluidic channels. (C) Overall illustration of the device (Inset: Close-up view of the axon/glia compartment showing culture medium flow during culture medium exchange process).

reservoirs for the axon/glia compartments, a medium outflow channel, and a medium exchange port. Using this design, six different conditions of culture medium can be loaded to each axon/glia compartment reservoir covering four axon/glia compartments. A negative pressure is applied to the culture medium exchange port, driving the culture medium inside the six axon/glia compartment reservoirs into the 24 axon/glia compartments. Used culture medium inside the axon/glia compartments is aspirated out via the culture medium outflow holes and collected at the culture medium exchange port (Figure 5.1C). This enables six different conditions of experiments with four sets of replicate to be performed in a single device while minimizing the number of pipetting steps for medium change and drug treatment.

5.3. Fabrication

The 24-compartment co-culture device is composed of three PDMS layers. The top and the bottom layers are replicated from PMMA masters that are fabricated by a CNC milling machine (MDX 40, Roland, Irvine, CA). The middle layer that incorporates 24 axon/glia compartments, one soma compartment, and a microfluidic channel array, is fabricated by the MMHSM fabrication technique shown in Section III. Compartments are first defined on a PMMA block using a CNC milling machine and the imprint master is hot-embossed against the PMMA block to transfer the microchannel patterns. The imprint master which has array of 3 μm high and 20 μm wide microridge structures was fabricated by anisotropically etching a Si wafer in a 40% KOH solution at 60°C. A

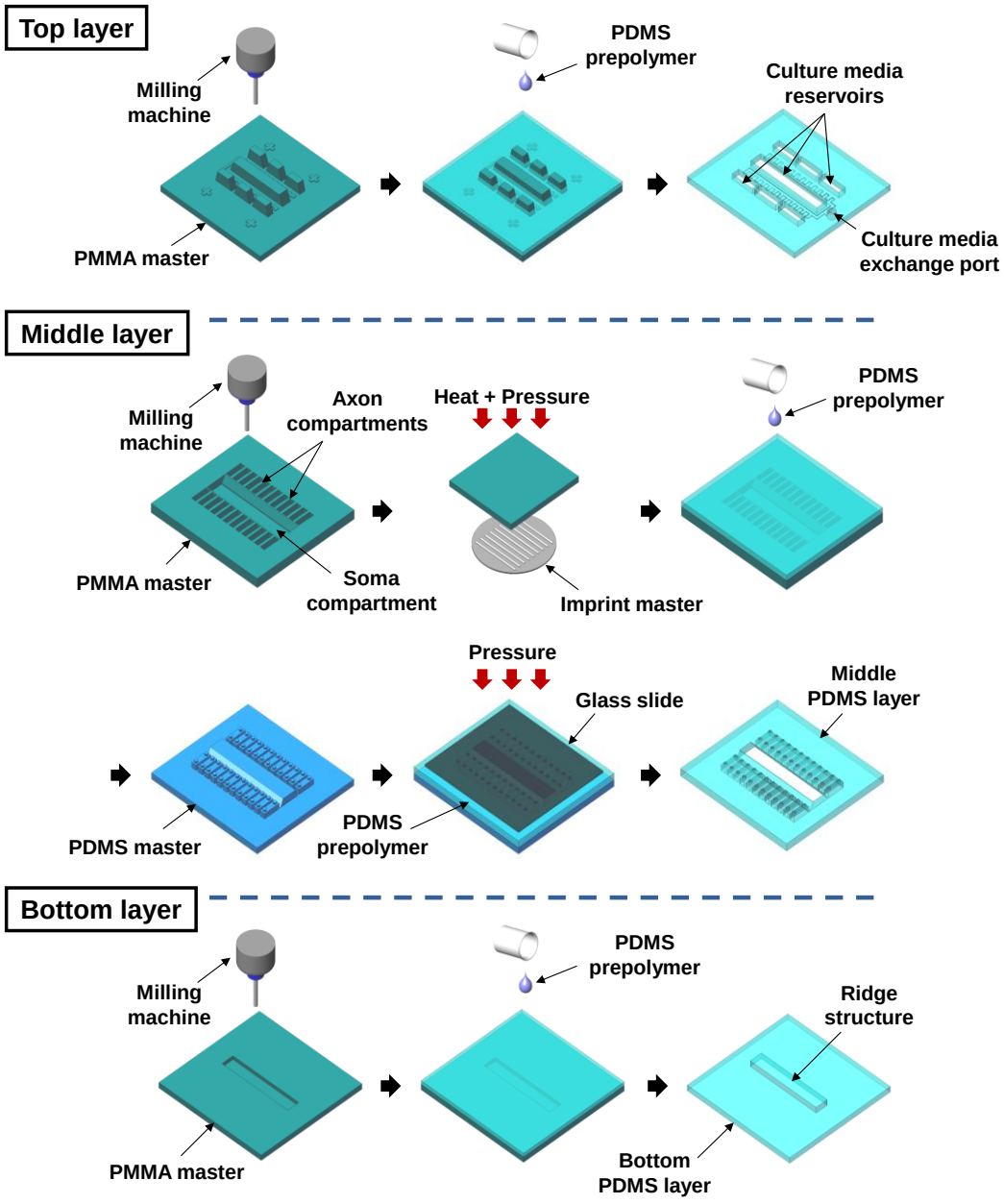

Figure 5.2. Fabrication process for the 24-compartment neuron/glia co-culture microdevice.

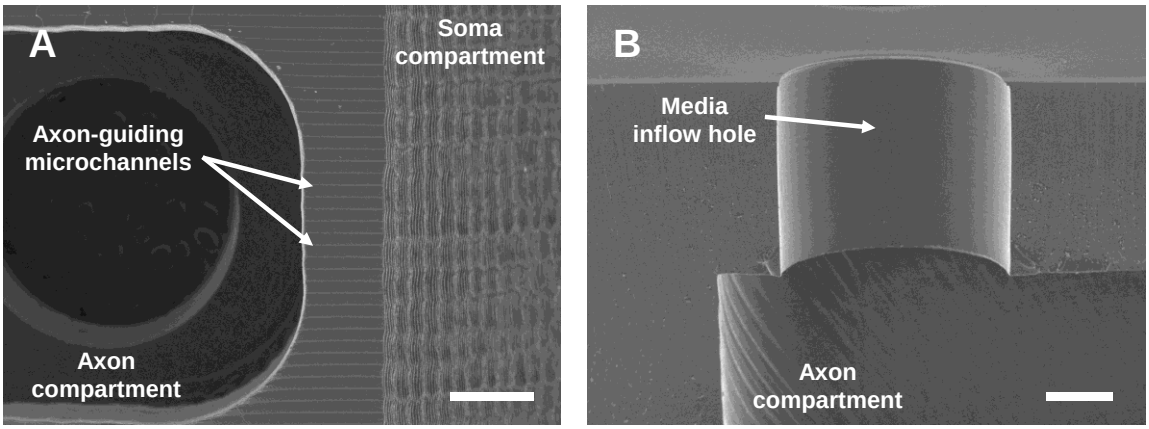

Figure 5.3. SEM images of the PDMS device. (A) Bottom side of the compartment layer showing the soma compartment and the axon compartment connected via arrays of axon-guiding microchannels. (B) An axon compartment showing culture medium inflow hole. Scale bars: 500 μm.

silicon nitride layer patterned by photolithography and RIE processes was used as the etch mask during the Si wet etching process. The silicon nitride etch mask was patterned at a 45° angle to the primary flat of the (100) wafer, resulting in microridge structures with vertical side walls when the silicon was etched in KOH.[114] The three PDMS layers were then exposed to oxygen plasma and assembled. The overall fabrication process is shown in Figure 5.2.

Using the MMHSM fabrication technique, 3.5mm high compartments connected by 3 μm high and 400 μm long microchannels could be replicated in significantly reduced time with great reproducibility as demonstrated in Section II. Through-holes on the top part of the axon compartments were made by covering the PDMS master with a glass slide coated with (tridecafluoro-1,1,2,2-tetrahydrooctyl) trichlorosilane (United Chemical Technologies, Inc., Bristol, PA) and applying constant pressure (0.43 kPa) during the PDMS polymerization process. As it can be seen in Figure 5.3, holes were clearly defined and a time-consuming manual punching process was not necessary.

5.4. Tissue dissociation

Neurons were prepared as described in Section 2.4.

5.5. Axon isolation

Neurons were added into the soma compartment at an areal density of 1000 cells/mm^2 and were cultured at 37°C in a humidified 5% CO_2 incubator. Neurons were

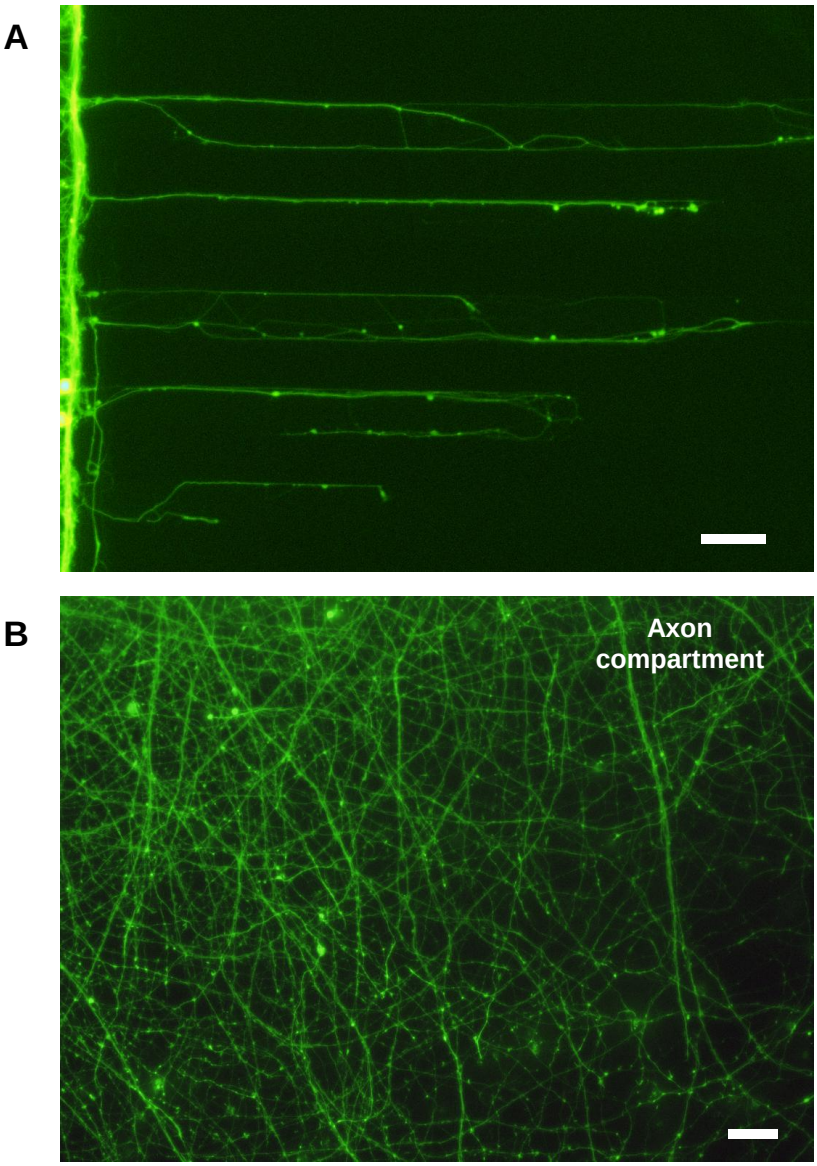

Figure 5.4. (A) Axons inside arrays of axon-guiding microchannels crossing into the neighboring axon compartment. (B) Isolated axonal layer inside the axon compartment of the 24-compartment neuron culture microdevice after two weeks of culture. Cells were stained with Calcein-AM for visualization. Scale bars: 50 μm.

successfully cultured inside the 24-compartment PDMS neuron culture platform without any toxicity issues and axons differentiated from neuronal somata crossed axon-guiding microchannels into the neighboring axon compartments for isolation (Figure 5.4A). After 14 days of culture, axons formed intense axonal layer inside the axon compartments and were ready for localized drug or biomolecular treatments (Figure 5.4B). Cells were stained with Calcein-AM for visualization and only axons were observed inside the axon compartment, demonstrating the axon isolation capability of the microdevice

5.6. Conclusion

A novel compartmentalized neuron culture platform composed of 24 axon compartments for performing multiple conditions of experiments in parallel has been developed. Neurons cultured inside the soma compartment grew inside the culture platform and axons from neuronal somata were successfully isolated inside the neighboring 24 axon/glia compartments. In addition, culture medium in the 24 axon /glia compartment could be changed out all together by a single pipetting step via the culture medium exchange port on the top layer. The axon isolation capability combined with the one-step culture medium replenishing feature make this device a true high-throughput cell culture microsystem and allow this device to be used not only for high-throughput screening of potential drugs that promote CNS axon degeneration/regeneration, but also for co-culturing isolated axons with glial cells to study axon-glia interactions.

VI. NEURAL PROGENITOR CELL AGGREGATE CULTURE MICROSYSTEM FOR CNS MYELINATION STUDY

6.1. Motivation

The function of the central nervous system (CNS) is critically dependent on proper physical and biochemical signaling and interactions among various cells and biomolecules at precise time and location during the development. For example, myelination is a sequential and multi-step process that requires reciprocal signaling between neurons and oligodendrocytes (OLs), the cells that produce myelin sheath, as well as other cells such as astrocytes in the CNS. Conventional two-dimensional (2D) cell culture in plastic plates has not been successful in proper functional growth of neural cells of the CNS. This lack of *in vitro* models that closely recapitulate the major events during CNS development has been a major roadblock in understanding the underlying mechanisms and regulating signals, as well as easy accessibility for drug testing.

In several areas including tissue engineering, stem cell biology, and cancer biology, it is now generally accepted that a three-dimensional (3D) cell culture provides a more *in vivo* like culture environment and results in more physiologically relevant functional development of living tissues and cells. Such 3D culture models also have more physiologically relevant responses, and are being considered as better model systems for drug discovery applications.[73-76] Recently, Koito *et al*. introduced a novel CNS neural progenitor aggregate culture system prepared from embryonic rat forebrains as an *in vitro* 3D model system to study neural development myelination.[79] Myelin was

generated much more robustly in aggregate cultures than those of conventional dissociated cultures where myelination was rarely observed. It has been assumed that the 3D nature of the aggregate culture system provides a microenvironment that closely mimics those of *in vivo*, and thereby enables proper development and differentiation of neural progenitors into mature neurons and glia. However, the extent of myelination in the current *in vitro* aggregate model system shows large dependency and variability on many factors that are difficult to control by conventional culture methods and not well understood, including the sizes of aggregates, the distance and axonal connectivity among aggregates, and glia lineage cell development, to name a few.

Therefore, we have developed a novel microfluidic *in vitro* 3D CNS neural progenitor cell aggregate model system that recapitulates major neural development processes. The system exhibits exquisite capabilities for spatial and temporal manipulations of aggregates, such as formation and position of large numbers of mono-disperse aggregates with predetermined dimensions, generation of 3D cultures, and treatment with biomolecules. In addition, establishing a true 3D co-culture environment will be a possibility where spatially patterned neural aggregates can be surrounded by glia cells in a 3D space through glia-extracellular matrix (ECM) mixture loading into the microfluidic system. Such 3D culture system could be broadly used for screening and investigating factors that play critical roles in various neurodevelopmental processes, leading to mechanistic understanding of these processes and to new therapeutics development.

6.2. Material and methods

6.2.1. Aggregate formation

Neural progenitor aggregates were prepared using two different methods, the spontaneous aggregates and the coerced aggregates. Spontaneous aggregates were prepared by suspending dissociated neural progenitor cells in a non-coated cell culture plate. Cells were resuspended inside the culture plate by manually pipetting them once a day for 3 days. Suspended neural progenitor cells spontaneously form aggregates after 3 days. Suspended cells were then filtered with 100 μm and 70 μm cell strainers to obtain 70-100 μm diameter neural aggregates. Spontaneously formed aggregates showed dense axonal and neurites growth and showed robust formation of myelin *in vitro*[79]; however, the size of spontaneously formed neural aggregate were not uniform and the number of myelin sheath formed in the culture showed dependency on the size of the aggregates. In order to generate neural aggregates with uniform size, dissociated neural progenitor cells were loaded inside array of microwells to form coerced aggregates (Figure 6.1). Array of microwells were fabricated by PDMS soft-lithography from a SU-8™ patterned Si master mold and were treated with oxygen plasma prior to adding cells to facilitate cell loading into microwells. After 3 days, neural progenitor cells inside the microwells formed spherical aggregates of uniform size and were collected for use.

6.2.2. Device design

The 3D CNS neural progenitor cell aggregate culture platform is made of a PDMS layer assembled on a glass coverslip and is composed of 4 culture chambers that are 150 μm

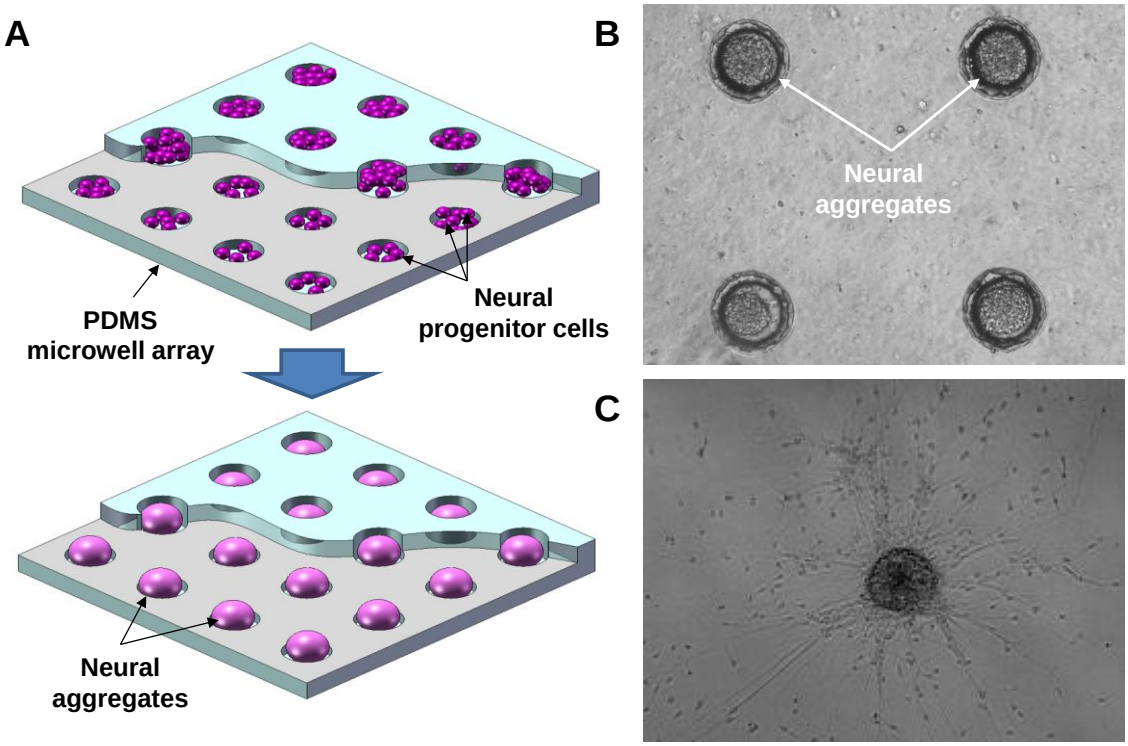

Figure 6.1. (A) Illustration of the coerced aggregate forming procedure. (B) Neural progenitors forming aggregate inside the microwell array. (C) Single aggregate showing neurite outgrowth (DIV 5).

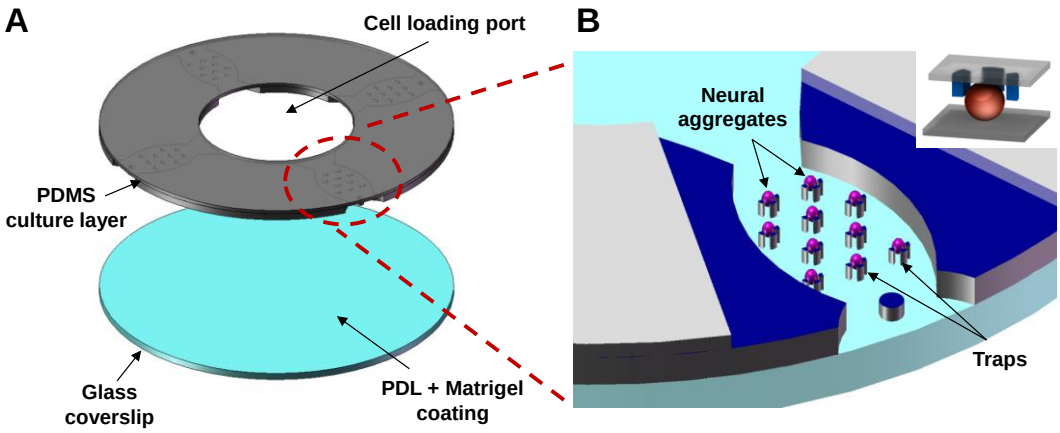

Figure 6.2. (A) Schematic illustration of the 3D neural progenitor aggregate culture platform. (B) Cross-sectional view of a culture chamber having 10 aggregate traps (Inset: A neural aggregate captured at a trapping site).

in height (Figure 6.2A). Each culture chamber has 10 aggregate trapping sites (400 μm trap-to-trap distance) composed of three pillar structure that connect the top and bottom of the culture chamber (Figure 6.2B). Culture chambers were initially designed to have 100 trapping sites per chamber, however degradation of axon bundles and loss of glial cells around the neural aggregate was observed after two weeks of culture (Figure 6.3). This was mainly due to extremely high concentration of cells per device that resulted in insufficient nutrient supply. Therefore, the number of traps per culture chamber has been reduced to 10%. In order to optimize the size and the design of the trapping sites, a commercial finite element method (FEM) simulation tool (COMSOL Multiphysics®, Inc., MA) was used to analyze the fluidic flow inside the culture chamber. Simulation results show that the fluidic flow inside the chamber is minimally interfered by the optimized trapping structures (Figure 6.4).

6.2.3. Fabrication and assembly

PDMS cell culture layer is replicated by soft-lithography from a PDMS master that has been cast molded from a SU-8™ patterned Si master mold. The cell culture layer having arrays of trapping structures was fabricated by multiple PDMS soft-lithography process because it was not easy to replicate high aspect ratio (HAR) trapping structures directly from the Si master mold. Using the multiple replication process, PDMS cell culture layer with HAR pillar structures could be successfully fabricated (Figure 6.5). The cell culture layer was then assembled on a glass coverslip after oxygen plasma treatment followed by autoclaving 30 min for sterilization.

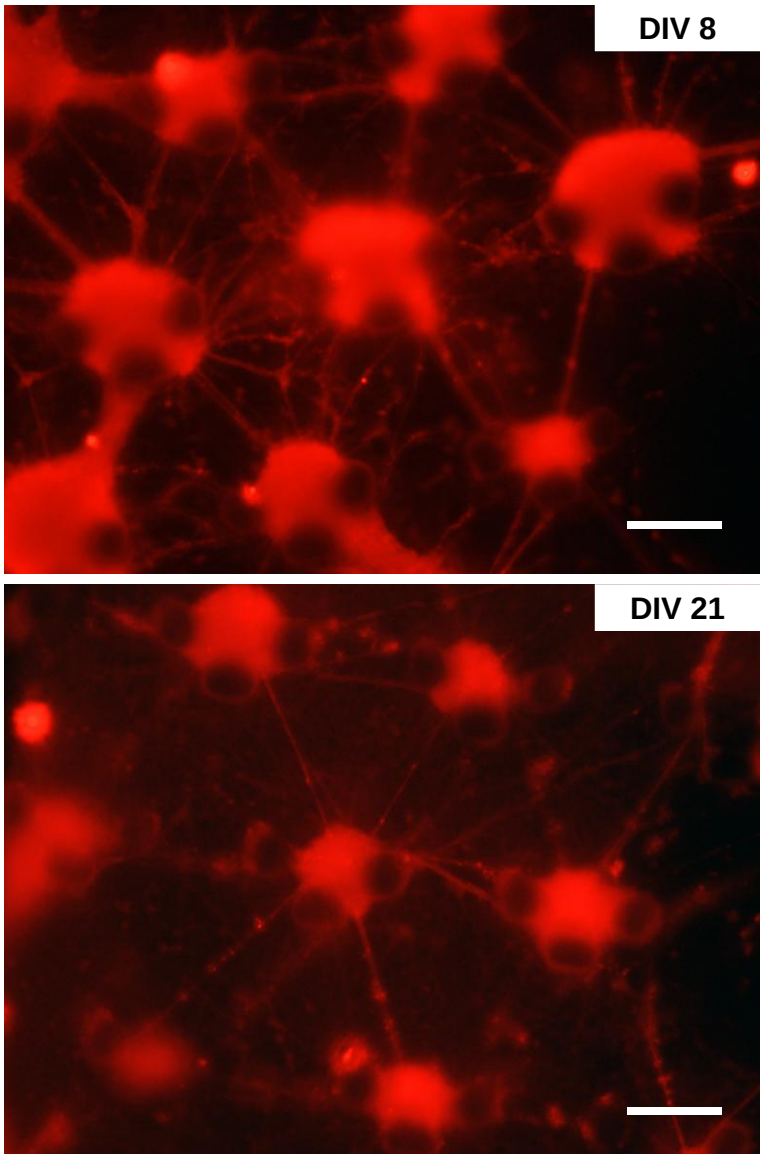

Figure 6.3. Fluorescently labeled (NF-red) images of neural aggregates captured inside the trapping structures. Axons grown from neural aggregates start to degrade after two weeks of culture inside the culture chamber having 100 trapping sites. Scale bars: 100 μm.

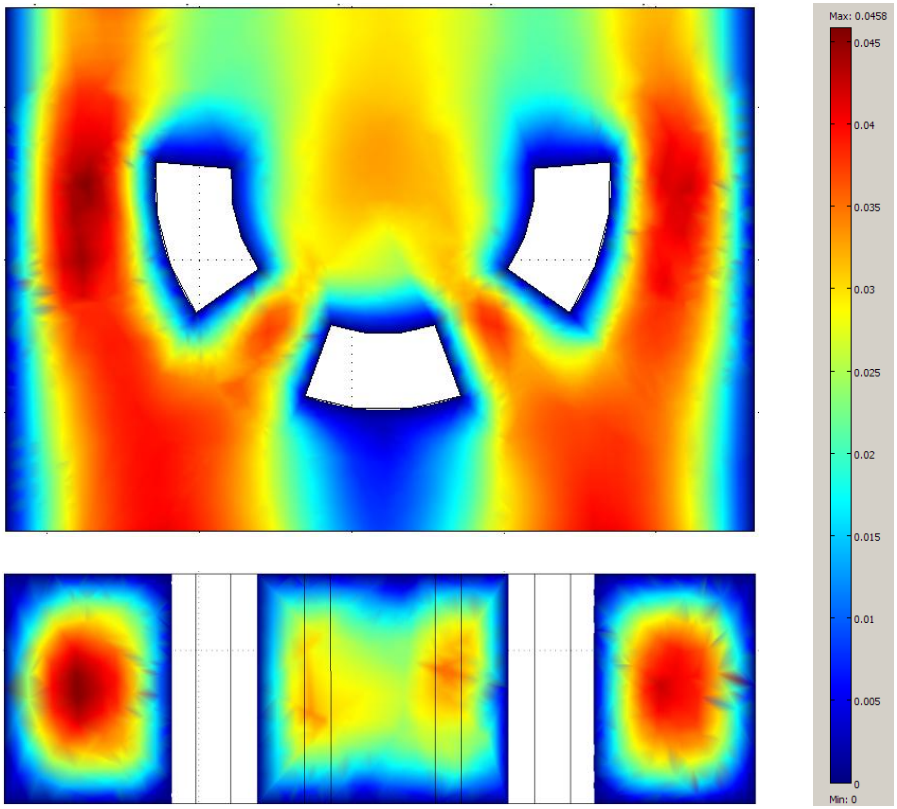

Figure 6.4. FEM simulation (COMSOL Multiphysics®) showing the velocity field around the aggregate trapping site. The fluidic flow inside the chamber was not obstructed by the trapping sites, indicating that cells will be captured at each trapping site during the cell loading process.

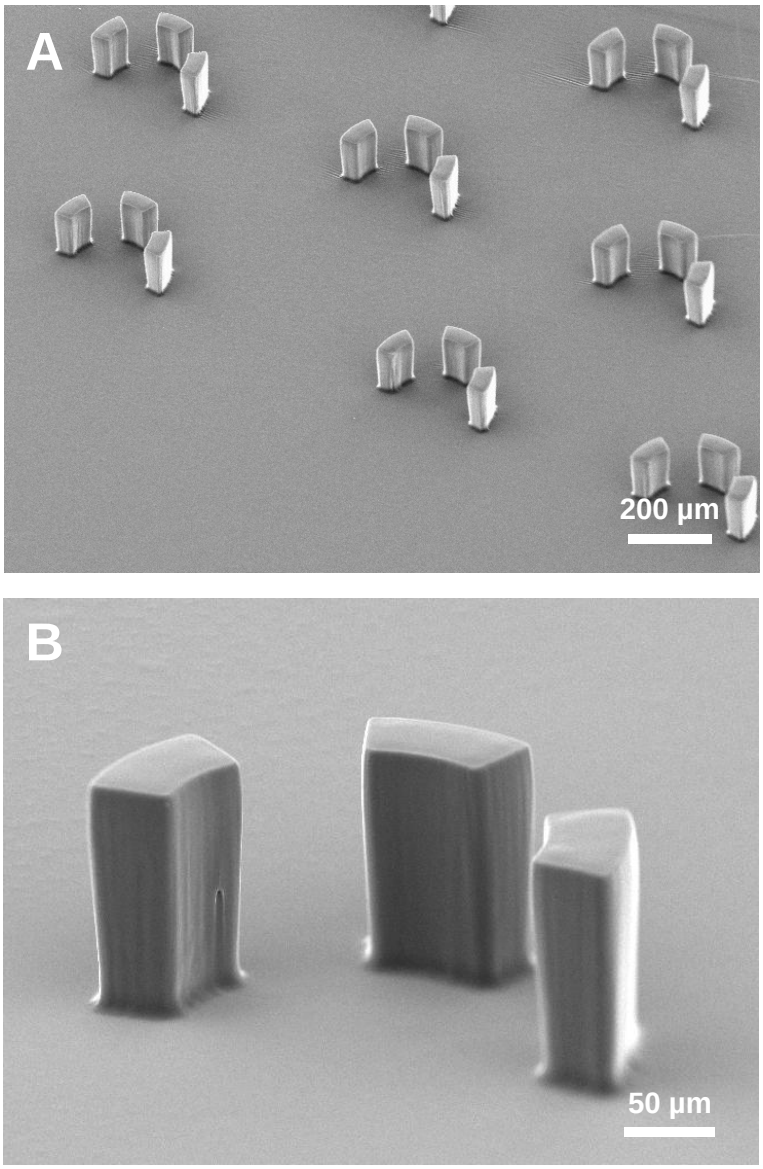

Figure 6.5. (A) Scanning electron microscopic image of PDMS cell culture chamber showing array of traps. (B) Close-up image of a single trap composed of three pillar structures.

6.3. 3D neural aggregate culture

Prepared neural aggregates were loaded into four culture chambers simultaneously via the cell loading port at the center of the device and were trapped at each trapping site for culture of up to 4 weeks. Glass coverslip substrate was coated with PDL prior to aggregate loading for promoting cell adhesion to the substrate. The aggregates successfully attached to the substrate but showed almost no axon growth even after two days of culture (Figure 6.6A). In order to promote the cell growth, Matrigel™ was additionally coated on top of the PDL coat. As it can be seen in Figure 6.6B, the Matrigel™ coat significantly enhanced the cell growth and dense neurite outgrowth could be observed.

Captured aggregates were cultured for 2 weeks prior to drug treatments for establishing dense axonal layer and glial cell development. As indicated by the white dotted circles in Figure 6.7, glial cells started to migrate from the neural aggregate at DIV 4 and high density of glial cells could be observed around the neural aggregate at DIV 11. After two weeks of aggregate culture inside the device, dense axonal network mixed with glial cells was formed inside the culture chambers. At DIV 16, cells were fixed and immunostained for neurofilament (NF-red) and myelin basic protein (MBP-green). As it can be seen in Figure 6.8, neural aggregates formed intense axonal networks inside the culture chamber and thick bundles of axons connected neighboring aggregates. Also many MBP expressing OLs (shows as green) were observed both inside and outside of the neuron aggregates. Since MBP is expressed only in mature OLs, this result

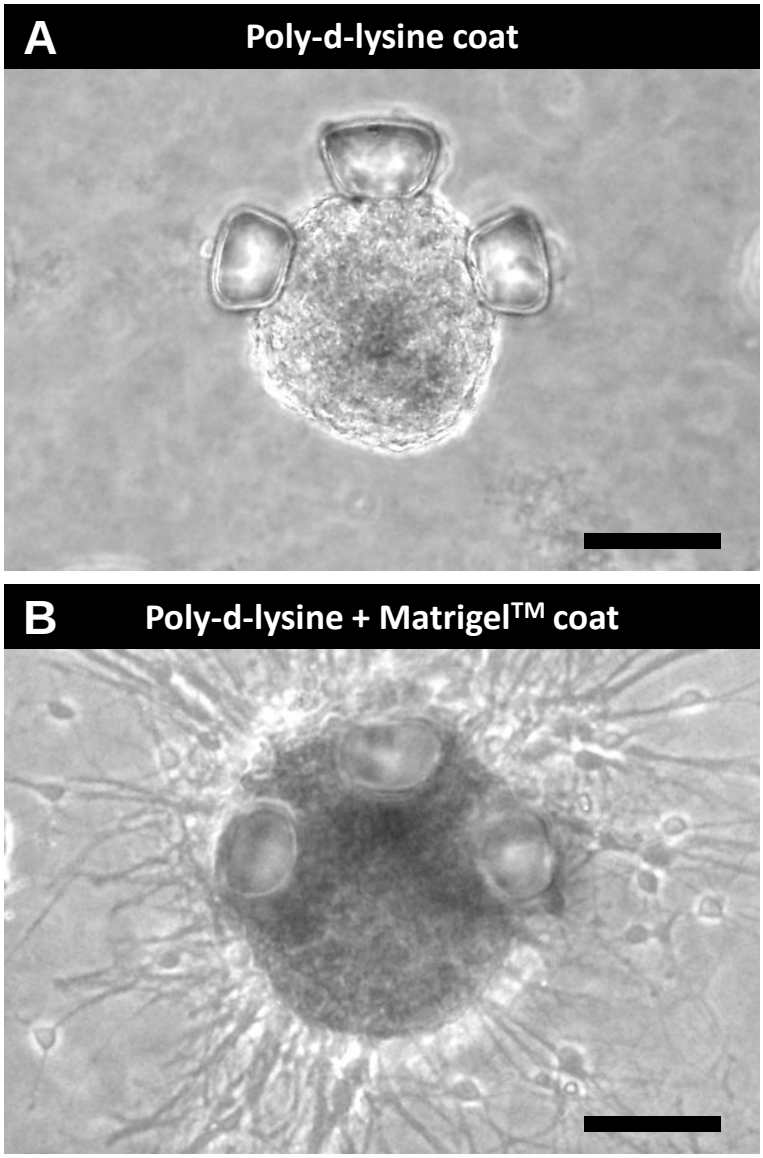

Figure 6.6. Neural progenitor aggregate captured and cultured inside a trapping structure with different substrate coatings at DIV 5. Scale bars: 100 μm.

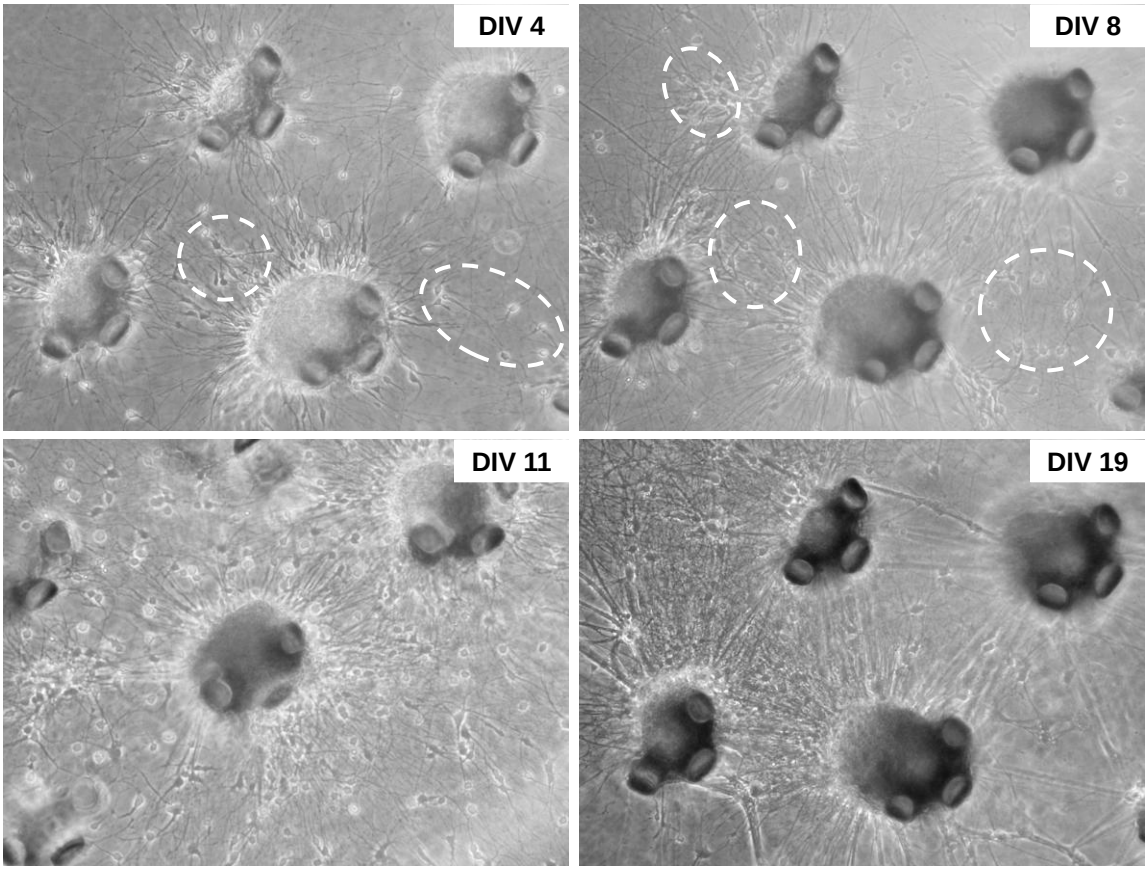

Figure 6.7. Neural progenitor aggregate cultured inside the device showing glial cell migration and axon growth. White dotted circles in upper images indicate glial cells migrated from neural aggregates.

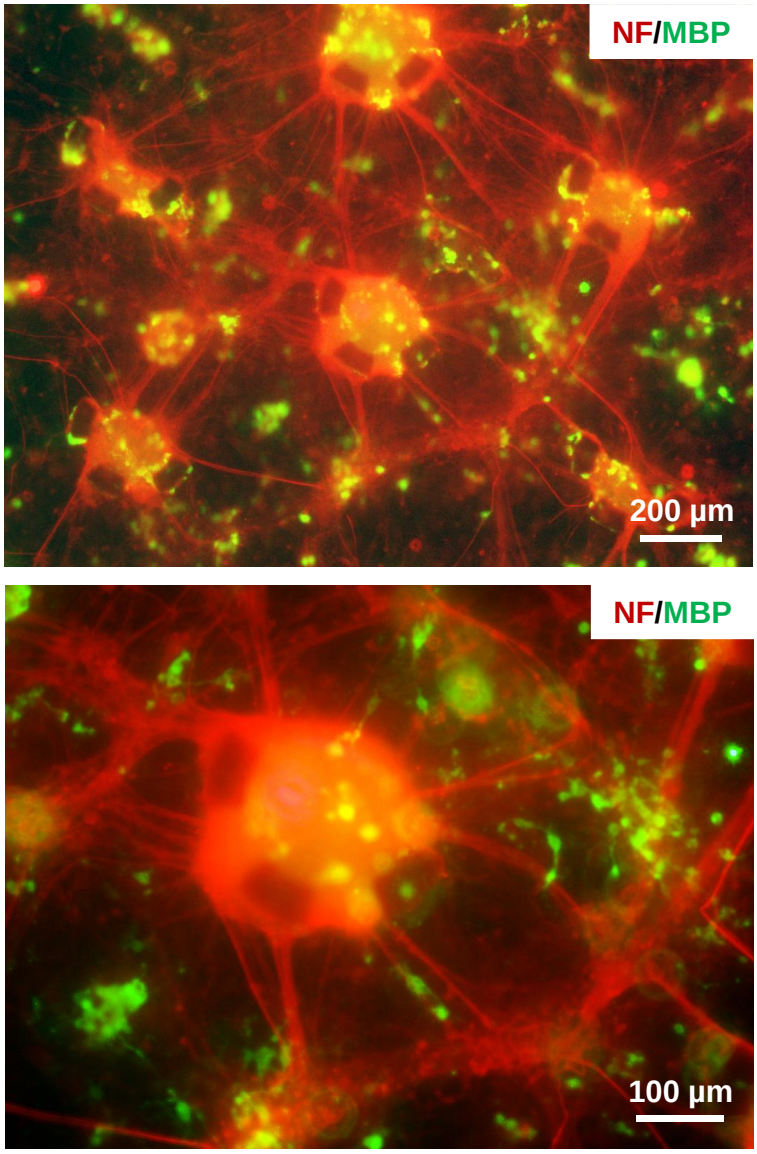

Figure 6.8. Immunostained images of mature OLs and neural aggregates inside the microdevice at DIV 16 (Axon: NF-red, mature OLs: MBP-green).

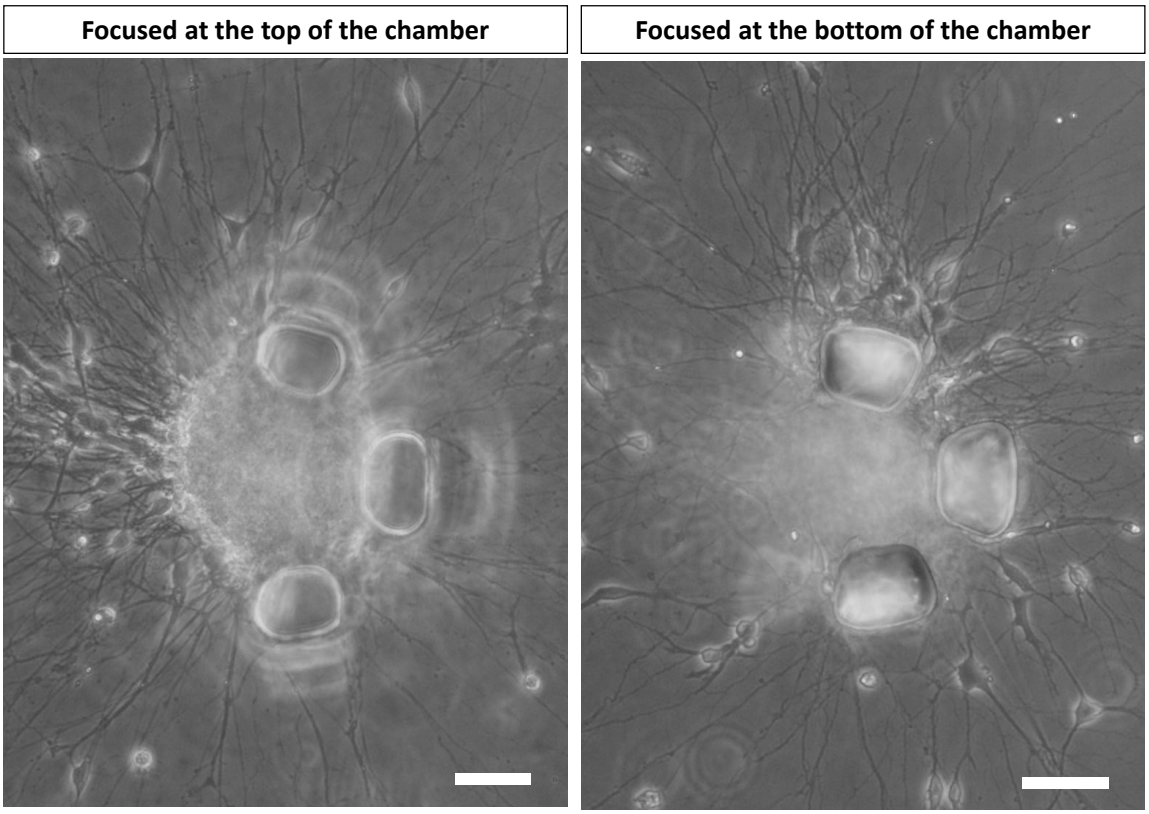

Figure 6.9. Images of axons growing on both the top and the bottom surface of the culture chamber at DIV 8. Scale bars: 50 μm.

indicates that OLs that migrated from neural aggregates successfully differentiated into mature OLs. In addition, due to the shallow height of the culture chamber, axons could not only grow on the bottom surface of the substrate but also on the top surface of the culture chambers, providing evidence that they are being cultured in 3D environment (Figure 6.9).

6.4. Biomolecular treatment

Huang *et al*. recently reported that retinoic acid (RA), which is a metabolite of vitamin A (retinol) that mediates the functions of vitamin A required for growth and development, accelerates CNS remyelination.[115] In order to investigate the effect of biomolecular treatments on CNS myelin formation *in vitro*, spatially controlled neural aggregates inside the 3D culture platform were treated with retinoic acid. First, neural progenitor cell aggregates were cultured inside the culture chambers for two weeks while maintaining a set aggregate-to-aggregate distance (400 μm) to form dense axonal network layer and to allow glial cells to develop. At DIV 17, 500 nM of retinoic acid, diluted in culture medium, was applied to aggregates via the cell loading port and cultured for 10 more days. At DIV 27, cells were fixed and stained against MBP to check myelin formation and to analyze the effect of retinoic acid treatment. Figure 6.10 shows neural aggregates immunostained against NF (green) and MBP (red). As it can be seen in the figure, much more robust myelin sheaths were formed when neural aggregates were treated with retinoic acid. A single OL forming multiple myelin sheaths

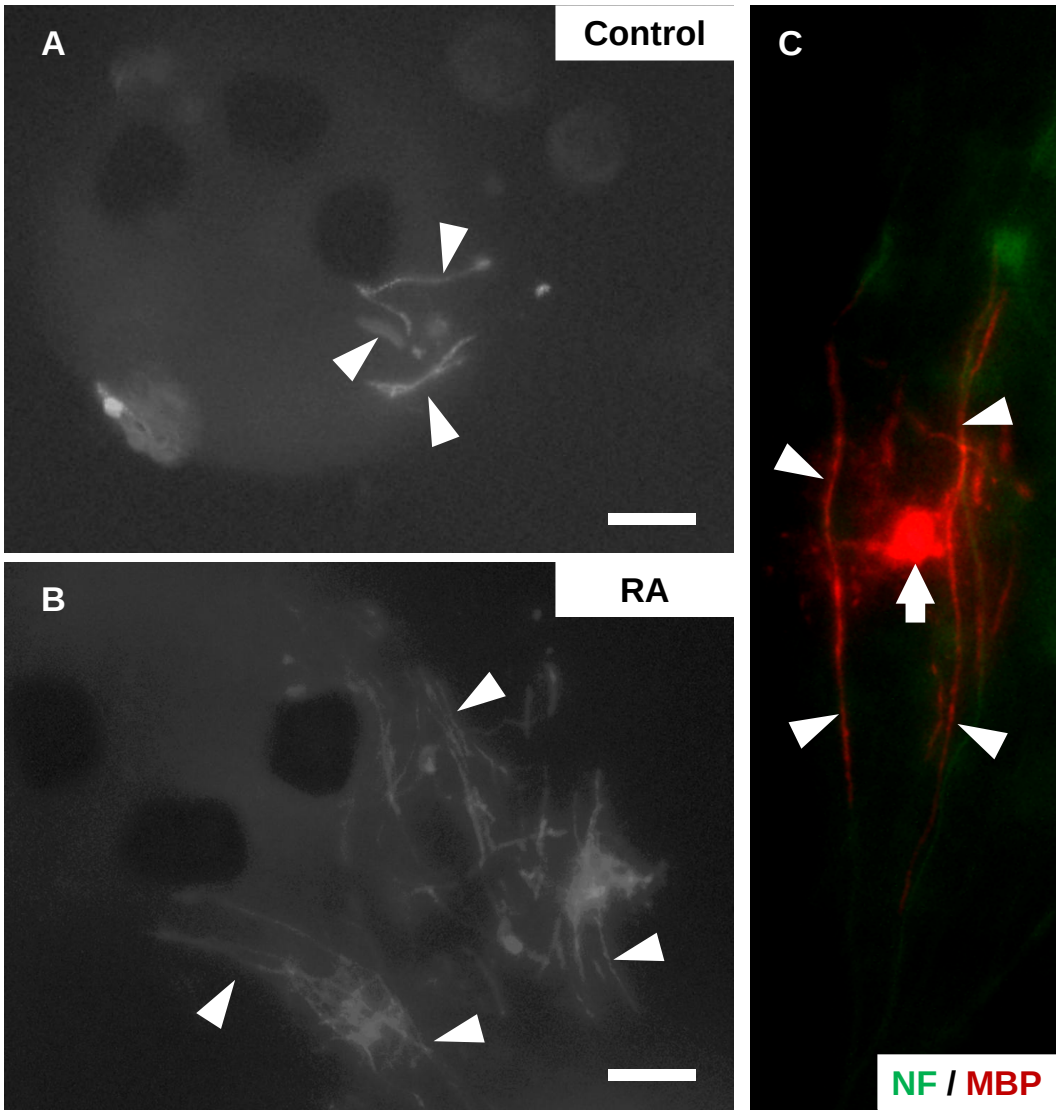

Figure 6.10. Immunostained images of neural aggregates at DIV 27 (A: Control, B-C: Retinoic acid treated). White arrow heads indicate myelin sheath formed by OLs. (C) Close-up view of an oligodendrocyte (white arrow) forming multiple myelin sheaths (white arrow heads) around neighboring axons (Axon: NF-green, mature OLs/myelin: MBP-red). Scale bars: 50 µm.

around axons could also be observed. By confining neural aggregates inside the trapping structures, aggregates could be cultured in more spatially controlled environment and experimental parameters that might affect the expression of myelin sheath, such as distance between aggregates, could be minimized for giving more reproducible results.

6.5. Conclusion

Novel 3D neural progenitor cell aggregate culture platform that can be used for *in vitro* CNS myelination studies have been developed. The 3D culture platform provided more *in vivo* like environment and neuron aggregates showed successful neurite outgrowth and formed intense axonal network inside the device. Also, OLs migrating from neural aggregates successfully differentiated into mature OLs and formed myelin sheath inside the culture platform. To the best to our knowledge, this is the first CNS myelin sheath formed inside a microfluidic device. Formation of robust CNS myelin sheath inside the proposed neural aggregate culture platform demonstrates that this microsystem can be used for studying *in vitro* CNS myelination and for screening potential drug candidates that promote CNS myelination under much more spatially and biochemically controlled environments with higher reproducibility.

VII. NEURON CULTURE MICROSYSTEM WITH INTEGRATED ELECTRODE ARRAY*

7.1. Motivation and design

Multi-electrode arrays (MEAs) are capable of electrically stimulating cells and recording electrical activities of cells with high spatial resolution.[116, 117] MEAs are commercially available and have been widely used to evoke spiking activity in dissociated CNS neuron cultures.[118-120] Recently, MEAs integrated with various micro cell culture platforms have been used for analyzing *in vitro* neuronal networking, drug screening, and for studying the electrical response of cells to localized chemical and electrical stimulations.[121-125]

Unlike dorsal root ganglion (DRG) neurons that are not spontaneously active *in vitro*, cortical neurons in culture are spontaneously active[126-128], and accumulating evidences from both *in vivo*[129, 130] and *in vitro*[131-135] studies have suggested that electrical activity of neurons may play a regulatory role in CNS myelination. However, the effect of localized electrical stimulation on CNS neurons has not yet been fully revealed.

---

*Reprinted with permission from "Micropatterning of poly(dimethylsiloxane) using a photoresist lift-off technique for selective electrical insulation of microelectrode arrays" by Jaewon Park, Hyun Soo Kim, Arum Han, 2009. *Journal of Micromechanics and Microengineering*, 19, 065016, Copyright 2009 by IOP Publishing Ltd.

7.2. Electrical insulation by PDMS patterning

7.2.1. Motivation

MEAs for recording/stimulation have to be electrically insulated from the solution as well as from each other except for the recording/stimulation sites of the electrodes to maximize the signal-to-noise ratio (SNR) and to prevent cross-talking of signals between electrodes. Insulation of these electrodes is typically done by depositing one or multiple layers of SiO_2 or Si_3N_4 on top of the electrodes using plasma-enhanced chemical vapor deposition (PECVD) processes.[136-138] The most widely used method to create openings in these insulation layers is a photolithography process followed by reactive ion etching (RIE). However, the method requires expensive equipment such as PECVD and RIE, and involves complicated multi-step fabrication processes. In addition, this method may not be suitable for flexible devices that require electrode insulation due to the cracking of hard insulating materials. Flexible neural probes fabricated by sandwiching sensing/stimulation electrodes between polyimide layers have been introduced but the method also involves complicated processes and requires specialized equipment for patterning the polyimide insulation layer.[139-141]

Poly(dimethylsiloxane) (PDMS), widely used in bio/medical microchips, is electrically nonconductive; hence, it can be used as an electrical insulation layer. One limitation of this material is that there is no easy way to directly pattern PDMS. PDMS is not a photosensitive material and although a few methods have been proposed to make PDMS photo-definable, the material preparation steps are complicated and not easy to follow, limiting its use.[142-144] Other PDMS patterning methods include plasma etching,

blade scratching and a parylene lift-off process. Patterning PDMS using blade scratching is a method that allows a relatively thick layer of PDMS to be patterned.[145] However, it is a manual process and cannot be used to create small patterns. Eon *et al.*[146] demonstrated that PDMS can be directly patterned using oxygen plasma etching, but the slow etch rate (7 nm/min) due to silicon-oxide-like layer formation on top and the rough surface after plasma etching limit its use. Tong *et al.*[147] introduced a precision PDMS patterning method using a parylene C layer lift-off process that provided a relatively smooth surface. In this method, PDMS was spin coated and cured on a parylene C layer that was deposited and patterned by a low-pressure chemical vapor deposition and a RIE. Parylene C was then peeled off by hand, leaving PDMS only at the area where the parylene C layer had openings. Although this method could provide thin PDMS layers (4 μm) having small features (5 μm), the type of patterns that can be generated is very limited. Since PDMS was removed by lifting off the parylene C layer, areas where PDMS has to be lifted off had to be all connected so that they could be removed along with the parylene C layer, making this method useful for only a limited set of designs. This method also requires equipment such as a parylene coater and a RIE, limiting its wide spread use and increasing the fabrication cost. Recently, a method combining both PDMS plasma etching and lift-off process to fabricate glass-PDMS-glass microfluidic channels was introduced.[148] The method provided a relatively faster PDMS etch rate using O_2 andCF_4 gas mixture, but the process produces particles on the PDMS surface after plasma etching and required a reactive ion etcher. Ostuni *et al.* and Jackman *et al.* proposed a method to obtain PDMS layers with openings by spin-coating

PDMS on top of an SU-8 patterned substrate and peeling it off after polymerization.[149, 150] This PDMS layer could be then used as a stencil/shadow mask or as an electrical insulation layer by placing the PDMS layer on top of sample substrates or electrodes. The main challenges of this method are difficulties in aligning the PDMS layer to the substrate and handling of the thin PDMS layers.

We have developed a simple, low-cost and easy to follow PDMS layer patterning method without any limitation on the type of designs. This photoresist lift-off-based method could be used to pattern thin PDMS layers regardless of whether all patterns are connected or not; hence, it can be easily used for selective passivation of microelectrode arrays, allowing an all PDMS microchip.

7.2.2. PDMS patterning process

PDMS layers having arrays of up to 1225 circular openings in three different diameters (15 μm, 30 μm, 50 μm) with four different center-to-center distances (100 μm, 200 μm, 300 μm, 500 μm) have been fabricated over a 147 mm^2 area on glass and poly(methyl methacrylate) (PMMA) substrates. The different sizes were selected to characterize how pattern sizes and distances between patterns affect the openings in the PDMS layer. The PDMS patterning steps are illustrated in Figure 7.1. To characterize how different thicknesses of sacrificial photoresist layers (NR2-20000P and NR4-8000P, Futurrex, Inc., Franklin, NJ) influence the PDMS patterns, photoresist patterns having thicknesses of 6.5 μm, 13 μm and 24 μm were fabricated. PDMS pre-polymer (10:1 mixture,

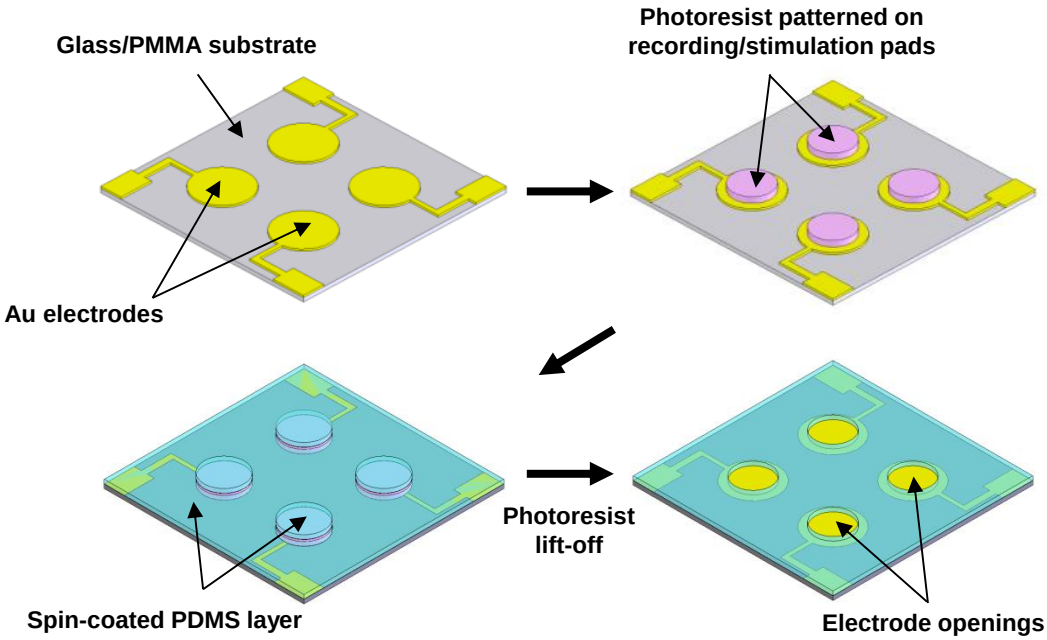

Figure 7.1. Schematics of the PDMS micropatterning steps using a photoresist lift-off process to selectively insulate electrodes.

Sylgard184, Dow Corning, Inc., Midland, MI) was then spin coated at different spin-coating speeds (2000, 4000 and 6000 rpm with an acceleration of 200 rpm/sec) on the photoresist-patterned substrate and baked inside an 85°C oven for 15 min for polymerization. For the PDMS layer to function as an electrical insulation layer without affecting the overall device, a relatively thin PDMS layer has to be obtained. PDMS is a material with relatively high viscosity (3900 mPa·s); thus to obtain a thin insulating layer, PDMS was diluted in toluene (Sigma Aldrich, St Louis, MO) at 1:1 and 1:2 ratios by weight. PDMS was diluted right before the spin-coating process in order to prevent evaporation of toluene which could change the viscosity of the diluted PDMS. Substrates coated with polymerized PDMS were then immersed in a photoresist remover (RR4, Futurrex, Inc., Franklin, NJ) and sonicated for 5 min to lift off the sacrificial photoresist layer, followed by rinsing with IPA and drying inside an 85°C oven. When patterning PDMS layers on top of electrode arrays, Cr/Au (10/250 nm thick) was deposited on the substrate and patterned using a conventional photolithography process followed by metal film etching prior to spin coating the PDMS. Also, to demonstrate that this fabrication method is not limited to discrete circular openings, straight, zigzag and serpentine-shaped lines having widths of 100 μm and lengths of 13-17 mm were patterned as well.

Table 7.1 shows how the different processing conditions affect the resulting PDMS patterns. 'O' in the table denotes that PDMS was successfully patterned over the whole substrate area and 'Δ' indicates that only parts of the overall substrate area were

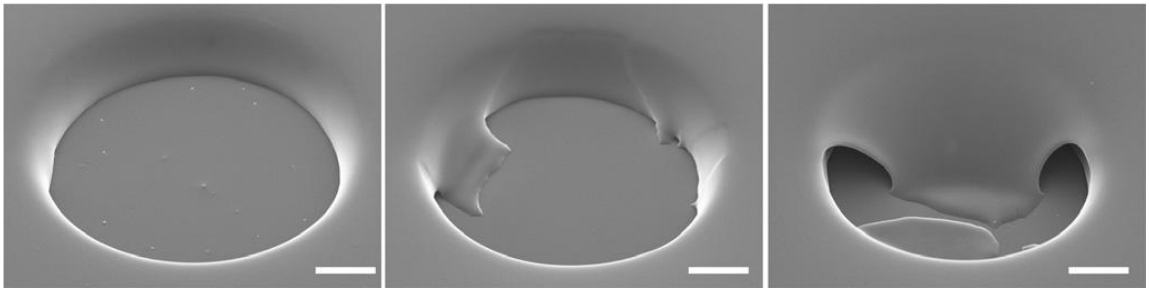

Figure 7.2. SEM images of patterned PDMS layers representing good (‘O’, left), partial (‘Δ’, center) and poor (‘X’, right) patterns. Diameter of circular patterns are 50 μm. Scale bars: 10 μm.

Table 7.1. PDMS patterning results under different processing conditions.

Spin-coating speed	2000 rpm			4000 rpm			6000 rpm		
PDMS:Toluene	1:0	1:1	1:2	1:0	1:1	1:2	1:0	1:1	1:2
PR thickness									
6.5 μm	X	X	X	X	X	X	X	X	O
13 μm	X	Δ	O	X	O	O	Δ	O	O
24 μm	Δ	O	O	O	O	O	O	O	O

successfully patterned with boundaries of the circular PDMS openings having residues. 'X' in the table denotes that the PDMS layer was not properly patterned and that most of the PDMS layer coated on top of the sacrificial photoresist patterns remained even after the photoresist lift-off process. Scanning electron microscopy (SEM) images representing each category ('O', 'Δ', 'X') are shown in Figure 7.2. When PDMS layers were patterned using appropriate processing conditions ('O' in Table 7.1), the size of the pattern openings as well as distances between the patterns did not affect the resulting PDMS patterns. On the other hand, PDMS layers were not patterned perfectly ('Δ' and 'X' in Table 7.1) by the developed lift-off process when the spin-coating speed or the PDMS dilution ratio was too low compared to the height of the sacrificial photoresist layer. Under these improper processing conditions, the size of the circular openings and the distance between the patterns influenced the final patterning results. Typically, patterns with smaller opening diameters and longer separation distances resulted in better patterning whereas circular patterns too large or too close to each other resulted in poor lift-off of the PDMS layer on top of the sacrificial photoresist layer. Figure 7.3A shows arrays of successfully patterned circular openings in a PDMS layer with different diameters (15 μm, 30 μm and 50 μm) but the same 100 μm center-to-center distance. Figure 7.3B shows arrays of 30 μm diameter openings with 100 μm, 200 μm and 300 μm center-to-center distances, all showing good results. This capability of creating holes in PDMS could not be achieved by the previously reported parylene lift-off-based PDMS patterning technique since it would have been impossible to remove the parylene

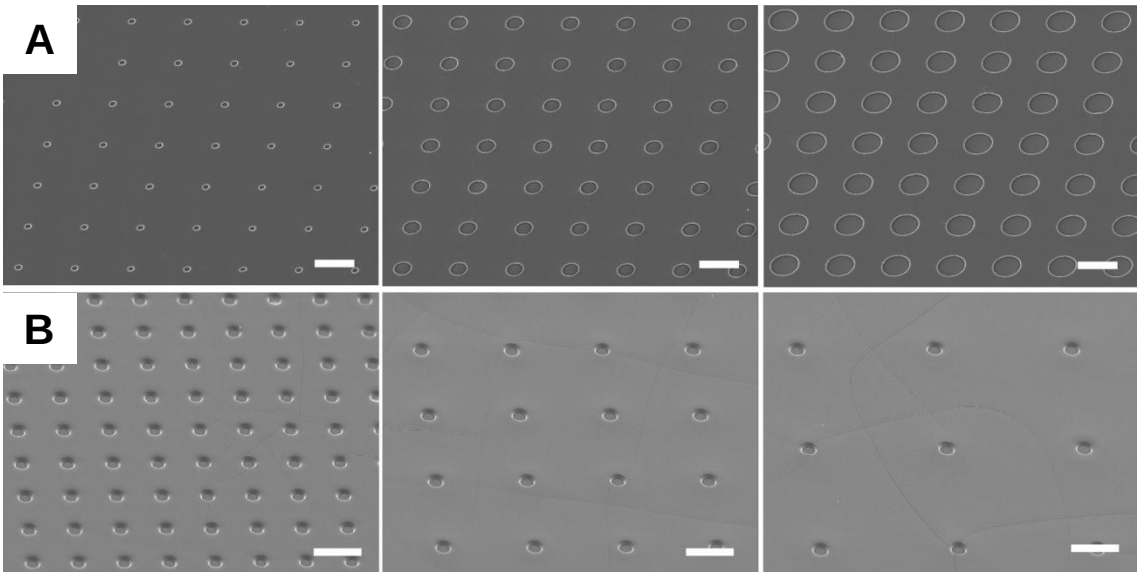

Figure 7.3. SEM images of successfully patterned PDMS layers having (A) circular openings of 15, 30 and 50 μm diameters (from left to right) with 100 μm center-to-center distances and (B) arrays of 30 μm circular openings with 100, 200 and 300 μm center-to-center distances (from left to right). Scale bars: 100 μm.

patterns from each of the holes by peeling them off. For some processing conditions, PDMS layers resulted in uneven surface thickness around the photoresist patterns even when the PDMS openings were clearly defined. This is due to the surface tension of the PDMS pre-polymer around the sacrificial photoresist patterns and occurred when the spin-coated PDMS thickness was too thin compared to the height of the photoresist pattern. Figure 7.4 shows undiluted PDMS spin coated at 6000 rpm on 24 μm thick photoresist patterns followed by photoresist lift-off. It can be seen that the PDMS around the sacrificial photoresist patterns was thicker than the rest of the area. However, such an uneven surface is typically not of any concern for most biosensing microdevice applications. Even for applications requiring an even surface, this problem was solved by selecting proper photoresist pattern thicknesses and PDMS spin-coating speeds, as can be seen in the smooth pattern surfaces in Figures 7.3A-B.

From the processing parameters resulting in good PDMS patterns, we further investigated how each processing parameter affects the final thickness of the patterned PDMS layer by measuring the thickness of the PDMS layer around the pattern boundaries. Table 7.2 shows the effect of each parameter on the final thickness of the patterned PDMS layer. It can be seen that the height of the sacrificial photoresist pattern had the most influence in determining the final thickness of the patterned PDMS layer, where increased photoresist thickness resulted in a thicker PDMS pattern. The thickness of the patterned PDMS layer decreased as the spin speed and the dilution ratio of PDMS increased. These results show that PDMS layers can be successfully patterned and their

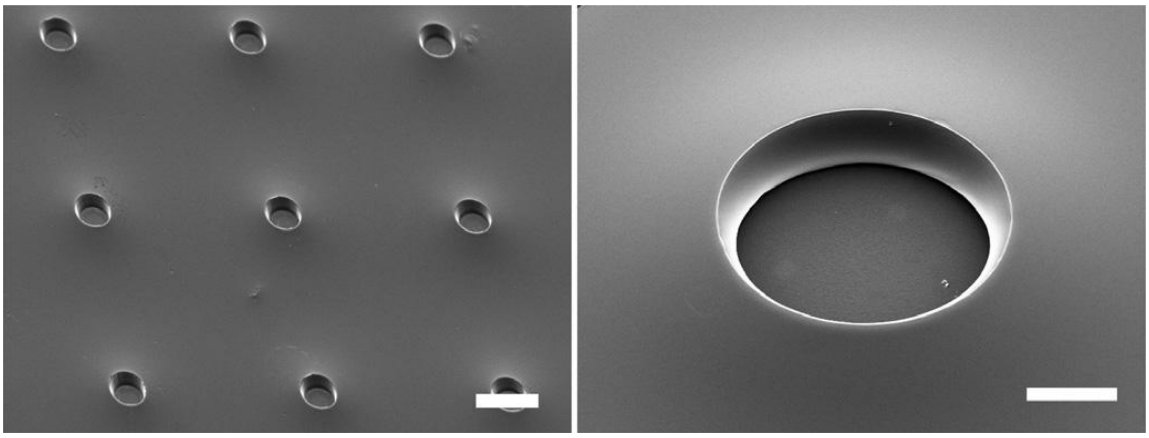

Figure 7.4. SEM images of PDMS layers having 50 μm diameter circular openings but with uneven thickness. Scale bars: 100 μm (left) and 20 μm (right).

Table 7.2. Effect of processing parameters (sacrificial photoresist layer thickness, PDMS spin-coat speed, PDMS dilution ratio) on the final thickness of the PDMS patterns.

1:2 dilution/6000 rpm	
PR Thickness	**Thickness (µm)**
6.5 µm	6.50 ± 0.36
13 µm	9.42 ± 0.12
24 µm	15.83 ± 0.21

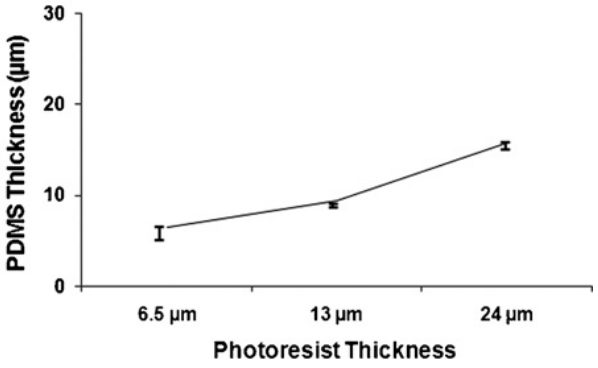

1:2 dilution/13 µm thick pattern	
Spin-speed	**Thickness (µm)**
2000 rpm	12.50 ± 0.22
4000 rpm	10.13 ± 0.35
6000 rpm	9.42 ± 0.12

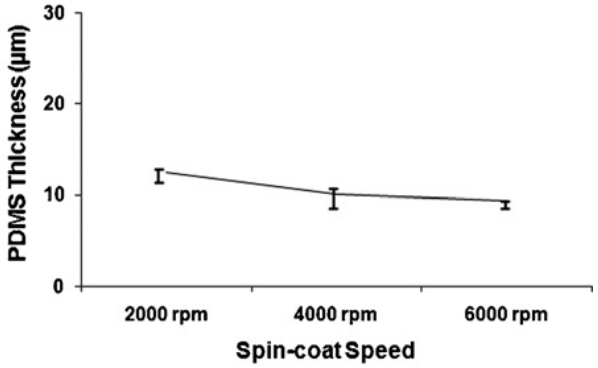

4000 rpm/24 µm thick pattern	
PDMS Dilution	**Thickness (µm)**
Undiluted	24.02 ± 0.22
1 to 1 (w/w)	19.86 ± 0.72
1 to 2 (w/w)	16.80 ± 0.28

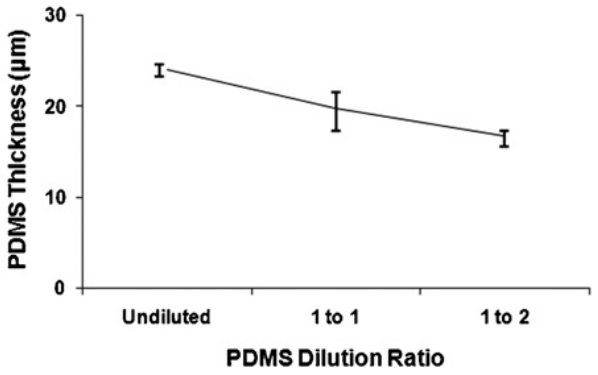

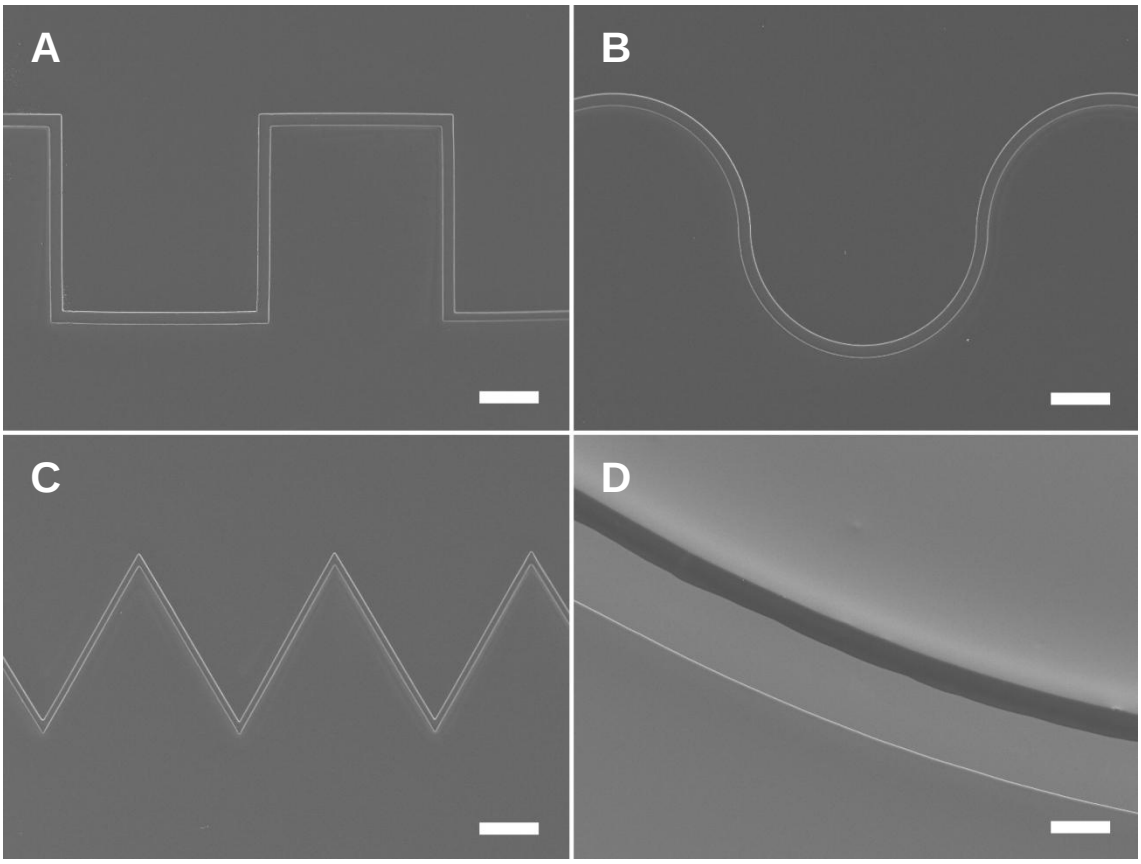

Figure 7.5. SEM images of 100 μm wide and 13–17 mm long (A-C) straight, serpentine and zigzag line-shaped PDMS patterns. Scale bars: 500 μm. (D) Close-up view of a serpentine line pattern. Scale bar: 50 μm.

thickness can be controlled as needed by adjusting the processing parameters. The PDMS patterning method developed here works not only for circular patterns but also for continuous line patterns. 100 μm wide and 13-17 mm long straight, zigzag and serpentine openings were successfully patterned in PDMS (Figure 7.5). NR4-8000P photoresist patterns with a thickness of 24 μm were used as a sacrificial photoresist layer and diluted PDMS (1:2 by weight in toluene) was spin coated at 6000 rpm.

7.3. Electrical insulation

The electrical resistance measured after applying PBS between adjacent bare sensing electrodes was 5-7 MΩ. When the electrodes were fully covered with PDMS without any openings, the measured resistance showed infinite after applying the PBS solution, indicating that the PDMS layer properly functioned as an electrical insulation layer. Finally, electrodes were insulated with a PDMS layer having circular openings made at the sensing sites of the electrodes (Figure 7.6A). The measured electrical resistance between adjacent electrodes after applying PBS was 5-7 MΩ, which is identical to the previously measured reference resistance value. The substrate containing PDMS-patterned electrodes were left in PBS for up to 3 days and electrical resistances were re-measured, but no change in resistivity was observed. These results show that the patterned PDMS layer can function properly as an electrical insulation layer. To show that this patterning method can also be applied for electrically insulating multi-electrode arrays on flexible devices, a PDMS layer having arrays of 50 μm openings at sensing

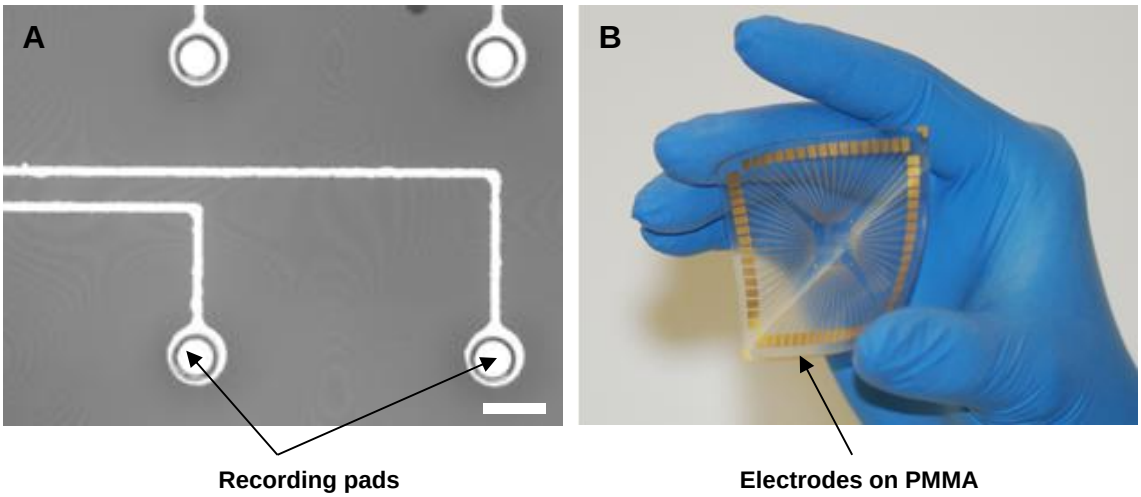

Figure 7.6. (A) A microscopic image of a PDMS layer with circular openings patterned on top of an MEA embedded glass substrate. Scale bar: 100 μm. (B) Photographic image of a flexible PMMA substrate with a multi-electrode array insulated by a patterned PDMS layer.

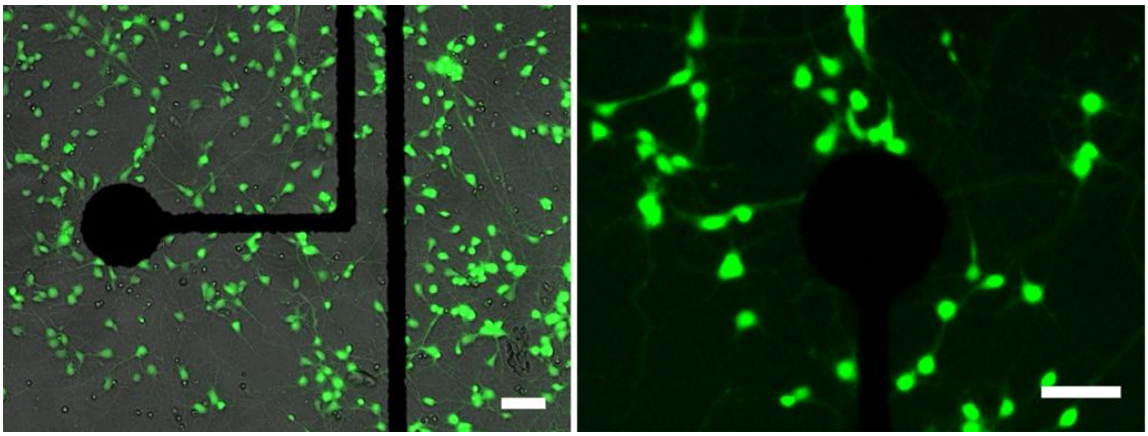

Figure 7.7. Fluorescence images of neuron cells at DIV 4 showing successful culture on top of an Au electrode array insulated with a patterned PDMS layer. Cell bodies and neurites were stained with Calcein-AM (green). Scale bars: 50 μm.

sites was patterned over a 500 μm thick flexible PMMA film (Figure 7.6B). The measured electrical resistances of 5-7 MΩ indicate that the patterned PDMS layer fully insulated the electrodes. Electrical resistances were measured again after bending the PMMA substrate multiple times using hand, but no noticeable changes in resistances were observed.

7.4. Biocompatibility

To investigate whether this PDMS patterning technology results in any biocompatibility issues, primary forebrain neuron cells from E16-18 rats were cultured on top of a glass substrate having electrode arrays insulated with a patterned PDMS layer. The patterned PDMS layer did not show any adhesion problem with the glass substrate with electrodes during the culture period. Neuron cells successfully attached to the substrate and started to form an extensive neuronal network on top of the PDMS insulation layer by DIV 4 as shown in Figure 7.7. Cells were successfully cultured on the device for up to two weeks and no noticeable negative effects from the patterned PDMS layer on the cultured neuron cells were observed.

7.5. Conclusion

We have developed a PDMS patterning method that utilizes a photoresist as a sacrificial layer for a PDMS lift-off process. The processing steps are simple and do not require expensive equipment other than a standard photolithography tool, and PDMS layers with different sizes and thicknesses could be successfully patterned on both glass and flexible

PMMA film substrates without any limitations. This method could be used to create any type of PDMS pattern designs regardless of whether they were all connected or not, making this a universal one-stop method for PDMS patterning. The patterned PDMS layer successfully functioned as an electrical insulation layer and the neuron cells were cultured on top of the patterned PDMS insulation layers for up to two weeks, showing extensive neurites growth. The results demonstrate that the developed PDMS patterning method can be applied for localized electrical stimulation as well as action potential recording of neurons cultured inside the compartmentalized microsystem. This work has been published in *Journal of Micromechanics and Microengineering*.[151]

VIII. DISSERTATION REVIEW AND CONCLUSIONS

The aim of the project is to develop *in vitro* CNS neuron culture platforms that provides more spatially and biochemically controlled microenvironments that could not be achieved in conventional cell culture methods for various CNS neuron studies including localized axon-glia interaction, axon growth analysis, high-throughput biomolecular screening, axon regeneration, and myelination. Due to the nature of conventional cell culture plate based method, performing localized manipulation of biochemical environments as well as physical guidance of cell components is not easy. The various CNS neuron culture platforms developed here through microfabrication techniques can overcome limitations of conventional culture methods.

We have developed a series of CNS neuron glia co-culture microfluidic platforms, including circular, six-compartment, and 24-compartment co-culture platforms for studying localized axon-glia interactions. A novel six-compartment neuron culture device capable of physically guiding axons during the culture period for quantitative axon growth analysis have also been developed for screening drugs or biomolecular factors that promote intrinsic growth capability of CNS axons. In addition, a 3D neural progenitor cell aggregate culture platform allowing spatially controlled 3D neuron culture was developed for studying CNS myelination *in vitro*. The main achievements are as following:

8.1. Circular CNS neuron/glia co-culture microdevice

The circular CNS neuron/glia co-culture microdevice has been developed for studying localized axon-glia interaction. The unique circular designed allowed higher axon crossing efficiency compared to previously reported square-design device, and axons could be successfully isolated from neuronal somata physically as well as fluidically. OPCs co-cultured on top of isolated axon layer successfully developed into mature OLs and expressed MBP.

8.2. Six-compartment CNS neuron/glia co-culture microdevice

CNS neuron-glia co-culture microsystem having six axon/glia compartments for enhanced throughput has been developed by utilizing a newly developed macro-micro hybrid soft-lithography master (MMHSM) fabrication technique. PDMS culture platform having six satellite axon/glia compartments that are only 400 μm apart from the soma compartment could be replicated in significantly reduced time without any manual aligning or punching process using this process. Six axon/glia compartments were fluidically isolated from each other and the configuration allowed six different experimental conditions to be carried out on a single device simultaneously. Localized ceramide treatment to OLs inside the six axon/glia compartments demonstrated its capability for parallel screening and OPCs co-cultured on top of isolated axons successfully developed into mature OLs.

8.3. Six-compartment neuron culture platform for quantitative CNS axon growth analysis

The previously developed six-compartment neuron co-culture platform has been modified for quantitatively analyzing CNS axon growth. The device utilizes microgrooves on the bottom substrate for isolating axons from neuronal somata whereas previous devices use microchannels connecting the soma compartment and the axon compartment. Microgrooves not only isolate axons from neuronal somata for localized biomolecular treatment but also continue to physically guide axons inside the axon compartment for growing them straight. This novel feature allowed average length of axons to be quantitatively analyzed. Five different ECMs (Matrigel^{TM}, laminin, fibronectin, collagen, CSPG) have been locally treated to neuronal somata and isolated axons respectively in order to screen conditions that promote CNS axon growth the most. Localized laminin, collagen, or Matrigel^{TM} treatment to neuronal somata increased axons to grow approximately two-folds while treatments to isolated axon showed only 50% increase. Neuronal somata treatment with CSPG had limited effect on isolated axons; however localized CSPG treatment in the axon compartment completely abrogated axonal growth and caused retraction of the established axons.

8.4. 24-compartment neuron culture microsystem

A compartmentalized neuron culture platform having 24 axon/glia compartments have been developed. The device integrates microfluidic components that enable culture medium or drug treatments in all 24 axon/glia compartments to be replenished by a

single pipetting step. Axons were successfully isolated from neuronal somata inside the 24 axon/glia compartments for localized treatments and the microfluidic components enabled culture medium in all 24 compartments to be replenished all together.

8.5. Neural progenitor cell aggregate culture microsystem for CNS myelination study

A novel microsystem capable of culturing neural progenitor aggregates in spatially controlled 3D environment for studying CNS myelination has been developed. Neural aggregates were captured inside the trapping structures during the culture for maintaining fixed aggregate-to-aggregate distance. Dense axonal network layer was formed inside the culture chambers after two weeks of culture and spatially controlled culture environments increased the experiment repeatability. Also, OLs migrated from the neural aggregate successfully developed into mature OLs and formed myelin sheaths inside the device demonstrating its capability for screening drugs that promote CNS myelination.

8.6. Neuron culture microsystem with integrated electrode array

A technique for pattering PDMS layer for utilizing it as an electrical insulation layer for neuron culture microsystem with MEAs has been developed. The developed method allowed precise controlling of the insulating layer thickness by adjusting the process parameters; PDMS dilution ratio, sacrificial layer thickness, and the spin-coating speed. The patterned PDMS layer properly functioned as an electrical insulation layer and

could also be applied for flexible devices. Neuron were cultured on top of PDMS insulated MEAs without any toxicity issues.

REFERENCES

1. Shim, J., Bersano-Begey, T.F., Zhu, X., Tkaczyk, A.H., Linderman, J.J. *et al.* Micro- and Nanotechnologies for Studying Cellular Function. *Current Topics in Medicinal Chemistry* **3**, 687-703 (2003).
2. Wheeler, A.R., Throndset, W.R., Whelan, R.J., Leach, A.M., Zare, R.N. *et al.* Microfluidic Device for Single-Cell Analysis. *Analytical Chemistry* **75**, 3581-3586 (2003).
3. Dertinger, S.K.W., Chiu, D.T., Jeon, N.L. & Whitesides, G.M. Generation of Gradients Having Complex Shapes Using Microfluidic Networks. *Analytical Chemistry* **73**, 1240-1246 (2001).
4. Taylor, A.M., Blurton-Jones, M., Rhee, S.W., Cribbs, D.H., Cotman, C.W. *et al.* A Microfluidic Culture Platforms for Cns Axonal Injury, Regeneration and Transport. *Nature Methods* **2**, 599-605 (2005).
5. Hong, J.W. & Quake, S.R. Integrated Nanoliter Systems. *Nature Biotechnology* **21**, 1179-1183 (2003).
6. Liu, Y., Garcia, C.D. & Henry, C.S. Recent Progress in the Development of Microtas for Clinical Analysis. *Analyst* **128**, 1002-1008 (2003).
7. Adamo, A. & Jansen, K.F. Microfluidic Based Single Cell Microinjection. *Lab on a Chip* **8**, 1258-1261 (2008).

8. Morton, K.J., Loutherback, K., Inglis, D.W., Tsui, O.K., Sturm, J.C. *et al.* Crossing Microfluidic Streamlines to Lyse, Label and Wash Cells. *Lab on a Chip* **8**, 1448-1453 (2008).

9. Chang, C., Takahashi, Y., Murata, T., Shiku, H., Chang, H. *et al.* Entrapment and Measurement of a Biologically Functionalized Microbead with a Microwell Electrode. *Lab on a Chip* **9**, 1185-1192 (2009).

10. Han, A., Yang, L. & Frazier, A.B. Quantification of the Heterogeneity in Breast Cancer Cell Lines Using Whole-Cell Impedance Spectroscopy. *Clinical Cancer Research* **13**, 139-143 (2007).

11. Han, A. & Frazier, A.B. Ion Channel Characterization Using Single Cell Impedance Spectroscopy. *Lab on a Chip* **6**, 1412-1414 (2006).

12. Nevill, J., Cooper, R., Dueck, M., Breslauer, D. & Lee, L. Integrated Microfluidic Cell Culture and Lysis on a Chip. *Lab on a Chip* **7**, 1689-1695 (2007).

13. Khine, M., Ionescu-Zanetti, C., Blatz, A., Wang, L.-P. & Lee, L.P. Single-Cell Electroporation Arrays with Real-Time Monitoring and Feedback Control. *Lab on a Chip* **7**, 457-462 (2007).

14. Huang, K.-S., Lin, Y.-C., Su, C.-C. & Fang, C.-S. Enhancement of an Electroporation System for Gene Delivery Using Electrophoresis with a Planar Electrode. *Lab on a Chip* **7**, 86-92 (2007).

15. Wu, C.-C., Saito, T., Yasukawa, T., Shiku, H., Abe, H. *et al.* Microfluidic Chip Integrated with Amperometric Detector Array for in Situ Estimating Oxygen

Consumption Characteristics of Single Bovine Embryos. *Sensors and Actuators, B: Chemical* **125**, 680-687 (2007).

16. Chen, C.S., Jiang, X. & Whitesides, G.M. Microengineering the Environment of Mammalian Cells in Culture. *Materials Research Bulletin* **30**, 194-201 (2005).
17. Hung, P.J., Lee, P.J., Sabounchi, P., Aghdam, N., Lin, R. *et al.* A Novel High Aspect Ratio Microfluidic Design to Provide a Stable and Uniform Microenvironment for Cell Growth in a High Throughput Mammalinan Cell Culture Array. *Lab on a Chip* **5**, 44-48 (2005).
18. Chung, B.G., Flanagan, L.A., Rhee, S.W., Schwartz, P.H., Lee, A.P. *et al.* Human Neural Stem Cell Growth and Differentiation in a Gradient-Generating Microfluidic Device. *Lab on a Chip* **5**, 401-406 (2005).
19. Tourovskaia, A., Figueroa-Masot, X. & Folch, A. Differentiation-on-a-Chip: A Microfluidic Platform for Long-Term Cell Culture Studies. *Lab on a Chip* **5**, 14-19 (2005).
20. Gu, W., Zhu, X., Futai, N., Cho, B.S. & Takayama, S. Computerized Microfluidic Cell Culture Using Elastomeric Channels and Braille Displays. *Proceedings of the National Academy of Sciences of the United States of America* **101**, 15861-15866 (2004).
21. Shackman, J.G., Dahlgren, G.M., Peters, J.L. & Kennedy, R.T. Perfusion and Chemical Monitoring of Living Cells on a Microfluidic Chip. *Lab on a Chip* **5**, 56-63 (2005).

22. Hediger, S., Fontannaz, J., Sayah, A., Hunziker, W. & Gijs, M.A.M. Biosystem for the Culture and Characterization of Epithelial Cell Tissues. *Sensors and Actuators, B: Chemical* **63**, 63-73 (2000).

23. Zhang, Z., Boccazzi, P., Choi, H.-G., Perozziello, G., Sinskey, A.J. *et al.* Microchemostat - Microbial Continuous Culture in a Polymer-Based, Instrumented Microbioreactor. *Lab on a Chip* **6**, 906-913 (2006).

24. Frevert, C.W., Boggy, G., Keenan, T.M. & Folch, A. Measurement of Cell Migration in Response to an Evolving Radial Chemokine Gradient Triggered by a Microvalve. *Lab on a Chip* **6**, 849-856 (2006).

25. Abhyankar, V.V., Lokuta, M.A., Huttenlocher, A. & Beebe, D.J. Characterization of a Membrane-Based Gradient Generator for Use in Cell-Signaling Studies. *Lab on a Chip* **6**, 389-393 (2006).

26. Jeon, N.L., Baskaran, H., Dertinger, S.K.W., Whitesides, G.M., Water, L.V.D. *et al.* Neutrophil Chemotaxis in Linear and Complex Gradients of Interleukin-8 Formed in a Microfabricated Device. *Nature Biotechnology* **20**, 826-830 (2002).

27. Takayama, S., Ostuni, E., LeDuct, P., Naruse, K., Ingber, D.E. *et al.* Subcellular Positioning of Small Molecules. *Nature* **411**, 1016 (2001).

28. Cho, Y., Kim, H.S., Frazier, A.B., Chen, Z., Shin, D.M. *et al.* Whole Cell Impedance Analysis for Highly-Metastatic and Poorly-Metastatic Cancer Cells. *Journal of Microelectromechanical Systems* **18**, 808-817 (2009).

29. Han, K.-H., Han, A. & Frazier, A.B. Microsystems for Isolation and Electrophysiological Analysis of Breast Cancer Cells from Blood. *Biosensors and Bioelectronics* **21**, 1907-1914 (2006).

30. Koltay, P., Steger, R., Bohl, B. & Zengerle, R. The Dispensing Well Plate: A Novel Nanodispenser for the Multiparallel Delivery of Liquids. *Sensors and Actuators, A: Physical* **116**, 483-491 (2004).

31. Vickerman, V., Blundo, J., Chung, S. & Kamm, R. Design, Fabrication and Implementation of a Novel Multi-Parameter Control Microfluidic Platform for Three-Dimensional Cell Culture and Real-Time Imaging. *Lab on a Chip* **8**, 1468-1477 (2008).

32. Xia, Y. & Whitesides, G.M. Soft Lithography. *Angewandte Makromolekulare Chemie* **37**, 550-575 (1998).

33. Becker, H. & Locascio, L.E. Polymer Microfluidic Devices. *Talanta* **56**, 267-287 (2002).

34. Whitesides, G.M., Ostuni, E., Takayama, S., Jiang, X. & Ingber, D.E. Soft Lithography in Biology and Biochemistry. *Annual Reviews in Biomedical Engineering* **3**, 335-373 (2001).

35. Baumann, N. & Pham-Dinh, D. Biology of Oligodendrocyte and Myelin in the Mammalian Central Nervous System. *Physiological Reviews* **81**, 871-927 (2001).

36. Li, J., Baud, O., Vartanian, T., Volpe, J.J. & Rosenberg, P.A. Peroxynitrite Generated by Inducible Nitric Oxide Synthase and Nadph Oxidase Mediates

Microglial Toxicity to Oligodendrocytes. *Proceedings of the National Academy of Sciences of the United States of America* **102**, 9936-9941 (2005).

37. Baumann, N. & Pham-Dinh, D. Biology of Oligodendrocyte and Myelin in the Mammalian Central Nervous System. *Physiological Reviews* **81**, 871-927 (2001).

38. Knusel, B., Winslow, J., Rosenthal, A., Burton, L., Seid, D. *et al.* Promotion of Central Cholinergic and Dopaminergic Neuron Differentiation by Brain-Derived Neurotrophic Factor but Not Neurotrophin 3. *Neurobiology* **88**, 961-965 (1991).

39. Taylor, A., Gifondorwa, D., Newbern, J., Robinson, M., Strupe, J. *et al.* Astrocyte and Muscle-Derived Secreted Factors Differentially Regulate Motoneuron Surviva. *Journal of Neuroscience* **27**, 634-644 (2007).

40. Nave, K.-A. & Salzer, J.L. Axonal Regulation of Myelination by Neuregulin 1. *Current Opinion in Neurobiology* **16**, 492-500 (2006).

41. Pfeiffer, S.E., Warrington, A.E. & Bansal, R. The Oligodendrocyte and Its Many Cellular Processes. *Trends in Cell Biology* **3**, 191-197 (1993).

42. Colognato, H. & ffrench-Constant, C. Mechanisms of Glial Development. *Current Opinion in Neurobiology* **14**, 37-44 (2004).

43. McCarthy, K.D. & de Vellis, J. Preparation of Separate Astroglial and Oligodendroglial Cell Cultures from Rat Cerebral Tissue. *Journal of Cell Biology* **85**, 890-902. (1980).

44. Barres, B.A. & Raff, M.C. Control of Oligodendrocyte Number in the Developing Rat Optic Nerve. *Neuron* **12**, 935-942 (1994).

45. Miller, R.H. Regulation of Oligodendrocyte Development in the Vertebrate Cns. *Progress in Neurobiology* **67**, 451-467 (2002).

46. McMorris, F.A. & McKinnon, R.D. Regulation of Oligodendrocyte Development and Cns Myelination by Growth Factors: Prospects for Therapy of Demyelinating Disease. *Brain Pathology* **6**, 313-329 (1996).

47. Waxman, S.G. Axon-Glia Interactions: Building a Smart Nerve Fiber. *Current Biology* **7**, R406-410 (1997).

48. Simons, M. & Trajkovic, K. Neuron-Glia Communication in the Control of Oligodendrocyte Function and Myelin Biogenesis. *Journal of Cell Science* **119**, 4381-4389 (2006).

49. Sherman, D.L. & Brophy, P.J. Mechanisms of Axon Ensheathment and Myelin Growth. *Nature Reviews* **6**, 683-690 (2005).

50. Millet, L., Stewart, M., Sweedler, J., Nuzzo, R. & Gillette, M. Microfluidic Devices for Culturing Primary Mammalian Neurons at Low Densities. *Lab on a Chip* **7**, 987-994 (2007).

51. Dowell-Mesfin, N.M., Abdul-Karim, M.A., Turner, A.M., Schanz, S., Craighead, H.G. *et al.* Topographically Modified Surfaces Affect Orientation and Growth of Hippocampal Neurons. *Journal of Neural Engineering* **1**, 78-90 (2004).

52. Prinz, C., Hallstrom, W., Martensson, T., Samuelson, L., Montelius, L. *et al.* Axonal Guidance on Patterned Free-Standing Nanowire Surfaces. *Nanotechnology* **19** (2008).

53. Dertinger, S.K.W., Jiang, X., Li, Z., Murthy, V.N. & Whitesides, G.M. Gradients of Substrate-Bound Laminin Orient Axonal Specification of Neurons. *Proceedings of the National Academy of Sciences of the United States of America* **99**, 12542-12547 (2002).

54. Heuschkel, M.O., Guerin, L., Buisson, B., Bertrand, D. & Renaud, P. Buried Microchannels in Photopolymer for Delivering of Solutions to Neurons in a Network. *Sensors and Actuators, B: Chemical* **48**, 356-361 (1998).

55. Geremia, N.M., Gordon, T., Brushart, T.M., Al-Majed, A.A. & Verge, V.M.K. Electrical Stimulation Promotes Sensory Neuron Regeneration and Growth-Associated Gene Expression. *Experimental Neurology* **205**, 347-359 (2007).

56. Stevens, B., Tanner, S. & Fields, R.D. Control of Myelination by Specific Patterns of Neural Impulses. *The Journal of Neuroscience* **18**, 9303-9311 (1998).

57. Wagenaar, D., Madhavan, R., Pine, J. & Potter, S. Controlling Bursting in Cortical Cultures with Closed-Loop Multi-Electrode Stimulation. *Journal of Neuroscience* **25**, 680-688 (2004).

58. Campenot, R.B. Local Control of Neurite Development by Nerve Growth Factor. *Proceedings of the National Academy of Sciences of the United States of America* **74**, 4516-4519 (1977).

59. Bi, J., Tsai, N.-P., Lin, Y.-P., Loh, H.H. & Wei, L.-N. Axonal Mrna Transport and Localized Translational Regulation of K-Opioid Receptor in Primary Neurons of Dorsal Root Ganglia. *Proceedings of the National Academy of Sciences of the United States of America* **103**, 19919-19924 (2006).

60. Ishibashi, T., Dakin, K.A., Stevens, B., Lee, P.R. & Fields, R.D. Astrocytes Promote Myelination in Response to Electrical Impulses. *Neuron* **49**, 823-832 (2006).

61. Ng, B.K., Chen, L., Mandemakers, W., Cosgaya, J.M. & Chan, J.R. Anterograde Transport and Secretion of Brain-Derived Neurotrophic Factor Along Sensory Axons Promote Schwann Cell Myelination. *The Journal of Neuroscience* **27**, 7597-7603 (2007).

62. Taylor, A.M., Rhee, S.W., Tu, C., Cribbs, D., Cotman, C. *et al.* Microfluidic Multicomparment Device for Neuroscience Research. *Langmuir* **19**, 1551-1556 (2003).

63. Taylor, A., Blurton-Jones, M., Rhee, S.W., Cribbs, D., Cotman, C. *et al.* Microfluidic Culture Platform for Neuroscience Research. *Nature Methods* **2**, 599-605 (2005).

64. Kim, Y., Karthikeyan, K., Chirvi, S. & Davé, D. Neuro-Optical Microfluidic Platform to Study Injury and Regeneration of Single Axons. *Lab on a Chip* **9**, 2576-2581 (2009).

65. Park, J.W., Vahid, B., Kim, H.J., Rhee, S.W. & Jeon, N.L. Quantitative Analysis of Cns Axon Regeneration Using a Microfluidic Neuron Culture Devices. *Biochip Journal* **2** (2008).

66. Lacour, S.P., Atta, R., FitzGeralsd, J.J., Blamire, M., Tarte, E. *et al.* Polyimide Micro-Channel Arrays for Peripheral Nerve Regenerative Implants. *Sensors and Actuators, A: Physical* **147**, 456-463 (2008).

67. Yang, I., Siddique, R., Hosmane, S., Thakor, N. & Höke, A. Compartmentalized Microfluidic Culture Platform to Study Mechanism of Paclitaxel-Induced Axonal Degeneration. *Experimental Neurology*, 124-128 (2009).

68. Zhang, K., Osakada, Y., Vrljic, M., Chen, L., Mudrakola, H. *et al.* Single-Molecule Imaging of Ngf Axonal Transport in Microfluidic Devices. *Lab on a Chip* **10**, 2566-2573 (2010).

69. Hur, E.M., Yang, I.H., Kim, D.H., Byun, J., Levchenko, A. *et al.* Engineering Neuronal Growth Cones to Promote Axon Regeneration over Inhibitory Molecules. *Proceedings of the National Academy of Sciences of the United States of America* **108**, 5057 (2011).

70. Lubetzki, C., Demerens, C., Anglade, P., Villarroya, H., Frankfurter, A. *et al.* Even in Culture, Oligodendrocytes Myelinate Solely Axons. *Proceedings of the National Academy of Sciences of the United States of America* **90**, 6820 (1993).

71. Meyer-Franke, A., Shen, S. & Barres, B. Astrocytes Induce Oligodendrocyte Processes to Align with and Adhere to Axons. *Molecular and Cellular Neuroscience* **14**, 385-397 (1999).

72. Thomson, C., Hunter, A., Griffiths, I., Edgar, J. & McCulloch, M. Murine Spinal Cord Explants: A Model for Evaluating Axonal Growth and Myelination in Vitro. *Journal of Neuroscience Research* **84**, 1703-1715 (2006).

73. Friedrich, J., Ebner, R. & Kunz-Schughart, L.A. Experimental Anti-Tumor Therapy in 3-D: Spheroids-Old Hat or New Challenge? *International Journal of Radiation Biology* **83**, 849-871 (2007).

74. Hirschhaeuser, F., Menne, H., Dittfeld, C., West, J., Mueller-Klieser, W. *et al.* Multicellular Tumor Spheroids: An Underestimated Tool Is Catching up Again. *Journal of Biotechnology* **148**, 3-15 (2010).

75. Hemmendinger, L., Garber, B., Hoffmann, P. & Heller, A. Target Neuron-Specific Process Formation by Embryonic Mesencephalic Dopamine Neurons in Vitro. *Proceedings of the National Academy of Sciences of the United States of America* **78**, 1264 (1981).

76. So, J. & Dickey, M. Inherently Aligned Microfluidic Electrodes Composed of Liquid Metal. *Lab on a Chip* (2011).

77. Ziegler, L., Grigoryan, S., Yang, I., Thakor, N. & Goldstein, R. Efficient Generation of Schwann Cells from Human Embryonic Stem Cell-Derived Neurospheres. *Stem Cell Reviews and Reports*, 1-10 (2010).

78. Widera, D., Mikenberg, I., Kaus, A., Kaltschmidt, C. & Kaltschmidt, B. Nuclear Factor-Kb Controls the Reaggregation of 3d Neurosphere Cultures in Vitro. *European Cells and Materials* **11**, 76-85 (2006).

79. Koito, H. & Li, J. Preparation of Rat Brain Aggregate Cultures for Neuron and Glia Development Studies. *Journal of Visualized Experiments* **31** (2009).

80. Watkins, T.A., Emery, B., Mulinyawe, S. & Barres, B.A. Distinct Stages of Myelination Regulated by R-Secretase and Astrocytes in a Rapidly Myelinating Cns Coculture System. *Neuron* **60**, 555-569 (2008).

81. Jin, H.-J., Cho, Y.-H., Gu, J.-M., Kim, J. & Oh, Y.-S. A Multicellular Spheroid Formation and Extraction Chip Using Removable Cell Trapping Barriers. *Lab on a Chip* **11**, 115-119 (2011).

82. Tekin, H., Anaya, M., Brigham, M.D., Nauman, C., Langer, R. *et al.* Stimuli-Responsive Microwells for Formation and Retrieval of Cell Aggregates. *Lab on a Chip* **10**, 2411-2418 (2010).

83. Kang, E., Choi, Y., Jun, Y., Chung, B. & Lee, S. Development of a Multi-Layer Microfluidic Array Chip to Culture and Replate Uniform-Sized Embryoid Bodies without Manual Cell Retrieval. *Lab on a Chip* **10**, 2651-2654 (2010).

84. Lee, K.H., No, D.Y., Kim, S.-H., Ryoo, J.H., Wong, S.F. *et al.* Diffusion-Mediated in Situ Alginate Encapsulation of Cell Spheroids Using Microscale Concave Well and Nanoporous Membrane. *Lab on a Chip* (2011).

85. Khoury, M., Bransky, A., Korin, N., Konak, L., Enikolopov, G. *et al.* A Microfluidic Traps System Supporting Prolonged Culture of Human Embryonic Stem Cells Aggregates. *Biomedical Microdevices*, 1-8 (2010).

86. Yu, L., Chen, M.C.W. & Cheung, K.C. Droplet-Based Microfluidic System for Multicellular Tumor Spheroid Formation and Anticancer Drug Testing. *Lab on a Chip* **10**, 2424-2432 (2010).

87. Liu, T., Lin, B. & Qin, J. Carcinoma-Associated Fibroblasts Promoted Tumor Spheroid Invasion on a Microfluidic 3d Co-Culture Device. *Lab on a Chip* **10**, 1671-1677 (2010).

88. Li, J., Ramenaden, E.R., Peng, J., Koito, H., Volpe, J.J. *et al.* Tumor Necrosis Factor Mediates Lipopolysaccharide-Induced Microglial Toxicity to Developing Oligodendrocytes When Astrocytes Are Present. *The Journal of Neuroscience* **28**, 5321 (2008).

89. Park, J., Koito, H., Li, J. & Han, A. Microfluidic Compartmentalized Co-Culture Platform for Cns Axon Myelination Research. *Biomedical Microdevices* **11**, 1145-1153 (2009).

90. Park, J.W., Vahidi, B., Taylor, A., Rhee, S.w. & Jeon, N.L. Microfluidic Culture Platform for Neuroscience Research. *Nature Protocols* **1**, 2128-2136 (2006).

91. Morales, R., Riss, M., Wang, L., Gavin, R., Rio, J.A.D. *et al.* Integrating Multi-Unit Electrophysiology and Plastic Culture Dishes for Network Neuroscience. *Lab on a Chip* **8**, 1896-1905 (2008).

92. Hong, C., Bao, D., Thomas, M.S., Clift, J.M. & Vullev, V.I. Print-and-Peel Fabrication of Microelectrodes. *Langmuir* **24**, 8439-8442 (2008).

93. McDonald, J.C., Duffy, D.C., Anderson, J.R., Chiu, D.T., Wu, H. *et al.* Fabrication of Microfluidic Systems in Poly(Dimethylsiloxane). *Electrophoresis* **21**, 27-40 (2000).

94. Desai, S.P., Freeman, D.M. & Voldman, J. Plastic Masters-Rigid Templates for Soft Lithography. *Lab on a Chip* **9**, 1631-1637 (2009).

95. Riboni, L., Prinetti, A., Bassi, R., Caminiti, A. & Tettamanti, G. A Mediator Role of Ceramide in the Regulation of Neuroblastoma Neuro2a Cell Differentiation. *Journal of Biological Chemistry* **270**, 26868 (1995).

96. Bielawska, A., Linardic, C.M. & Hannun, Y.A. Modulation of Cell Growth and Differentiation by Ceramide. *FEBS Letters* **307**, 211-214 (1992).

97. Geilen, C., Wieder, T. & Orfanos, C.E. Ceramide Signalling: Regulatory Role in Cell Proliferation, Differentiation and Apoptosis in Human Epidermis. *Archives of Dermatological Research* **289**, 559-566 (1997).

98. Chao, M.V. Ceramide: A Potential Second Messenger in the Nervous System. *Molecular and Cellular Neuroscience* **6**, 91-96 (1995).

99. Brugg, B., Michel, P.P., Agid, Y. & Ruberg, M. Ceramide Induces Apoptosis in Cultured Mesencephalic Neurons. *Journal of Neurochemistry* **66**, 733-739 (1996).

100. Park, J., Li, J. & Han, A. Micro-Macro Hybrid Soft-Lithography Master (Mmhsm) Fabrication for Lab-on-a-Chip Applications. *Biomedical Microdevices* **12**, 345-351 (2010).

101. Qiu, J., Cai, D. & Filbin, M. Glial Inhibition of Nerve Regeneration in the Mature Mammalian Cns. *Glia* **29**, 166-174 (2000).

102. Fitch, M. & Silver, J. Cns Injury, Glial Scars, and Inflammation: Inhibitory Extracellular Matrices and Regeneration Failure. *Experimental Neurology* **209**, 294-301 (2008).

103. Harel, N. & Strittmatter, S. Can Regenerating Axons Recapitulate Developmental Guidance During Recovery from Spinal Cord Injury? *Nature Reviews Neuroscience* **7**, 603-616 (2006).

104. Yiu, G. & He, Z. Glial Inhibition of Cns Axon Regeneration. *Nature Reviews Neuroscience* **7**, 617-627 (2006).

105. Park, K., Liu, K., Hu, Y., Smith, P., Wang, C. *et al.* Promoting Axon Regeneration in the Adult Cns by Modulation of the Pten/Mtor Pathway. *Science's STKE* **322**, 963-966 (2008).

106. Dal Toso, R., Giorgi, O., Soranzo, C., Kirschner, G., Ferrari, G. *et al.* Development and Survival of Neurons in Dissociated Fetal Mesencephalic Serum-Free Cell Cultures: I. Effects of Cell Density and of an Adult Mammalian Striatal-Derived Neuronotrophic Factor (Sdnf). *The Journal of Neuroscience* **8**, 733 (1988).

107. Goldberg, J.L., Klassen, M.P., Hua, Y. & Barres, B.A. Amacrine-Signaled Loss of Intrinsic Axon Growth Ability by Retinal Ganglion Cells. *Science* **296**, 1860 (2002).

108. Benowitz, L.I., Goldberg, D.E. & Irwin, N. Inosine Stimulates Axon Growth in Vitro and in the Adult Cns. *Progress in Brain Research* **137**, 389-399 (2002).

109. Goldberg, J.L., Vargas, M.E., Wang, J.T., Mandemakers, W., Oster, S.F. *et al.* An Oligodendrocyte Lineage-Specific Semaphorin, Sema5a, Inhibits Axon Growth by Retinal Ganglion Cells. *The Journal of Neuroscience* **24**, 4989 (2004).

110. Park, J., Koito, H., Li, J. & Han, A. Multi-Compartment Cns Neuron-Glia Co-Culture Platform. *Micro Total Analysis Systems* **13**, 1318-1320 (2009).

111. Hosmane, S., Yang, I.H., Ruffin, A., Thakor, N. & Venkatesan, A. Circular Compartmentalized Microfluidic Platform: Study of Axon–Glia Interactions. *Lab on a Chip* **10**, 741-747 (2010).

112. Wang, H., Katagiri, Y., McCann, T.E., Unsworth, E., Goldsmith, P. *et al.* Chondroitin-4-Sulfation Negatively Regulates Axonal Guidance and Growth. *Journal of Cell Science* **121**, 3083 (2008).

113. Lingor, P., Teusch, N., Schwarz, K., Mueller, R., Mack, H. *et al.* Inhibition of Rho Kinase (Rock) Increases Neurite Outgrowth on Chondroitin Sulphate Proteoglycan in Vitro and Axonal Regeneration in the Adult Optic Nerve in Vivo. *Journal of Neurochemistry* **103**, 181-189 (2007).

114. Cho, Y., Park, J., Park, H., Cheng, X., Kim, B. *et al.* Fabrication of High-Aspect-Ratio Polymer Nanochannels Using a Novel Si Nanoimprint Mold and Solvent-Assisted Sealing. *Microfluidics and Nanofluidics* **9**, 163-170 (2009).

115. Huang, J.K., Jarjour, A.A., Oumesmar, B.N., Kerninon, C., Williams, A. *et al.* Retinoid X Receptor Gamma Signaling Accelerates Cns Remyelination. *Nature Neuroscience* (2010).

116. Wagenaar, D. & Potter, S. A Versatile All-Channel Stimulator for Electrode Arrays, with Real-Time Control. *Journal of Neural Engineering* (2004).

117. James, C., Spence, A., Dowell-Mesfin, N., Hussain, R., Smith, K. *et al.* Extracellular Recordings from Patterned Neuronal Networks Using Planar Microelectrode Arrays. *IEEE Transactions on Biomedical Engineering* **51**, 1640-1646 (2004).

118. Gross, G.W., Rhoades, B.K., Reust, D.L. & Schwalm, F.U. Stimulation of Monolayer Networks in Culture through Thin-Film Indium-Tin Oxide Recording Electrodes. *Journal of Neuroscience Methods* **50**, 131-143 (1993).

119. Maher, M.P., Pine, J., Wright, J. & Tai, Y.C. The Neurochip: A New Multielectrode Device for Stimulating and Recording from Cultured Neurons. *Journal of Neuroscience Methods* **87**, 45-56 (1999).

120. Wagenaar, D.A., Pine, J. & Potter, S.M. Effective Parameters for Stimulation of Dissociated Cultures Using Multi-Electrode Arrays. *Journal of Neuroscience Methods* **138**, 27-37 (2004).

121. Dworak, B.J. & Wheeler, B.C. Novel Mea Platform with PDMS Microtunnels Enables the Detection of Action Potential Propagation from Isolated Axons in Culture. *Lab on a Chip* **9**, 404-410 (2009).

122. Ravula, S.K., Wang, M.S., Asress, S.A., Glass, J.D. & Frazier, A.B. A Compartmented Neuronal Culture System in Microdevice Format. *Journal of Neuroscience Methods* **159**, 78-85 (2007).

123. Ravula, S., McClain, M., Wang, M., Glass, J. & Frazier, A. A Multielectrode Microcompartment Culture Platform for Studying Signal Transduction in the Nervous System. *Lab on a Chip* **6**, 1530-1536 (2006).

124. Morin, F., Nishimura, N., Griscom, L., LePioufle, B., Fujita, H. *et al.* Constraining the Connectivity of Neuronal Networks Cultured on Microelectrode Arrays with Microfluidic Techniques: A Step Towards Neuron-Based Functional Chips. *Biosensors and Bioelectronics* **21**, 1093-1100 (2006).

125. Claverol-Tinture, E., Ghirardi, M., Fiumara, F., Rosell, X. & Cabestany, J. Multielectrode Arrays with Elasomeric Microstructured Overlays for Extracellular Recordings from Patterned Neurons. *Journal of Neural Engineering* **2**, L1-L7 (2005).

126. Murphy, T.H., Blatter, L.A., Wier, W.G. & Baraban, J.M. Spontaneous Synchronous Synaptic Calcium Transients in Cultured Cortical Neurons. *Journal of Neuroscience* **12**, 4834-4845 (1992).

127. Meda, L., Cassatella, M.A., Szendrei, G.I., Otvos, L., Jr., Baron, P. *et al.* Activation of Microglial Cells by Beta-Amyloid Protein and Interferon-Gamma. *Nature* **374**, 647-650. (1995).

128. Opitz, T., De Lima, A.D. & Voigt, T. Spontaneous Development of Synchronous Oscillatory Activity During Maturation of Cortical Networks in Vitro. *Journal of Neurophysiology* **88**, 2196-2206 (2002).

129. Gyllensten, L. & Malmfors, T. Myelinization of the Optic Nerve and Its Dependence on Visual Function--a Quantitative Investigation in Mice. *Journal of Embryology and Experimental Morphology* **11**, 255-266 (1963).

130. Tauber, H., Waehneldt, T.V. & Neuhoff, V. Myelination in Rabbit Optic Nerves Is Accelerated by Artificial Eye Opening. *Neuroscience Letters* **16**, 235-238 (1980).

131. Demerens, C., Stankoff, B., Logak, M., Anglade, P., Allinquant, B. *et al.* Induction of Myelination in the Central Nervous System By electrical activity.

Proceedings of the National Academy of Sciences of the United States of America **93**, 9887-9892 (1996).

132. Stevens, B., Tanner, S. & Fields, R.D. Control of Myelination by Specific Patterns of Neural Impulses. *Journal of Neuroscience* **18**, 9303-9311 (1998).

133. Itoh, K., Stevens, B., Schachner, M. & Fields, R.D. Regulated Expression of the Neural Cell Adhesion Molecule L1 by Specific Patterns of Neural Impulses. *Science* **270**, 1369-1372 (1995).

134. Barres, B.A. & Raff, M.C. Axonal Control of Oligodendrocyte Development. *Journal of Cell Biology* **147**, 1123-1128 (1999).

135. Yuan, X., Eisen, A.M., McBain, C.J. & Gallo, V. A Role for Glutamate and Its Receptors in the Regulation of Oligodendrocyte Development in Cerebellar Tissue Slices. *Development* **125**, 2901-2914 (1998).

136. Huang, Y. & Rubinsky, B. Microfabricated Electroporation Chip for Single Cell Membrane Permeabilization. *Sensors and Actuators, A: Physical* **89**, 242-249 (2001).

137. Lin, L. & Pisano, A.P. Silicon-Processed Microneedles. *Journal of Microelectromechanical Systems* **8**, 78-84 (1999).

138. Pancrazio, J., Bey, P., Loloee, A., Manne, S., chao, H.-c. *et al.* Description and Demonstration of a Cmos Amplifier-Based-System with Measurement and Stimulation Capability for Bioelectrical Signal Transduction. *Biosensors and Bioelectronics* **13**, 971-979 (1998).

139. Mercanzini, A., Cheung, K., Buhl, D.L., Boers, M., Maillard, A. *et al.* Demonstration of Cortical Recording Using Novel Flexible Polymer Neural Probes. *Sensors and Actuators, A: Physical* **143**, 90-96 (2008).

140. Lee, K., Singh, A., He, J., Massia, S., Kim, B. *et al.* Polyimide Based Neural Implants with Stiffness Improvement *Sensors and Actuators, B: Chemical* **102**, 67-72 (2004).

141. Duport, S., Millerin, Muller & Correges A Metallic Multisite Recording System Designed for Continuous Long-Term Monitoring of Electrophysiological Activity in Slice Cultures. *Biosensors and Bioelectronics* **14**, 369-376 (1999).

142. Chiang, W.-Y. & Shu, W.-J. Preparation and Properties of Uv-Curable Polydimethylsiloxane Urethane Acrylate. *Angewandte Makromolekulare Chemie* **160**, 41-66 (1987).

143. Choi, K.M. & Rogers, J.A. Novel Chemical Approach to Achieve Advanced Soft Lithography by Developing New Stiffer, Photocurable PDMS Stamp Materials. *Material Research Society* **820**, O6.2.1-O6.2.8 (2004).

144. Tsougeni, K., Tserepi, A. & Gogolides, E. Photosensitive Poly(Dimethylsiloxane) Materials for Microfluidic Applications. *Microelectronic Engineering* **84**, 1104-4108 (2007).

145. Ryu, K.S., Wang, X., Shaikh, K. & Liu, C. A Method for Precision Patterning of Silicone Elastomer and Its Applications. *Journal of Microelectromechanical Systems* **13**, 568-575 (2004).

146. Eon, D., Poucques, L.d., Peignon, M.C., Cardinaud, C., Turban, G. *et al.* Surface Modification of Si-Containing Polymers During Etching for Bilayer Lithography. *Microelectronic Engineering* **61-62**, 901-906 (2002).

147. Tong, J., Simmons, C.A. & Sun, Y. Precision Patterning of PDMS Membranes and Applications. *Journal of Micromechanics and Microengineering* **18**, 037004 (2008).

148. Oh, S.R. Thick Single-Layer Positive Photoresist Mold and Poly(Dimethylsiloxane) (PDMS) Dry Etching for the Fabrication of a Glass-PDMS-Glass Microfluidic Device. *Journal of Micromechanics and Microengineering* **18**, 115025 (2008).

149. Ostuni, E., Kane, R., Chen, C.S., Ingber, D.E. & Whitesides, G.M. Patterning Mammalian Cells Using Elastomeric Membranes. *Langmuir* **16**, 7811-7819 (2000).

150. Jackman, R.J., Duffy, D.C., Cherniavskaya, O. & Whitesides, G.M. Using Elastomeric Membranes as Dry Resists and for Dry Lift-Off. *Langmuir* **15**, 2973-2984 (1999).

151. Park, J., Kim, H.S. & Han, A. Micropatterning of Poly(Dimethylsiloxane) Using a Photoresist Lift-Off Technique for Selective Electrical Insulation of Microelectrode Arrays. *Journal of Microelectromechanical Systems* **19**, 065016 (2009).

152. Bhagat, A.A.S., Jothimuthu, P., Pais, A. & Papautsky, I. Re-Usable Quick-Release Interconnect for Characterization of Microfluidic Systems. *Journal of Micromechanics and Microengineering* **17**, 42-49 (2007).

153. Christensen, A., Chang-Yen, D. & Gale, B. Characterization of Interconnects Used in PDMS Microfluidic Systems. *Journal of Micromechanics and Microengineering* **15**, 928-934 (2005).

154. Thorsen, T., Maerki, S.J. & Quake, S.R. Microfluidic Large-Scale Integration. *Science* **298**, 580-585 (2002).

APPENDIX A

1. OTHER APPLICATIONS OF MMHMS PROCESS

A PDMS microfluidic device having integrated fluidic interfaces and reservoirs was fabricated to show the validity of the method for a one-step integrated world-to-chip interface fabrication process. The device ($50 \times 50 \times 3.5$ mm^3) was composed of 40 sets of 1.2 mm diameter fluidic interfaces for connection with commonly used 1.58 mm diameter polymer tubings, and two 6 mm diameter reservoirs connected through 500 μm wide and 20 μm high microfluidic channels (Figure A.1A). The device was fabricated using the same process introduced in the previous section. Figure A.1B-D shows SEM images of the PMMA master, PDMS master, and PDMS device for the 40 fluidic interfaces integrated microdevice fabricated by the MMHSM process. The bottom part of the 1.2 mm diameter pillars was enlarged to 1.8 mm to make it more mechanically robust (Figure A.1C). In order to confirm that the original geometry of the pattern was not distorted during the MMHSM fabrication process, average width/depth of microchannels from the PMMA master, the PDMS master, and the PDMS device were compared using SEM images and optical surface profile measurements (Figure A.2). The average width and depth of channels changed from 515.8 ± 5.9 μm (PMMA master, $n = 10$) to 515.7 ± 2.7 μm (PDMS device, $n = 4$) and from 21.3 ± 0.8 μm (PMMA master, $n = 8$) to 21.7 ± 0.8 μm (PDMS device, $n = 6$), respectively. The dimension changes were less than 1.88%, showing that almost no changes had been made during the replication process and that this process is very reliable.

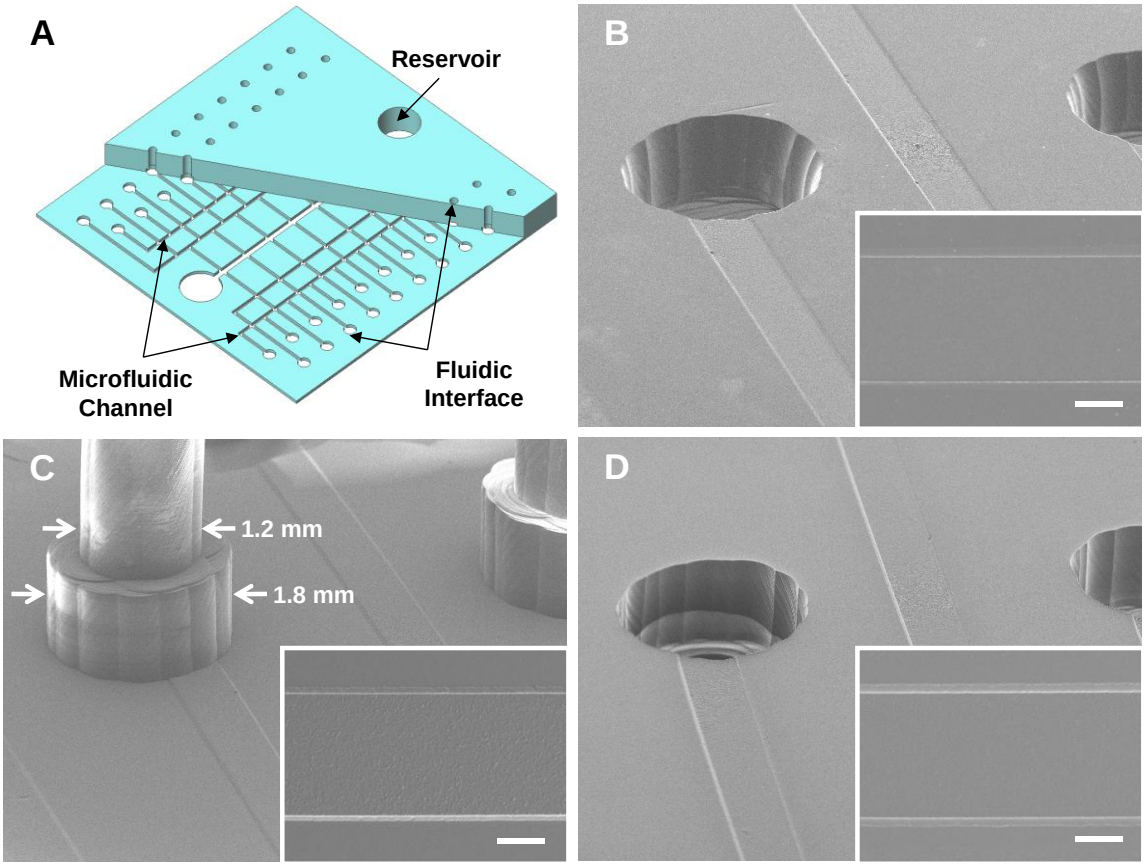

Figure A.1. (A) Schematic illustrations of PDMS microfluidic device with 40 integrated fluidic interfaces and two reservoirs. (B) PMMA master, (C) PDMS master, and (D) PDMS device showing microchannels connected to millimeter-scale fluidic interfaces (Insets: Enlarged view of 500 μm wide channels). Scale bars: 200 μm.

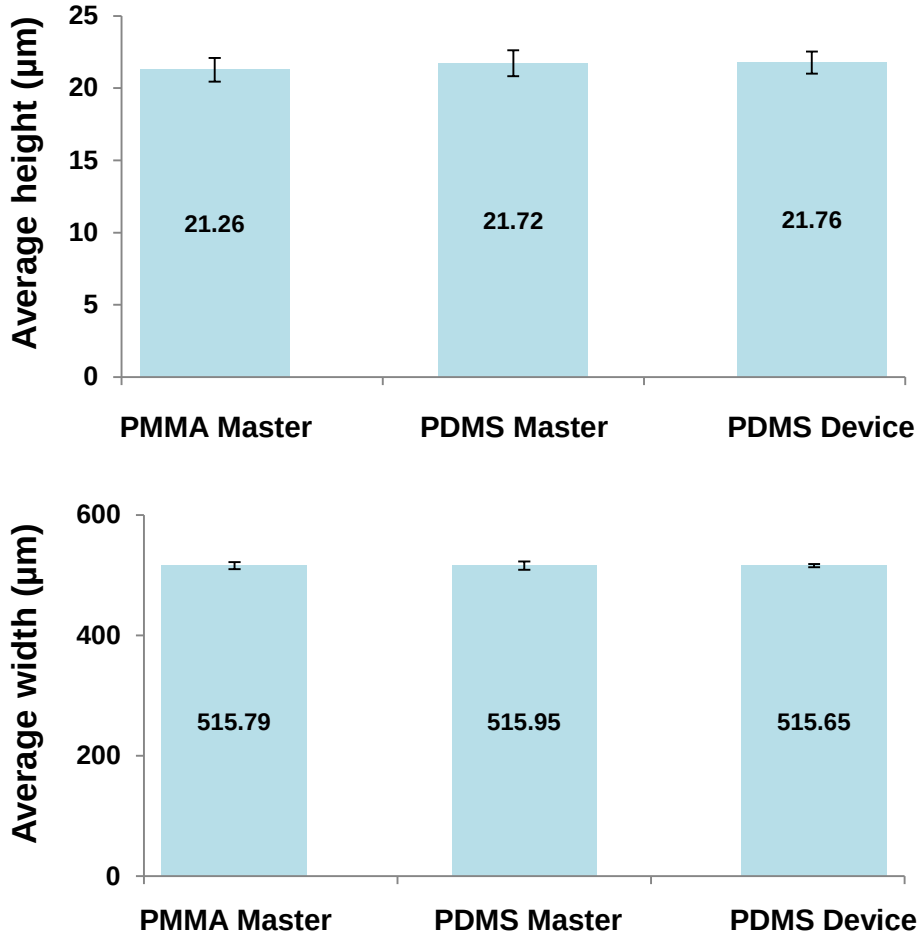

Figure A.2. Average height and width of the microchannels in the PMMA master, PDMS master and final PDMS device fabricated through the MMHSM process.

Finally, 40 Teflon FEP tubings (Ø 1.58 mm) were inserted into the PDMS device with integrated fluidic interfaces (Figure A.3A). Fluids were introduced through the 40 fluidic inlets and were successfully collected at two reservoirs without any leakage at the interface. To further investigate the robustness of the fluidic interface, a pressure threshold experiment was conducted. Schematic illustration of the experimental setup is shown in Figure A.3B. A PDMS device with the integrated fluidic interfaces was bonded on a glass substrate after oxygen plasma treatment, followed by Teflon® tubing insertion. Water droplets were applied around the inserted tubings to observe leakage while applying pressure to the fluidic interface. The fluidic interface did not show any leakage for applied pressure of up to 345 kPa. Although some fluidic connections using clamps provide stronger pressure tolerance[152], most bio/medical microfluidic experiments do not require high pressure. The pressure tolerance of 345 kPa obtained through our fluidic interface is comparable to other widely used press-fit type fluidic interfaces.[153, 154] The MMHSM fabrication process presented in this paper is not limited to fluidic interfaces or reservoirs, and can be widely used for a broad range of applications requiring both micro and macro scale structures in a single system.

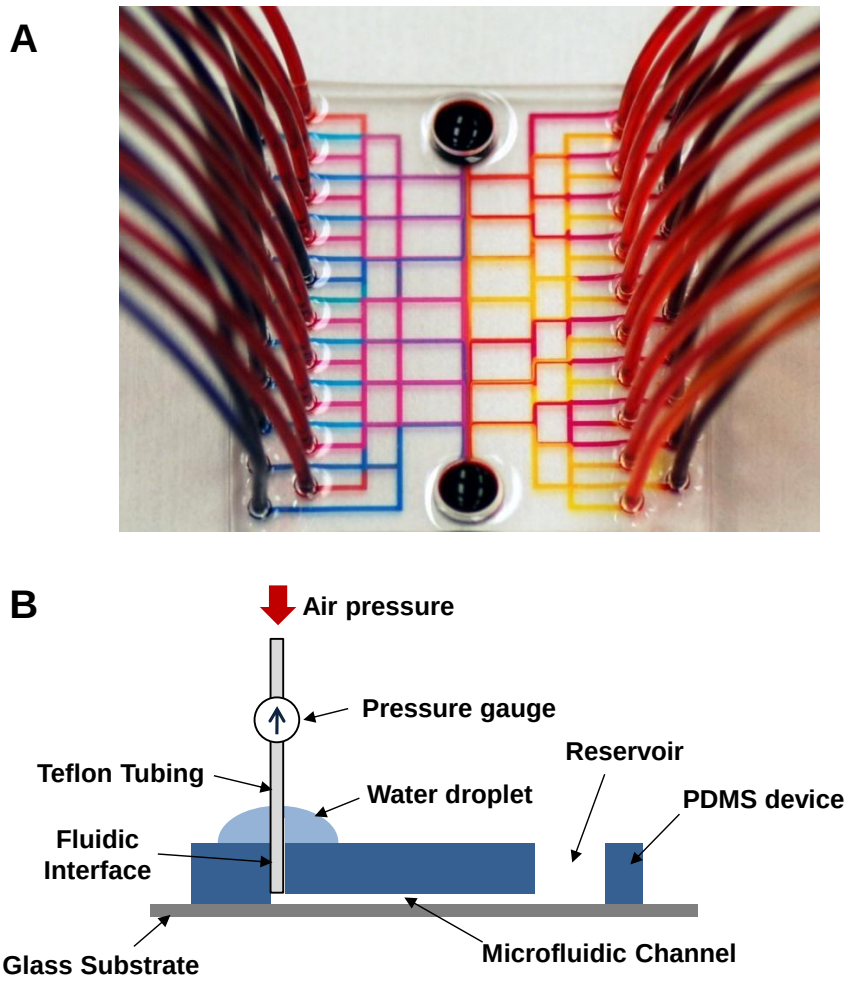

Figure A.3. (A) A photographic image of a 3.5 mm thick PDMS microfluidic device (50 × 50 mm^2) with 40 Teflon tubings connected to the integrated fluidic interfaces. Four different color dyes were used for visualization. (B) Schematic illustration showing the pressure threshold experimental setup.

APPENDIX B

1. MASKS

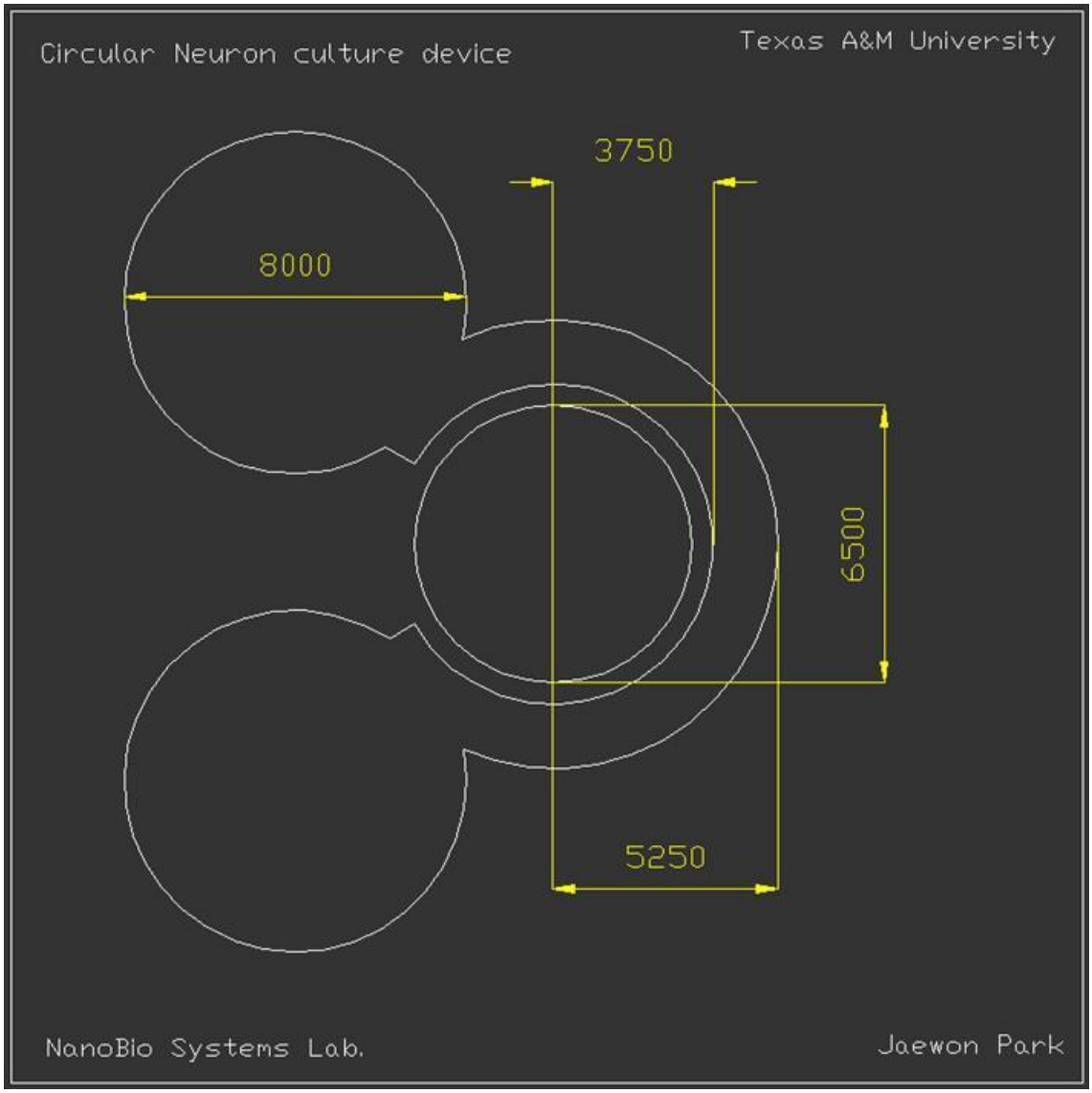

Figure B. 1. Circular neuron co-culture device, cell culture chamber (Circular chamber.dwg).

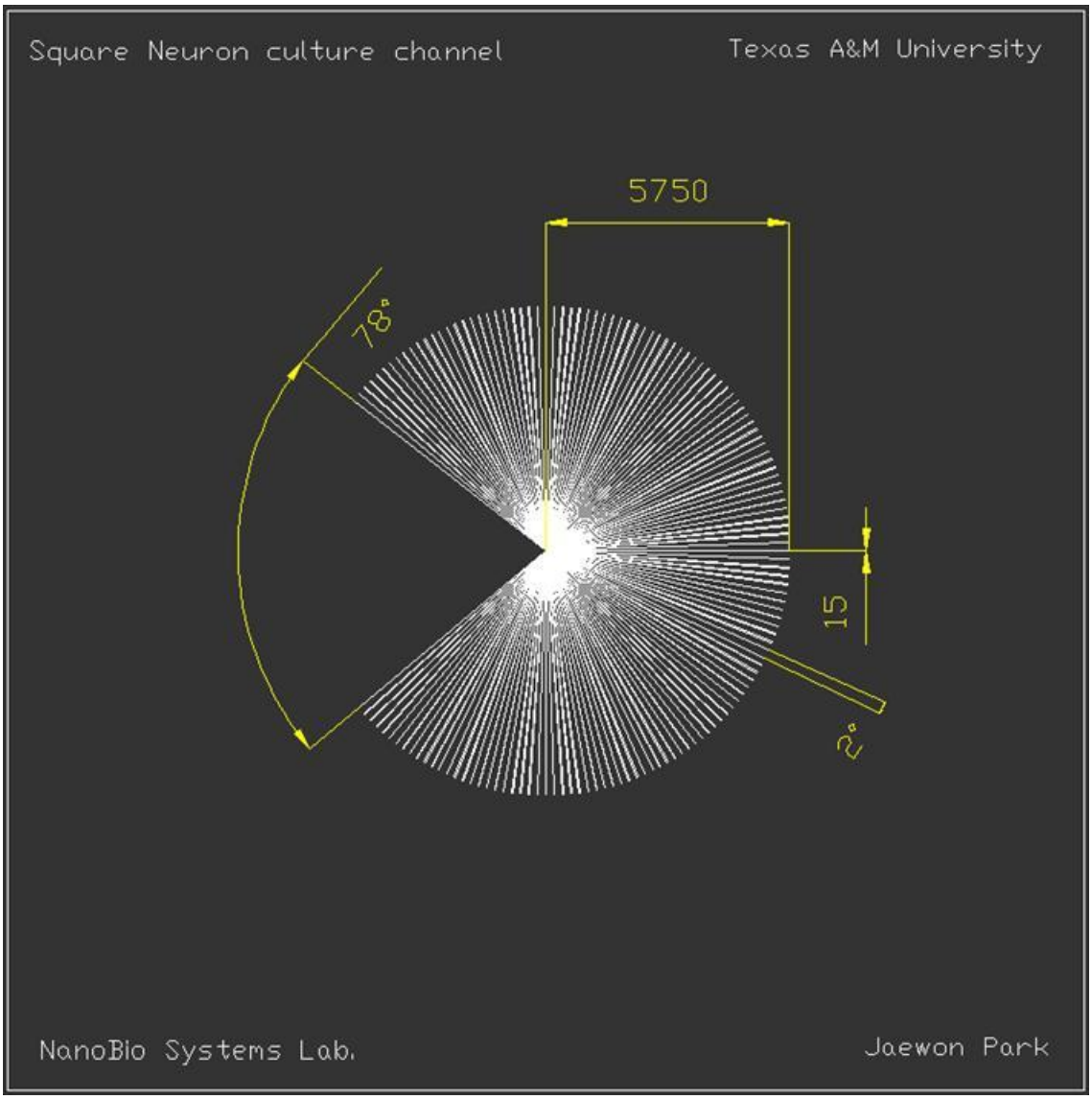

Figure B. 2. Circular neuron co-culture device, axon-guiding channels (Circular channel.dwg).

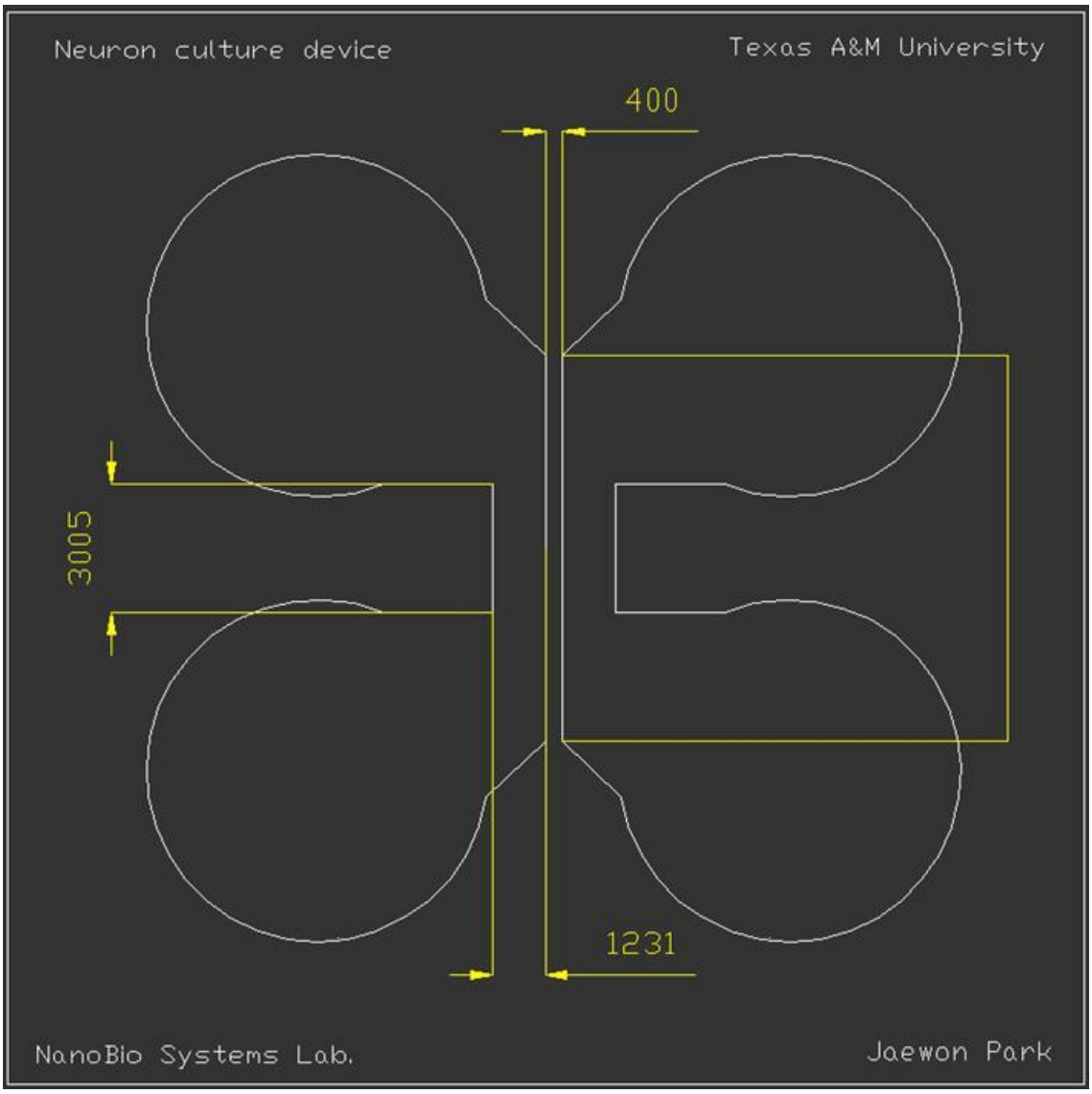

Figure B. 3. Square neuron co-culture device, cell culture chamber (Square chamber.dwg).

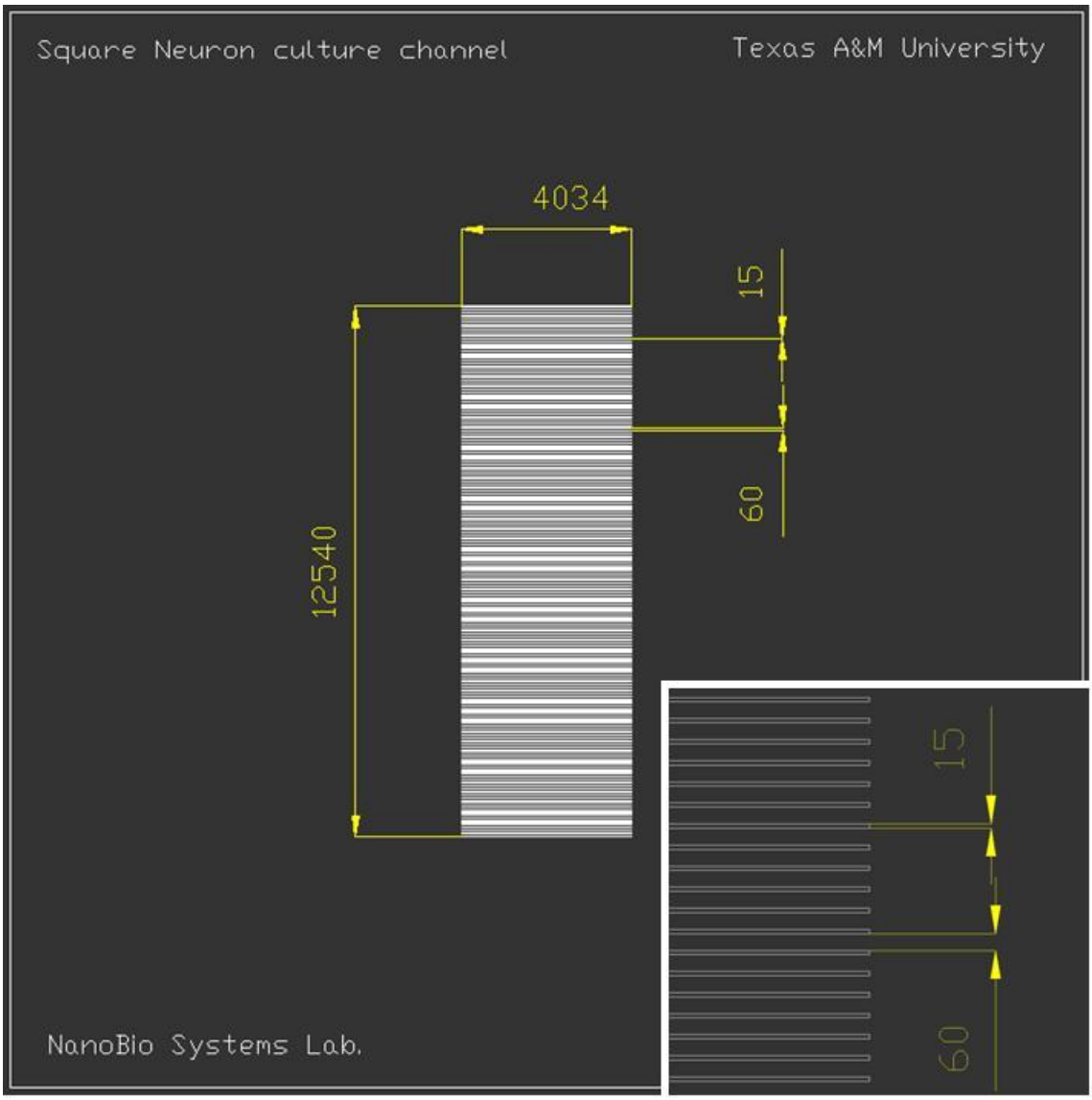

Figure B. 4. Square neuron co-culture device, axon-guiding channels (Square channel.dwg).

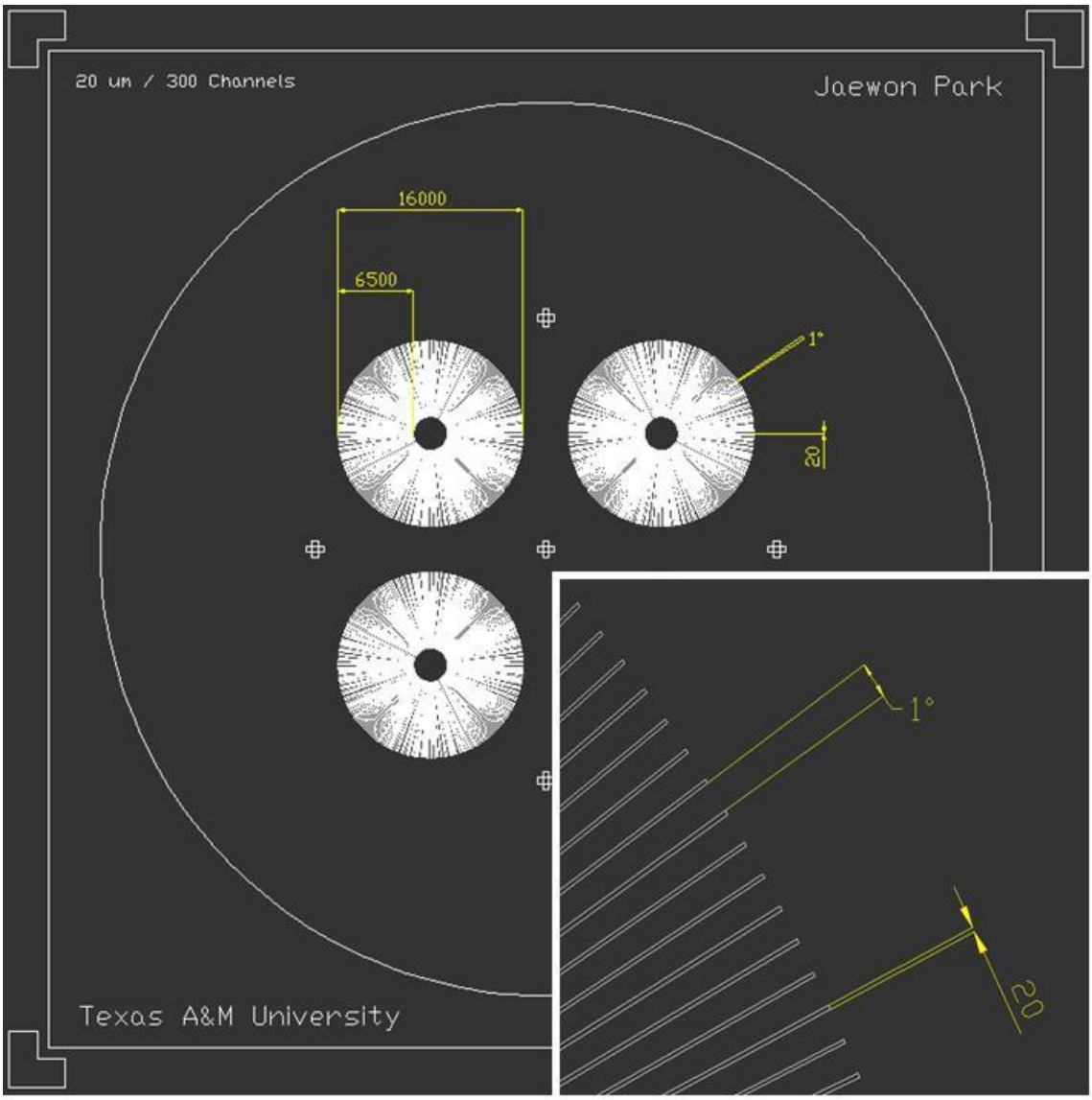

Figure B. 5. Six compartment neuron co-culture device, imprint master (Six compartment imprint master.dwg).

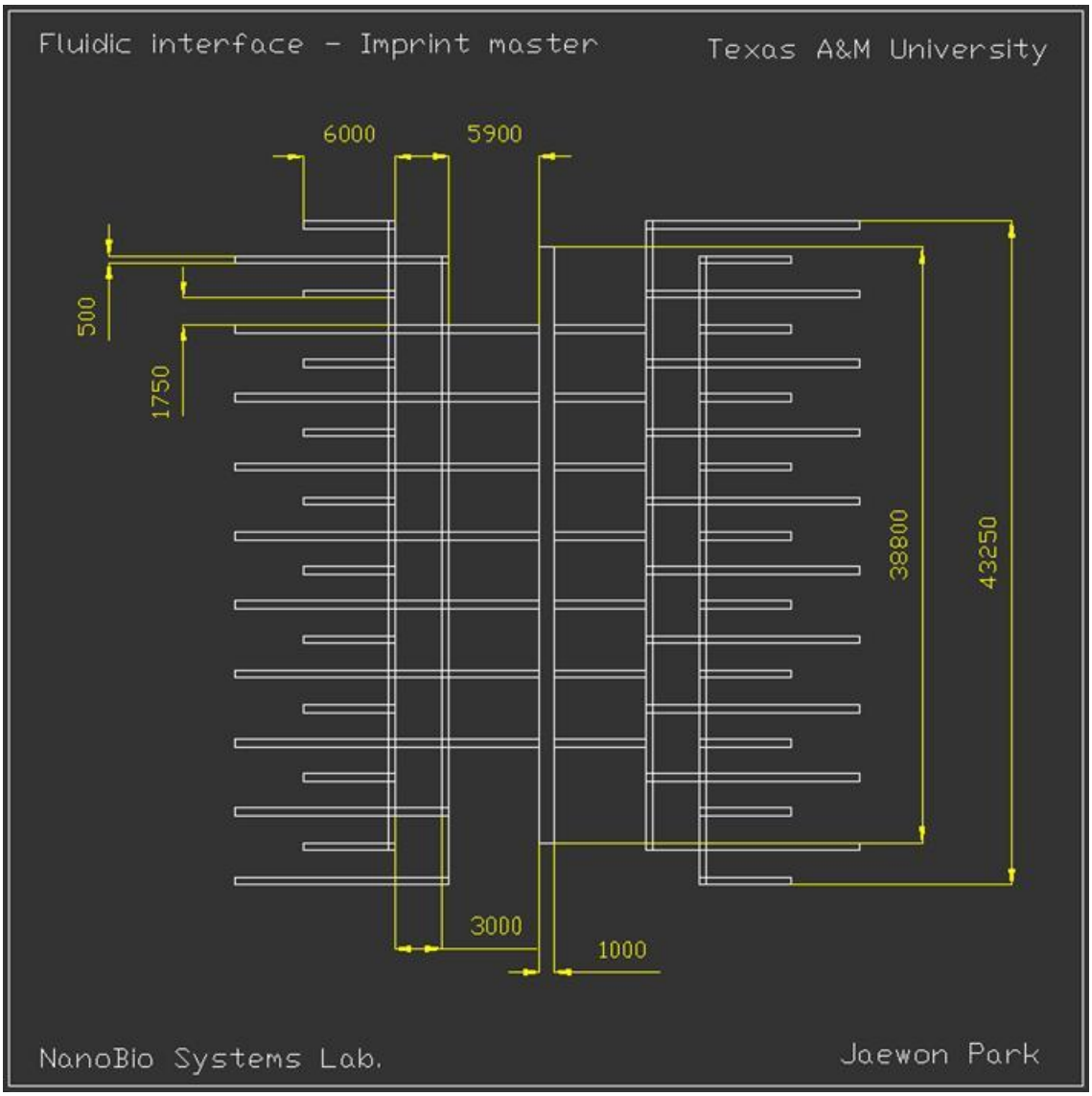

Figure B. 6. MMHSM fluidic interface application, imprint master (Fluidic interface for MMHSM.dwg).

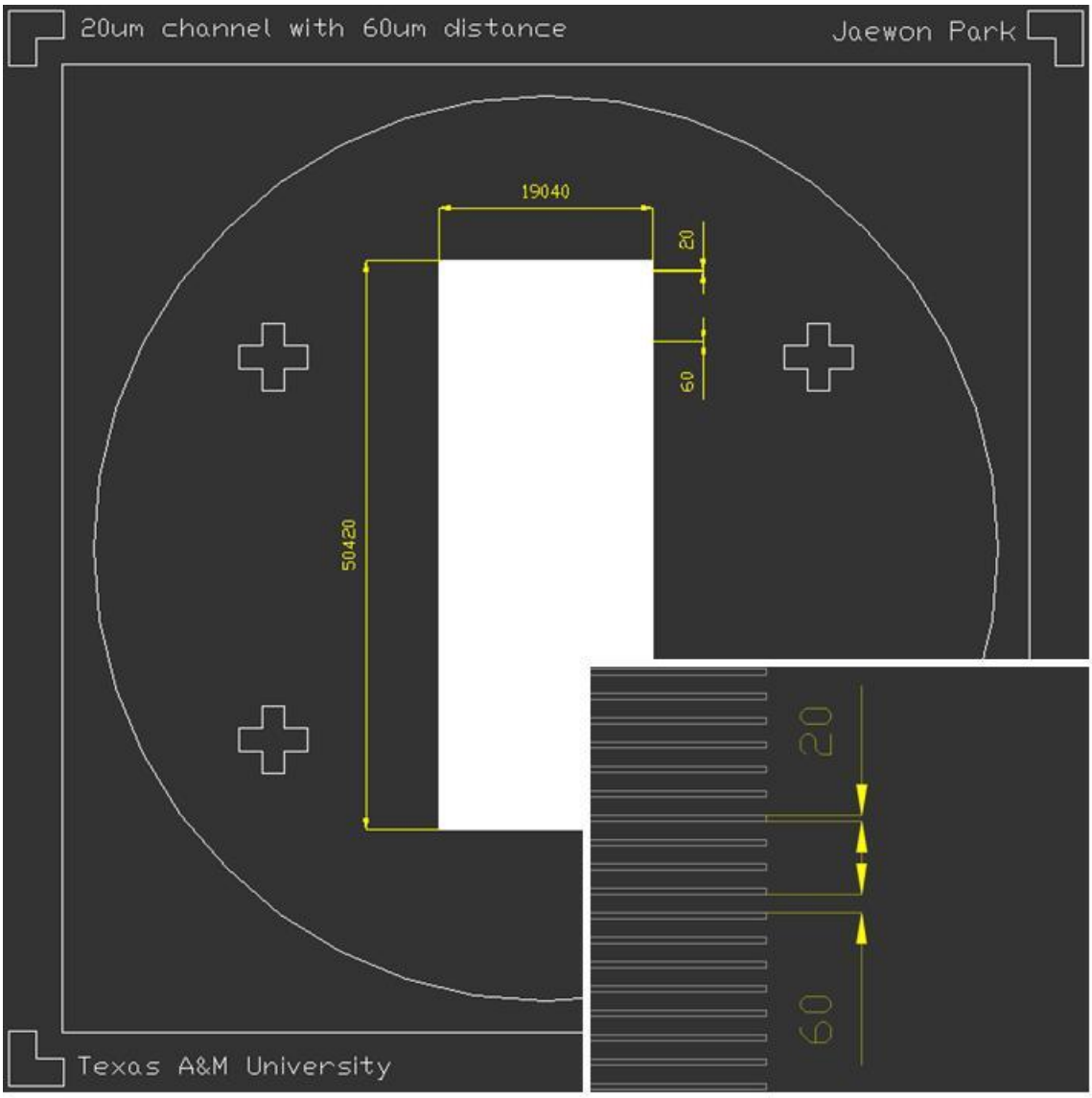

Figure B. 7. 24-compartment neuron co-culture device, imprint master (24 compartment channels.dwg).

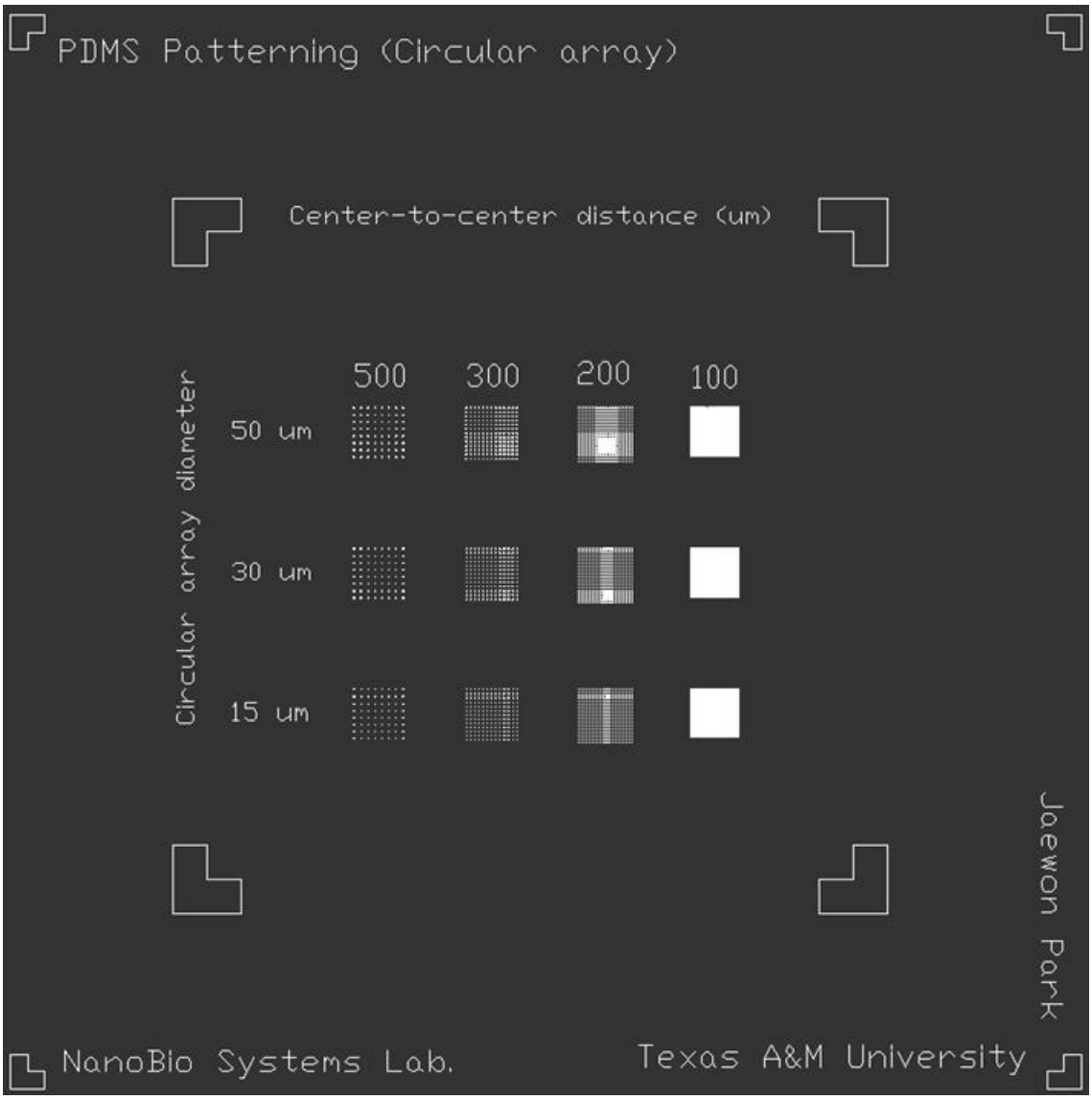

Figure B. 8. Circular arrays for PDMS lift-off patterning characterization (PDMS Patterning-circular array.dwg).

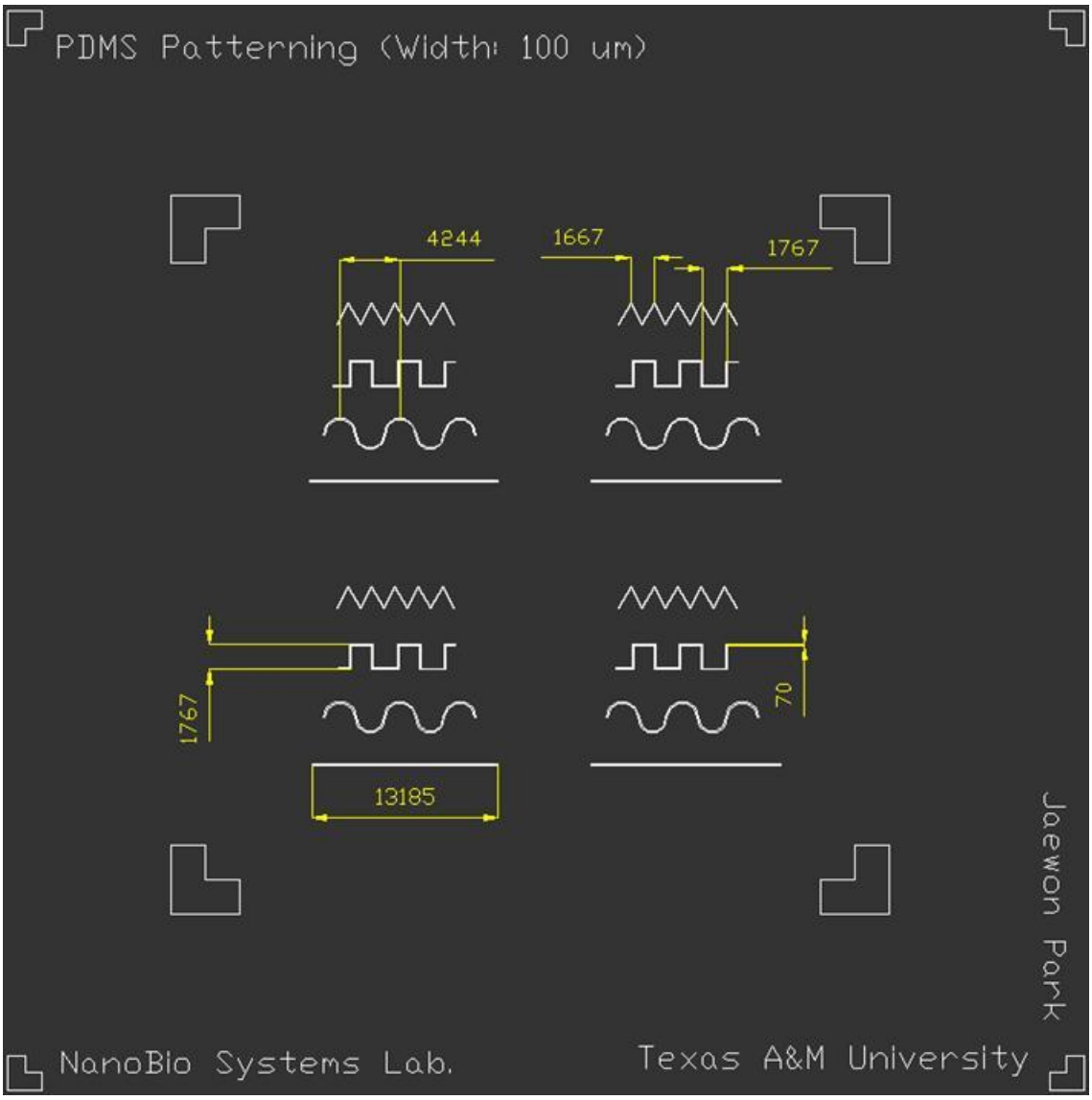

Figure B. 9. Various channel designs for PDMS lift-off patterning (PDMS Patterning-channels.dwg).

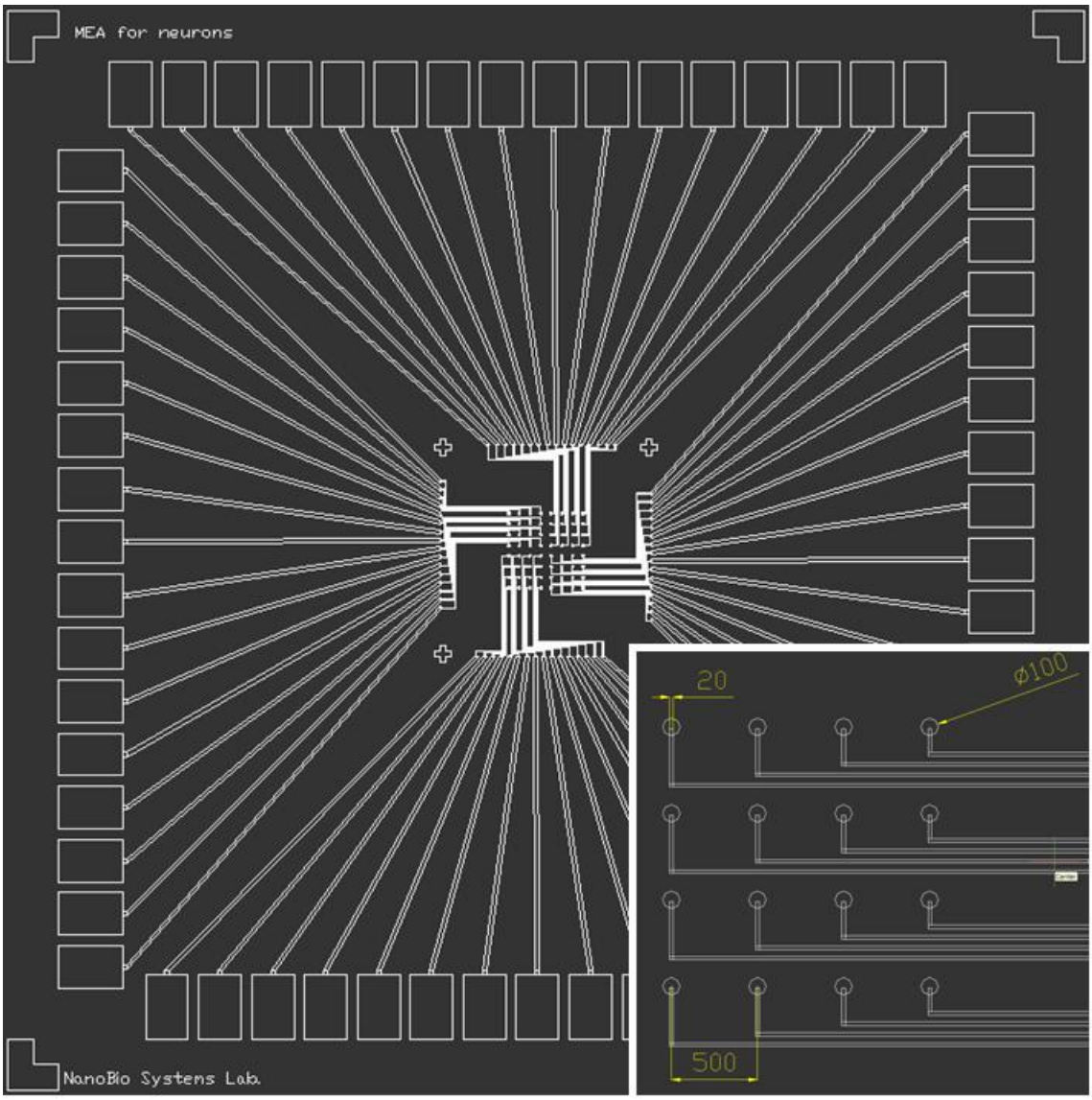

Figure B. 10. Multi-electrode array for electrical stimulation/recording of neurons (MEA for neurons.dwg).

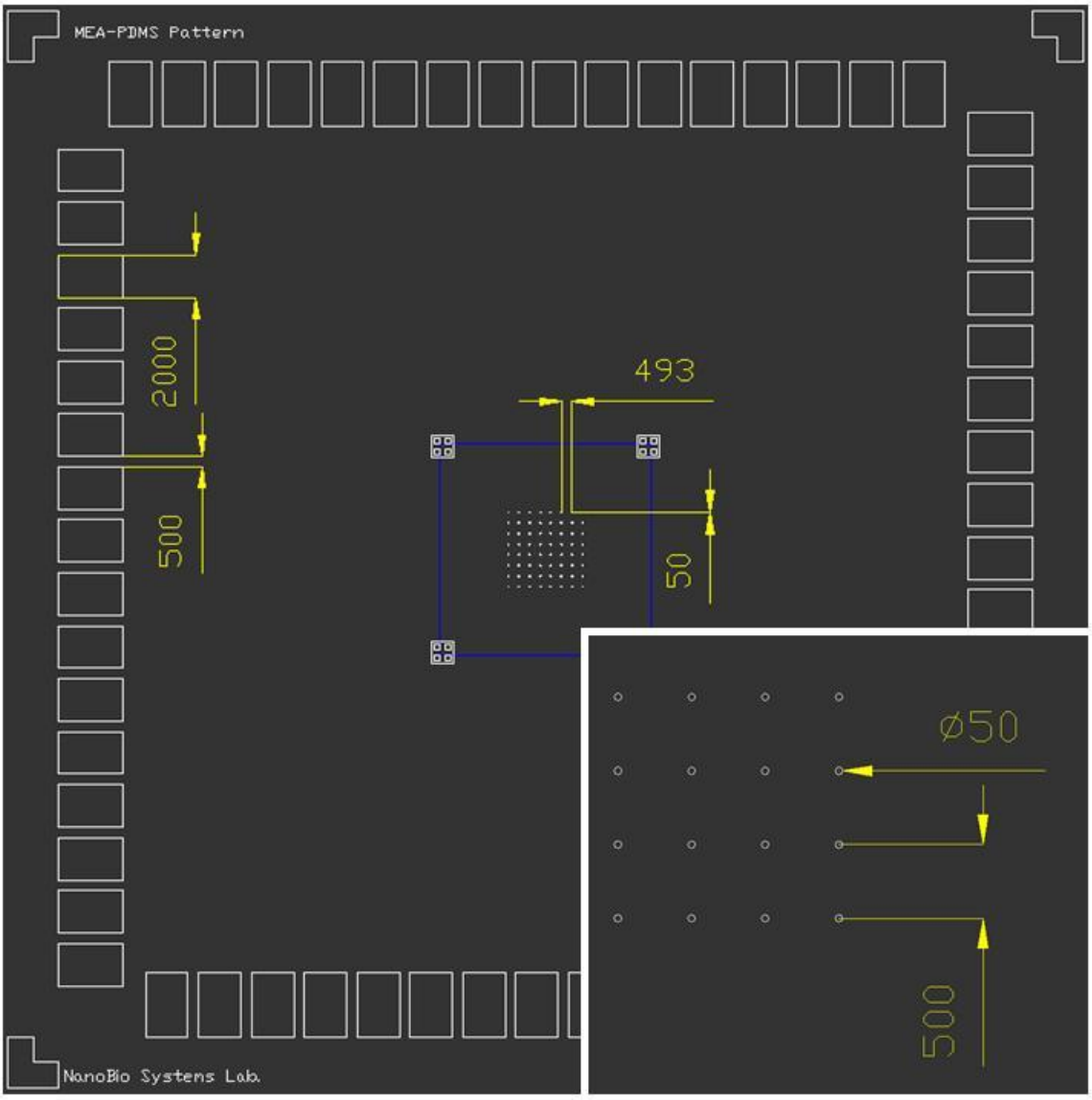

Figure B. 11. PDMS patterning sacrificial layer for MEA recording pads (PDMS patterning for MEA.dwg).

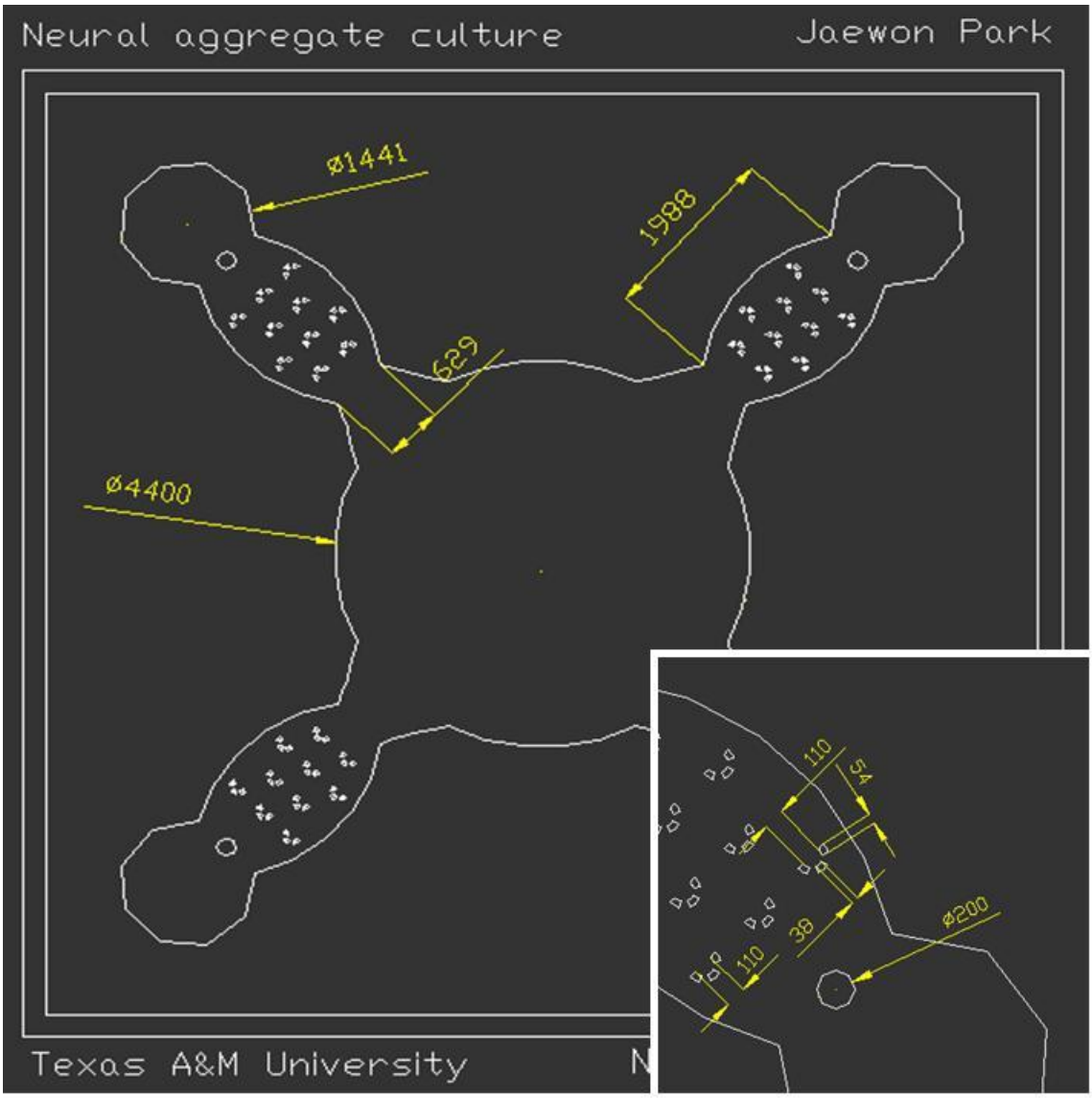

Figure B. 12. Neural aggregate culture platform for CNS myelination study (Neuron aggregate.dwg).

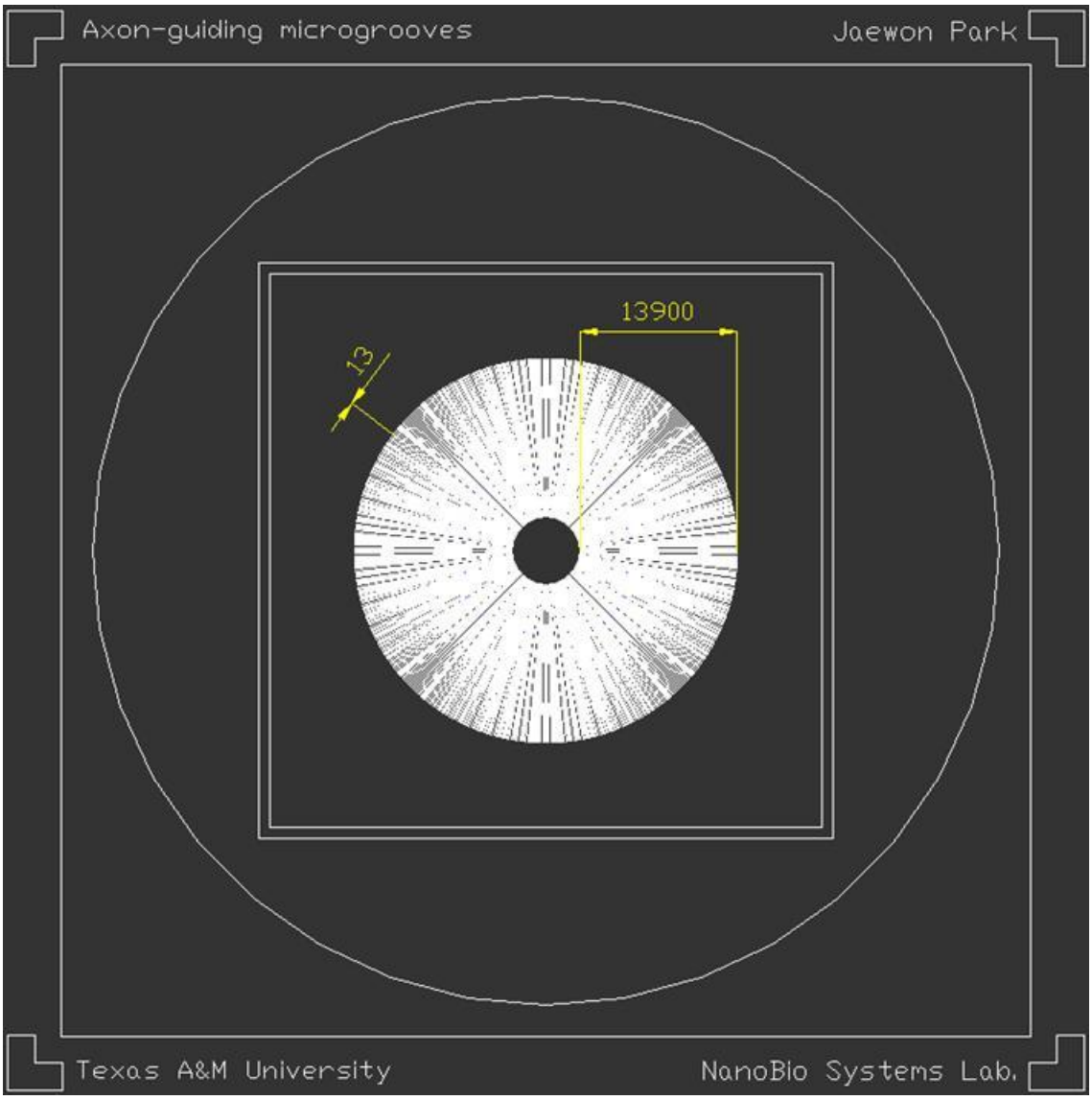

Figure B. 13. Axon-guiding microgrooves for six compartment device (Axon-guiding microchannels.dwg).

2. PMMA MOLD DESIGNS

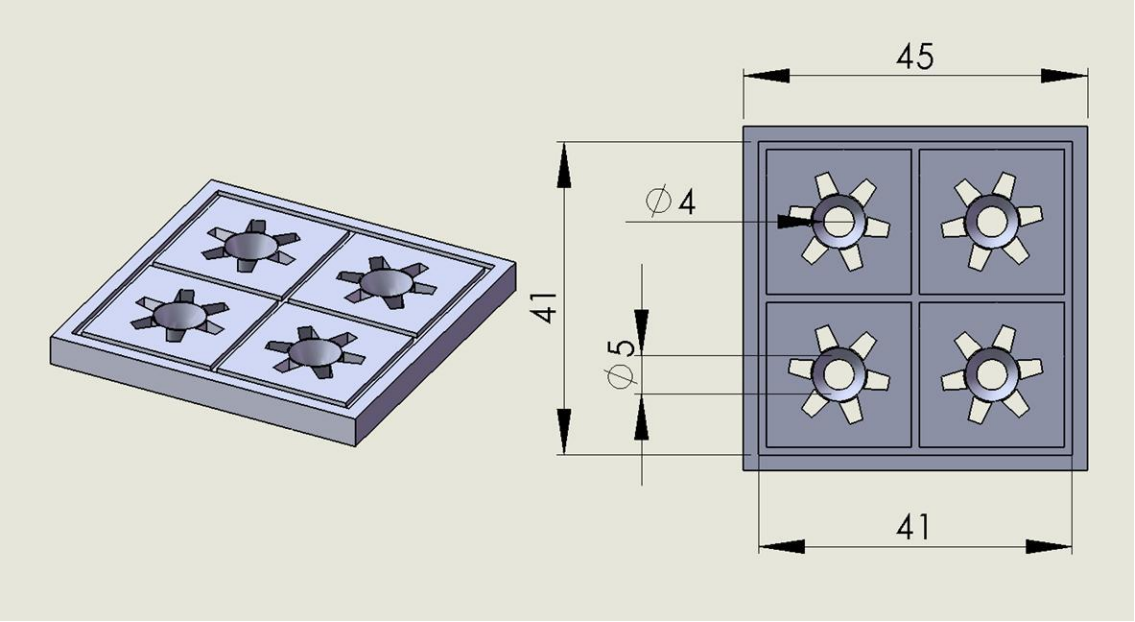

Figure B. 14. Six-compartment neuron co-culture device.

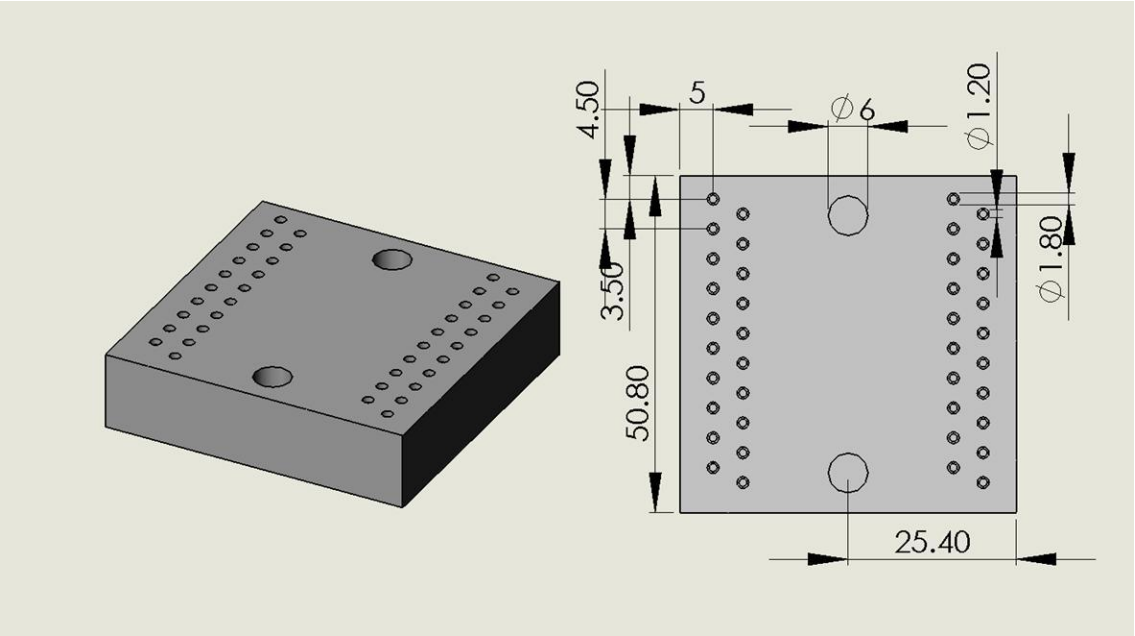

Figure B. 15. MMHSM fluidic interface application.

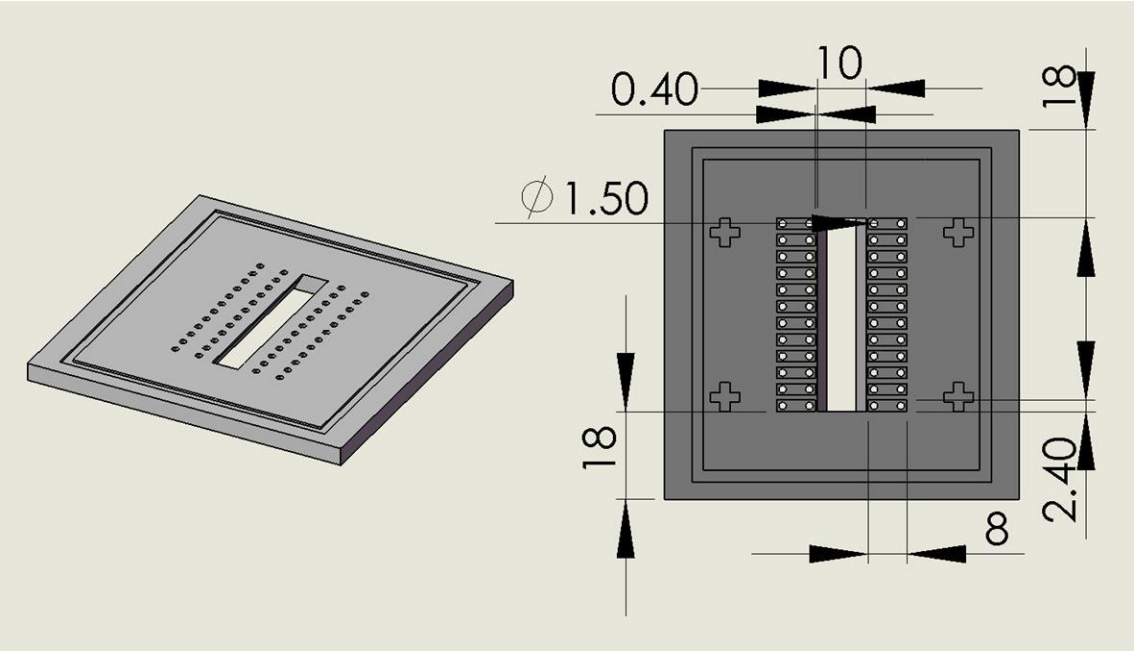

Figure B. 16. 24-compartment neuron culture device, compartment layer mold.

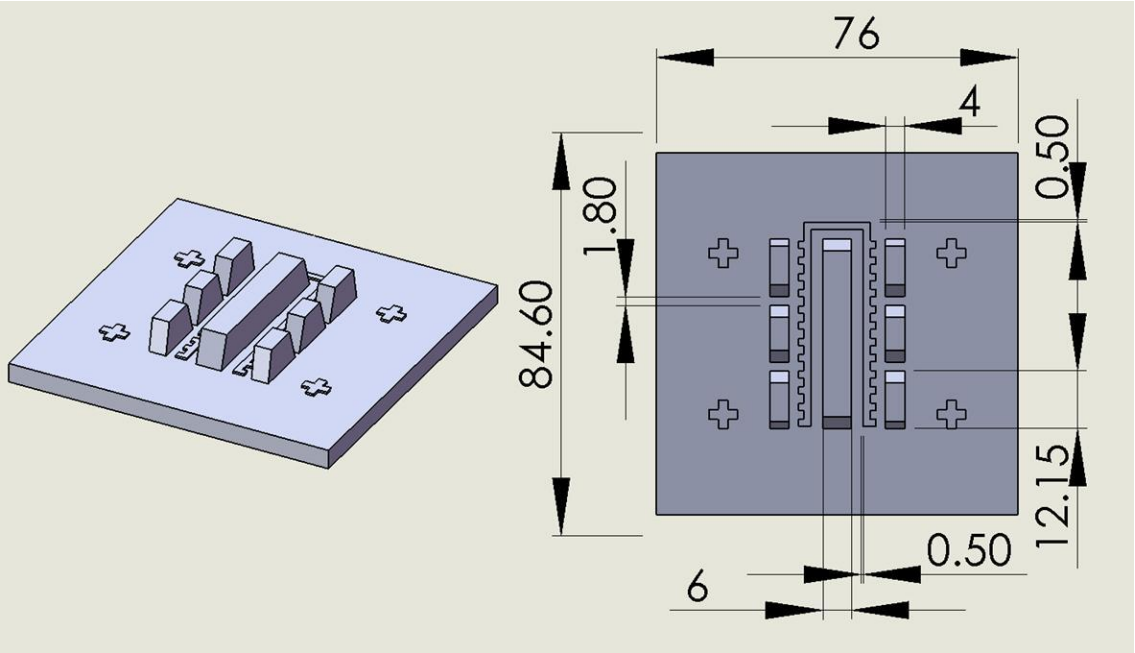

Figure B. 17. 24-compartment neuron culture device, cell loading layer mold.

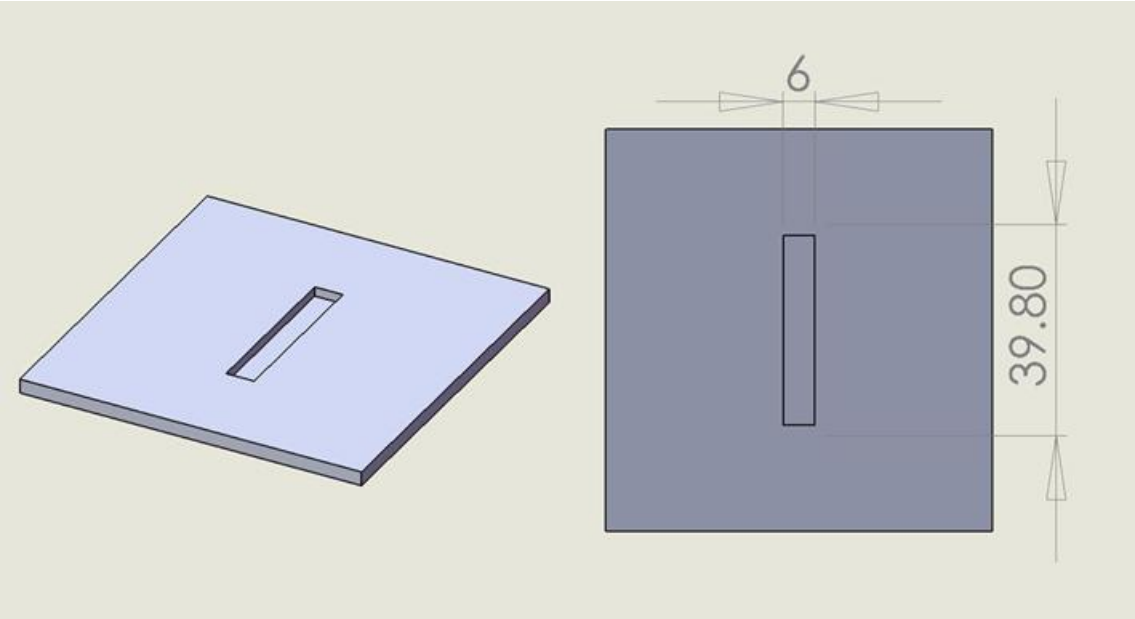

Figure B. 18. 24-compartment neuron culture device, substrate layer mold.

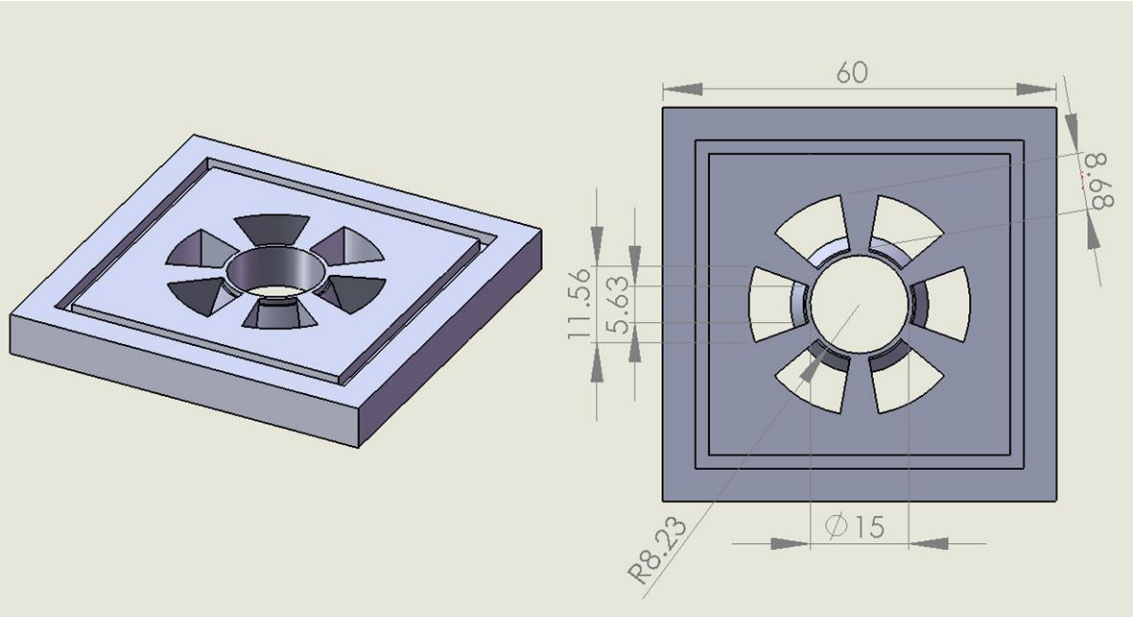

Figure B. 19. Six-compartment axon growth analysis platform, compartment layer.

APPENDIX C

Protocol I. PDMS Soft-lithography

- Mix PDMS pre-polymer (Sylgard 184, Dow corning, Inc.) with curing agent (10:1 w/w)
- Pour the PDMS mixture over the soft-lithography master mold
- Remove bubbles by degassing the PDMS mixture inside a vacuum chamber for 10-30 min
- Place the degassed PDMS inside a leveled 85°C oven for at least 45 min for polymerization
- Peel off the polymerized PDMS layer from the master mold

Protocol II. Soft-lithography Master Mold Surface Coating

- Vapor coat PDMS soft-lithography master mold with (tridecafluoro-1,1,2,2-tetrahydrooctyl) trichlorosilane inside a vacuum chamber for 5-15 min
- Rinse the coated sample with IPA
- Dry IPA with N_2 gas

Protocol III. Circular CNS Neuron/Glia Co-Culture Microdevice

- Silicon master mold fabrication: Photolithography
    - ✓ Axon-guiding microchannels
        - Photoresist: SU-8™ 2002
        - Spin-coat: 30 sec at 750 rpm
        - Soft bake: 5 min at 95 °C
        - Exposure: 105 mJ/cm^2 (MJB3, Karl Suss)
        - Post exposure bake: 5 min at 95 °C
        - Develop in Thinner P
    - ✓ Cell culture compartments
        - Photoresist: SU-8™ 2075
        - Spin-coat: 5 sec at 500 rpm + 30 sec at 2000 rpm
        - Soft bake: 5 min at 65 °C + 20 min at 95 °C
        - Exposure: 230 mJ/cm^2 (MJB3, Karl Suss)
        - Post exposure bake: 5 min at 65 °C + 15 min at 95 °C
        - Develop in Thinner P
- Surface coating (Protocol II)
- Device replication
    - ✓ PDMS soft-lithography (Protocol I)
- Punch the soma compartment and reservoirs using a 7 mm punch bit
- Treat PDMS device with oxygen plasma
- Immerse the PDMS device in 70% EtOH for sterilization for 15-30 min

- Dry EtOH with N_2 gas inside a biosafety cabinet
- Assemble the dry PDMS device on top of PDL coated cell culture plate or PDL coated glass coverslip
- Fill reservoirs with culture medium and incubate overnight inside a humidified 37°C incubator
- Aspirate the culture medium and load neurons into the soma compartment
- Replace half of the culture medium every 3-4 days
- Load OPCs to the axon/glia compartment at DIV 14 for co-culture
- Fix cells with 4% PFA at DIV 24-30

Protocol IV. Six-Compartment CNS Neuron/Glia Co-Culture Microdevice

- Glass imprint master
  - ✓ Deposit Cr/Au on a glass wafer: Glass etch mask layer
  - ✓ Photolithography
    - Photoresist: S1818
    - Spin-coat: 30 sec at 4000 rpm
    - Soft bake: 5 min at 110 °C
    - Exposure: 84 mJ/cm^2 (MA6, Karl Suss)
    - Develop in MF-319
  - ✓ Pattern Cr/Au layer by wet etching
  - ✓ Glass wet etching (3 μm)
  - ✓ Remove Cr/Au etch mask
  - ✓ Rinse with DI water
- PMMA master
  - ✓ Cut 3.5-4 mm deep reservoirs on a PMMA block (75 x 75 x 18.8 mm^3) using a CNC milling machine
  - ✓ Transfer the pattern on the imprint master using a temperature controlled hydraulic press
    - Pressure: 1,082 kPa
    - Temperature: 115°C
    - Time: 5 min
  - ✓ Sonicate the PMMA master in IPA

- ✓ Dry the PMMA master with N_2 gas

- PDMS master
  - ✓ PDMS soft-lithography from the PMMA master (Protocol I)
- PDMS master surface coating (Protocol II)
- Sonicate PDMS master in IPA for 5 min
- Device replication
  - ✓ PDMS soft-lithography (Protocol I)
- Device assembly and sterilization
  - ✓ On culture plate
    - Treat PDMS device with oxygen plasma
    - Immerse the PDMS device in 70% EtOH for sterilization for 15-30 min
    - Dry EtOH with N_2 gas inside a biosafety cabinet
    - Assemble the dry PDMS device on top of PDL coated cell culture plate
  - ✓ On glass coverslip
    - Treat the PDMS device and a glass coverslip with oxygen plasma
    - Permanently bond the device on a glass coverslip
    - Immerse in DI water and autoclave for sterilization
    - Coat the assembled device with PDL
- Fill reservoirs with culture medium and incubate overnight inside a humidified 37°C incubator

- Aspirate the culture medium and load neurons into the soma compartment
- Replace half of the culture medium every 3-4 days
- Load OPCs or astrocytes to the axon/glia compartments at DIV 14 for co-culture
- Fix cells with 4% PFA at DIV 24-30

Protocol V. 24-Compartment CNS Neuron Culture Microsystem

Compartment layer

- Silicon imprint master
    - ✓ Deposit nitride layer on Si wafer
    - ✓ Photolithography : Silicon nitride etch mask layer
        - Photoresist: S1818
        - Spin-coat: 30 sec at 4000 rpm
        - Soft bake: 5 min at 110 °C
        - Exposure: 84 mJ/cm^2 (MA6, Karl Suss)
        - Develop in MF-319
    - ✓ Pattern nitride layer using RIE
    - ✓ Remove photoresist etch mask layer
    - ✓ Silicon wet etching
        - Etchant: KOH (40%)
        - Temperature: 70 °C
    - ✓ Rinse with DI water
- PMMA master
    - ✓ Cut compartments on a PMMA block (75 x 75 x 18.8 mm^3) using a CNC milling machine
    - ✓ Transfer the pattern on the imprint master using a temperature controlled hydraulic press
        - Pressure: 1,082 kPa

        - Temperature: 115°C
        - Time: 5 min
    - ✓ Sonicate the PMMA master in IPA
    - ✓ Dry the PMMA master with N_2 gas
- PDMS master
    - ✓ PDMS soft-lithography from the PMMA master (Protocol I)
- PDMS master surface coating (Protocol II)
- Sonicate PDMS master in IPA for 5 min
- Device replication
    - ✓ PDMS soft-lithography (for a PDMS device with defined through holes)
        - Pour sufficient amount of degassed PDMS mixture on the PDMS master
        - Place a surface coated glass wafer on the PDMS master (Bubble should not be trapped under the glass wafer)
        - Put a weight (100 g) on the glass wafer
        - Place inside a leveled 85°C oven for at least 45 min
        - Remove the glass wafer and peel off the PDMS device from the PDMS master

Reservoir layer

- PMMA master

  - ✓ Cut compartments on a PMMA block (75 x 75 x 18.8 mm^3) using a CNC milling machine

- Device replication
  - ✓ PDMS soft-lithography from the PMMA master (Protocol I)

Substrate layer

- PMMA master
  - ✓ Cut compartments on a PMMA block (75 x 75 x 18.8 mm^3) using a CNC milling machine
- Device replication
  - ✓ PDMS soft-lithography from the PMMA master (Protocol I)

Assembly

- Treat three layers with oxygen plasma
- Align and permanently bond PDMS layers
- Immerse in DI water and autoclave for sterilization

Cell culture

- Coat the assembled device with PDL
- Fill reservoirs with culture medium and incubate overnight inside a humidified 37°C incubator
- Aspirate the culture medium and load neurons into the soma compartment

- Replace half of the culture medium every 3-4 days
- Stain isolated axons with Calcein-AM for visualization

Protocol VI. Micropatterning of PDMS using a Photoresist Lift-off Technique

- Sacrificial photoresist layer patterning: Photolithography
    - ✓ Photoresist: Futurrex NR2-20000P, NR4-8000P
- Pour PDMS mixture on photoresist patterned substrate
    - ✓ Dilute PDMS with toluene if necessary
- Spin-coat PDMS poured substrate with an acceleration rate of 200 rpm/s
- Place the sample inside a leveled 85°C oven for 15 min
- Immerse PDMS spin-coated substrate in a photoresist remover and sonicate for 5 min to lift-off the sacrificial photoresist layer
- Rinse the sample with IPA
- Dry inside a leveled 85°C oven

Protocol VII. Six-compartment Device for Axon Growth Analysis

Axon-guiding Layer

- Silicon master mold fabrication: Photolithography
    - ✓ Photoresist: SU-8™ 2002
    - ✓ Spin-coat: 30 sec at 750 rpm
    - ✓ Soft bake: 5 min at 95 °C
    - ✓ Exposure: 200 mJ/cm^2 (MA6, Karl Suss)
    - ✓ Post exposure bake: 5 min at 95 °C
    - ✓ Develop in Thinner P
- Surface coating (Protocol II)
- PDMS soft-lithography (Protocol I)

Compartment Layer

- PMMA master
    - ✓ Cut compartments on a PMMA block (75 x 75 x 18.8 mm^3) using a CNC milling machine
- PDMS master
    - ✓ PDMS soft-lithography from the PMMA master (Protocol I)
- PDMS master surface coating (Protocol II)
- Sonicate PDMS master in IPA for 5 min
- Device replication
    - ✓ PDMS soft-lithography (Protocol I)

Ridge structure

- PDMS soft-lithography from petri dish (thickness: 2mm, Protocol I)
- Punch with 10 mm punch bit

Assembly

- Treat two layers and the ridge structure with oxygen plasma
- Align and permanently bond PDMS layers and the ridge structure
- Immerse in DI water and autoclave for sterilization
- Coat the assembled device with PDL

Cell culture

- Coat the assembled device with PDL
- Fill reservoirs with culture medium and incubate overnight inside a humidified 37°C incubator
- Aspirate the culture medium and load neurons into the soma compartment
- Replace half of the culture medium every 3-4 days
- Localized ECM treatments to either neuronal somata or isolated axons at DIV 7
- Stain isolated axons with Calcein-AM for visualization and analyze the axon growth at DIV 11

Protocol VIII.Neural progenitor cell aggregate culture microdevice

- Silicon master mold fabrication: Photolithography
    - ✓ Photoresist: SU-8™ 2075
    - ✓ Spin-coat: 60 sec at 1000 rpm with 30 sec acceleration
    - ✓ Soft bake: over 24 hours at 65 °C + 45 min at 95 °C
    - ✓ Exposure: 370 mJ/cm^2 (MA6, Karl Suss)
    - ✓ Post exposure bake: 20 min at 65 °C + 40 min at 95 °C
    - ✓ Develop in Thinner P
- Silicon master surface coating (Protocol II)
- PDMS soft-lithography (Protocol I) for PDMS master
- PDMS master surface coating (Protocol II)
- Sonicate PDMS master in IPA for 5 min
- Device replication from the PDMS master
    - ✓ PDMS soft-lithography (Protocol I)
- Punch the center loading port with 4 mm punch bit
- Punch the whole device with 10 mm punch bit for defining outlets
- Treat PDMS device with oxygen plasma and assemble it on glass coverslip
- Immerse in DI water and autoclave for sterilization
- Coat the assembled device with PDL and Matrigel™
- Fill the device with culture medium and incubate overnight inside a humidified 37°C incubator

- Aspirate the culture medium and load neural progenitor aggregates into the center loading port
- Replace half of the culture medium every 3-4 days
- Biomolecular treatment at DIV 14-17
- Fix cells with 4% PFA at DIV 24-30

Protocol IX. Culture Medium Preparation

NBB27: Neuron Medium

- 100 ml of Neurobasal Medium
- 2 ml B27 supplement (50X)
- 250 µL GluMax (200mM)
- 1 ml (6.3 mg) N-acetyl cysteine
- 2 ml Penicillin/Streptomycin (100X)

NBB27/Glutamate: 1st week of Neuron Culture

- 200 ml of Neurobasal Medium
- 4 ml B27 supplement
- 29.23 mg L-glutamine
- 0.846 mg L-Glutamic Acid
- 12.6 mg N-acetyl cysteine
- 2 ml Penicillin/Streptomycin

DMEM/NBB27: **Neuron/OL co-culture, neural aggregate culture**

- 100 ml Neurobasal Medium
- 4 ml B27 supplement
- 750 µl GluMax
- 6.3 mg N-acetyl cysteine
- 100 ml DMEM

- 11 mg Sodium Pyruvate
- 2 ml SATO (100X)
- 50 µL D-Biotin
- 2 ml Penicillin/Streptomycin
- 200 µL Insulin (1st week of co-culture)

DMEM10S (10% FBS): **Neuronal medium**

- 200 ml DMEM
- 22 ml FBS (heat inactivated)
- 2.2 ml Penicillin/Streptomycin
- 22 mg Sodium Pyruvate
- 29.23 mg L-Glutamine

Protocol X. Rat Dissection for Neurons

1. Take brains from E16 Sprague-Dawley rat to dissection medium (10 mM HEPES/ HBSS without Ca^{2+} and Mg^{2+}) on ice pack.
2. Remove the meninges on each brain.
3. Remove hemispheres from midbrain/hindbrain, and transfer the cleaned forebrain to new a plate with dissection medium on ice pack.
4. Remove dissection medium from forebrain and add 4 ml of papain/L-cystaine solution.
5. Transfer to a 50 ml tube and incubate in a 37°C water bath for 5 min.
6. Remove the papain/L-cysteine solution by pipette.
7. Add 5 ml trypsin inhibitor solution and incubate for 2-3 min at 37°C water bath.
8. Remove Trypsin inhibitor solution.
9. Repeat steps 7-8 (3 times).
10. Add 20 ml NBB27/DMEM.
11. Triturate 20 times after clumps have disappeared.
12. Centrifuge at 100 x G for 7min.
13. Remove supernatant and wash pellet with 20 ml NBB27/DMEM.
14. Centrifuge at 100 x G for 7min.
15. Remove supernatant and add 10-15 ml NBB27/DMEM.
16. Suspend cells and sieve through a 70 μm mesh.

Protocol XI. Rat Dissection for Glial Cells

1. Place the rat pups on the ice block to anaesthetize them.
2. Dip the pups in the beaker of 70% EtOH and place in the empty petri dish on the right (if you have more than 5 pups, you will need to do multiple batches).
3. Use the large scissors and decapitate the pups, dropping the heads into the first dish of HBSS+ (on the right) and disposing of the body in the carcass bag. (Repeat steps 2-3 until all the pups have been decapitated.)
4. Using the small forceps, transfer the heads into the 2nd petri dish of HBSS+.
5. Using the spring scissors, cut the skin down the center of the skull (cranially).
6. Cut the skull cranially.
7. Use one spatula to remove the brain, leaving the skull in the empty petri dish on the left.
8. Use the second spatula to "cut" off the hind brain and place the fore-brain in one of the petri dishes with HBSS+ on the ice pack. (Repeat Steps 5-8 until all the brains are removed.)
9. Using the jeweler's forceps, remove the meninges from the forebrain (this may be done under a microscope inside the biosafety cabinet) and place the clean brain in the other petri dish with HBSS+ on the ice pack. (If you have more than 15 brains, divide the brains into two separate petri dishes with HBSS+.)
10. Gently suck out the HBSS+ from the petri dish.
11. Chop the brains with a sterile razor blade into ~1mm chunks. (Use the alligator forceps to hold the blade.)

12. Add 13.6 ml HBSS+, 0.8 ml DNase and 0.6 ml trypsin to each plate. (Optional to transfer the contents to a 50 ml tube at this time.)
13. Incubate in the 37°C incubator for 15 min. (DO NOT USE WATER BATH.)
14. Add 25 ml of DMEM10S to each conical tube and transfer the contents of the petri dishes to the tubes. Triturate gently 5 times to break up the trypsinized tissue.
15. Spin down at 100 x G for 7 min.
16. Suck off supernatant with a 25 ml pipette.
17. Add 25 ml DMEM10S and triturate the tissue with a 10 ml pipette up to 8 times to begin homogenizing the tissue.
18. Repeat steps 15-16.
19. Add 25 ml DMEM10S and triturate the tissue with a 10 ml pipette until nearly homogenous (very few small clumps).
20. Let the tissue settle for 10 min.
21. Pass the suspension (avoiding the pellet) through a 70 μm Nylon cell strainer and collect in a clean 50 ml tube.
22. Repeat steps 19-21.
23. If you are using multiple tubes, spin down and suck off the supernatant. Gently re-suspend the pellets and combine in a single tube.
24. Plate at 1.5 brains/flask in PDL coated T75 flasks with 10 ml DMEM10S per flask.
25. Spread medium with cells over the entire flask surface.
26. Label the flasks with the date and type of cell.
27. Feed the cells with complete medium changes (every 2 days).

28. 10 days and 17 days after plating, mixed glia cultures can be shaken for oligodendrocyte cultures.

Protocol XII. OPC Collection from Mixed Glial Culture

1. After culturing mixed glia for 10 days, shake the flasks at 200 rpm 1 hour at 37°C
2. Rinse with complete medium (10% DMEM, 10 ml) to remove floating cells.
3. Wash the cells with 10 ml, pre-warmed PBS, 2 times.
4. Add 10% DMEM and place inside the 37°C culture chamber for additional 4-5 hours. The culture is subjected to overnight (approx. 14 hours) shaking (250 rpm, 37°C)
5. Pre-plate cells on 100 mm petri-dish with 20 ml for 1 hour (37°C, 5% CO_2).
6. Sieve the OL cell suspension through a 20 μm nylon mesh into a 50 ml tube
7. Centrifuge at 100 x G for 7 min
8. Resuspend cells with 5ml of BDM media
9. Count and plate cells (at approx. 60% of confluency)
10. Culture OPCs in 10% DMEM for 5-16 hours and change to differentiation medium.

Protocol XIII.Astrocyte Collection from Mixed Glial Culture

After removing microglia, the flasks were shaken overnight to separate pre-OLs from the astrocyte layer. Astrocytes were purified from the astrocyte layer in the flask that has been exposed to the specific microglia toxin L-leucine methyl ester (1 mM) for 1 h, followed by one to two cycles of subculture and repeated exposure to L-leucine methyl ester. The enriched astrocytes were consistently more than 95% pure with pre-OLs being the major contaminating cells.

Detailed protocol for astrocyte LME treatment (L-leucine methyl ester hydeochloride)

Stock solution: 100 mM in PBS (-20°C)

1. Add 100ul of LME directly to the 75T flask (10ml D10S); final 1mM.
2. Incubate 1 hour at CO_2 incubator.
3. Wash with pre-warmed PBS (sterile) 2 times to remove serum.
4. Add 5ml 1X trypsin –EDTA and incubate for 3 min.
5. Add 5ml D10S and resuspend.
6. Collect to the 50ml conical tube and add 30ml D10S.
7. Spin for 5 min.
8. Wash with 30ml D10S.
9. Finally resuspend to 10ml D10S and count the cell.

Protocol XIV. Neural progenitor cell aggregate preparation

1. Suspend neurons in NBB27/DMEM medium with 1x Sato, 10 ng/ml CNTF, and 10 μM forskolin to a final density of ~ $2x10^6$ cells/ml.
2. Place 2 ml into each well of a 6-well plate (uncoated).
3. Incubate overnight.
4. Use a 1 ml pipette to gently resuspend once per day for 3 days, allowing the cells to form aggregates.
5. 3 days later, sieve aggregate suspension through a 200 μm mesh into a 50 ml tube and allow them to settle (3 min).
6. Remove supernatant by pipette.
7. Wash several times with medium to remove small aggregates and dead cells.
8. Gently resuspend the aggregates in NBB27/DMEM with 1x Sato, 10 ng/ml CNTF, 10 μM forskolin.

Protocol XV. Immunocytochemistry (NF, MBP)

Cell fix

- Aspirate culture medium and rinse with PBS one time.
- Aspirate PBS.
- Apply 4% paraformaldehyde (PFA) and leave at room temperature for 10-20 min.
- Aspirate PFA.
- Rinse with PBS (5 min).

Blocking

- Wash fixed sample with TBS-T three times (5-10 min each).
- Add 5% goat serum-TBS-T.
- Store at room temperature for 1 hour

Immunocytochemistry

- Aspirate goat serum blocking solution.
- Add primary antibody diluted in 5% goat serum-TBS-T
- Store at 4°C overnight. (Do not let sample dry.)
- Wash three time with TBS-T (5-10 min each)
- Add secondary antibody diluted in 5% goat serum -TBS-T
- Store at room temperature for 1 hour
- Wash three time with TBS-T (5-10 min each)

VITA

Name: Jaewon Park

Address: Department of Electrical and Computer Engineering

Texas A&M University, TAMU 3128

College Station, TX 77843-3128, USA

Email Address: jwpark717@gmail.com

Education: B.E., Electrical Engineering, Korea University, Seoul, Korea, 2004

Ph.D., Electrical Engineering, Texas A&M University,
College Station, USA, 2011

Research interest:

- Cell culture and analysis microsystems for central nervous system axon-glia interaction, myelination, and axon regeneration
- Nanochannel fabrication and applications
- Hybrid Nano-Micro/Bio Packaging
- Portable Disease Diagnosis/Pathogen Detection Microsystems